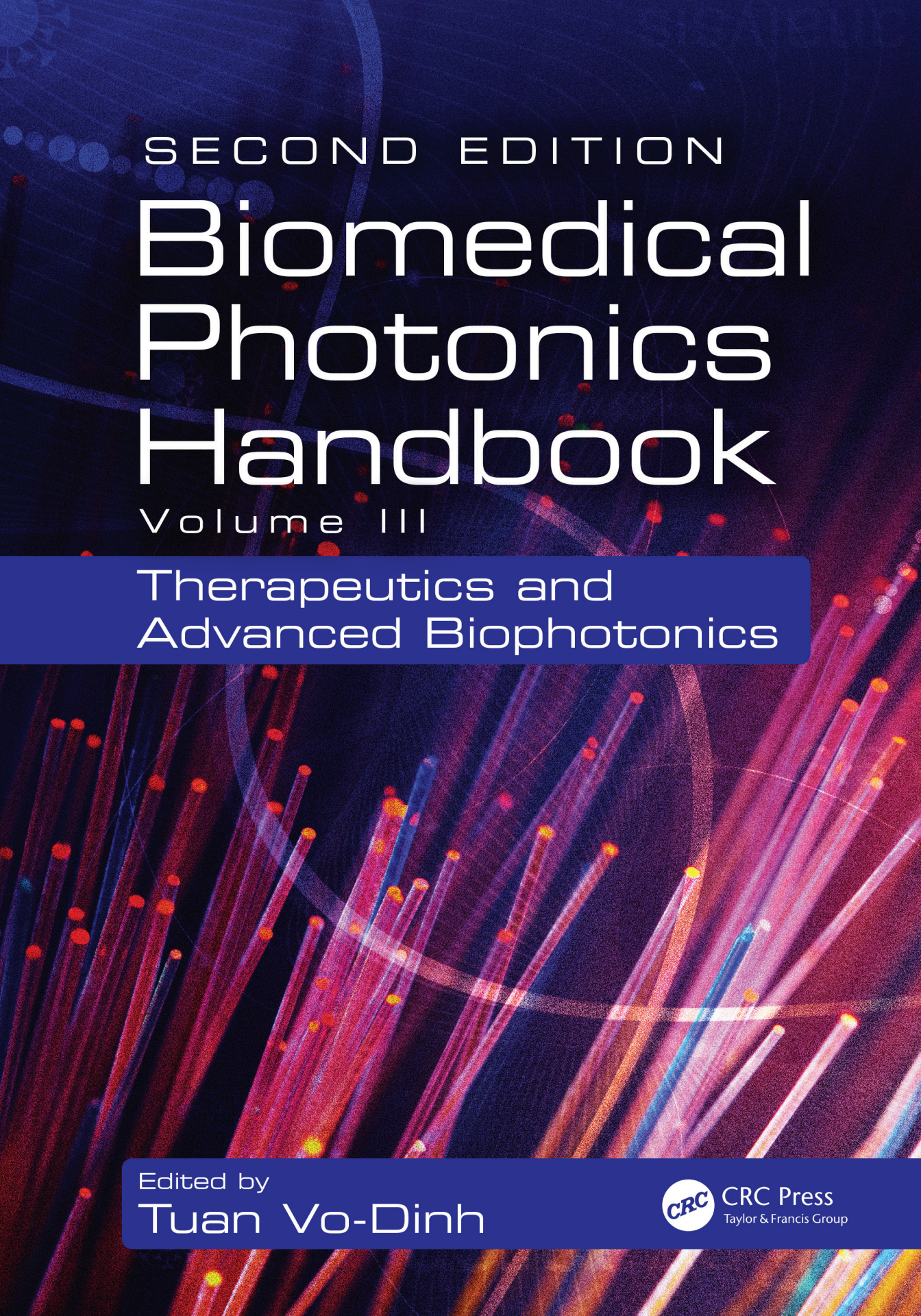
SECOND EDITION
Biomedical Photonics Handbook
Volume III
Therapeutics and Advanced Biophotonics
Edited by
Tuan Vo-Dinh
CRC Press
Taylor & Francis Group

SECOND EDITION

Biomedical Photonics Handbook

Volume III

Therapeutics and Advanced Biophotonics

Biomedical Photonics Handbook, Second Edition

Volume I: Fundamentals, Devices, and Techniques

Volume II: Biomedical Diagnostics

Volume III: Therapeutics and Advanced Biophotonics

SECOND EDITION

Biomedical Photonics Handbook

Volume III

Therapeutics and Advanced Biophotonics

Edited by
Tuan Vo-Dinh
Duke University
Durham, North Carolina, USA

CRC Press
Taylor & Francis Group
Boca Raton London New York

CRC Press is an imprint of the
Taylor & Francis Group, an **informa** business

CRC Press
Taylor & Francis Group
6000 Broken Sound Parkway NW, Suite 300
Boca Raton, FL 33487-2742

© 2015 by Taylor & Francis Group, LLC
CRC Press is an imprint of Taylor & Francis Group, an Informa business

No claim to original U.S. Government works
Version Date: 20140311

International Standard Book Number-13: 978-1-4200-8517-4 (eBook - PDF)

This book contains information obtained from authentic and highly regarded sources. Reasonable efforts have been made to publish reliable data and information, but the author and publisher cannot assume responsibility for the validity of all materials or the consequences of their use. The authors and publishers have attempted to trace the copyright holders of all material reproduced in this publication and apologize to copyright holders if permission to publish in this form has not been obtained. If any copyright material has not been acknowledged please write and let us know so we may rectify in any future reprint.

Except as permitted under U.S. Copyright Law, no part of this book may be reprinted, reproduced, transmitted, or utilized in any form by any electronic, mechanical, or other means, now known or hereafter invented, including photocopying, microfilming, and recording, or in any information storage or retrieval system, without written permission from the publishers.

For permission to photocopy or use material electronically from this work, please access www.copyright.com (http://www.copyright.com/) or contact the Copyright Clearance Center, Inc. (CCC), 222 Rosewood Drive, Danvers, MA 01923, 978-750-8400. CCC is a not-for-profit organization that provides licenses and registration for a variety of users. For organizations that have been granted a photocopy license by the CCC, a separate system of payment has been arranged.

Trademark Notice: Product or corporate names may be trademarks or registered trademarks, and are used only for identification and explanation without intent to infringe.

Visit the Taylor & Francis Web site at
http://www.taylorandfrancis.com

and the CRC Press Web site at
http://www.crcpress.com

Inspired by the love and
infinite patience of
my wife, Kim-Chi, and
my daughter, Jade

This book is dedicated to the
memory of my parents,
Vo Dinh Kinh and Dang Thi Dinh

Contents

SECTION II Advanced Biophotonics and Nanophotonics

Preface

In the tradition of the *Biomedical Photonics Handbook*, the second edition is intended to serve as an authoritative reference source for a broad audience involved in the research, teaching, learning, and practice of medical technologies. Biomedical photonics is defined as the science that harnesses light and other forms of radiant energy to provide the solution of problems arising in medicine and biology. This research field has recently experienced an explosive growth due to its noninvasive or minimally invasive nature and the cost-effectiveness of photonic modalities in medical diagnostics and therapy.

The field of biomedical photonics did not emerge as a well-defined, single research discipline like chemistry, physics, or biology. Its development and growth have been shaped by the convergence of three scientific and technological revolutions of the twentieth century: the *quantum theory revolution*, the *technology revolution*, and the *genomics revolution*.

The quantum theory of atomic phenomena provides a fundamental framework for molecular biology and genetics because of its unique understanding of electrons, atoms, molecules, and light itself. Out of this new scientific framework emerged the discovery of the structure of DNA, the molecular nature of cell machinery, and the genetic cause of diseases, all of which form the basis of molecular medicine. The formulation of quantum theory not only gave birth to the field of molecular spectroscopy but also led to the development of a powerful set of photonics tools—lasers, scanning tunneling microscopes, and near-field nanoprobes—for exploring nature and understanding the cause of disease at the fundamental level.

Advances in technology also played, and continue to play, an essential role in the development of biomedical photonics. The invention of the laser was an important milestone. Laser is now the light source most widely used to excite tissues for disease diagnosis as well as to irradiate tumors for tissue removal in interventional surgery (*optical scalpels*). The microchip is another important technological development that has significantly accelerated the evolution of biomedical photonics. While the laser has provided a new technology for excitation, the miniaturization and mass production of integrated circuits, sensor devices, and their associated electronic circuitry made possible the development of the microchip, which has radically transformed the ways detection and imaging of molecules, tissues, and organs can be performed in vivo and ex vivo. Recently, nanotechnology, which involves research on materials and species at length scales between 1 and 100 nm, has been revolutionizing important areas in biomedical photonics, especially diagnostics and therapy at the molecular and cellular level. The combination of photonics and nanotechnology has already led to a new generation of devices for probing the cell machinery and elucidating intimate life processes occurring at the molecular level that were heretofore invisible to human inquiry. This will open the possibility of detecting and manipulating atoms and molecules using nanodevices, which have the potential for a wide variety of medical uses at the cellular level. The marriage of electronics, biomaterials, and photonics is expected to revolutionize many areas of medicine in the twenty-first century.

A wide variety of biomedical photonic technologies have already been developed for clinical monitoring of early disease states or physiological parameters such as blood pressure, blood chemistry, pH, temperature, and the presence of pathological organisms or biochemical species of clinical importance. Advanced optical concepts using various spectroscopic modalities (e.g., fluorescence, scattering, reflection, and optical coherence tomography) are emerging in the important area of functional imaging. Many photonic technologies originally developed for other applications (e.g., lasers and sensor systems in defense, energy, and aerospace) have now found important uses in medical applications. From the brain to the sinuses to the abdomen, precision navigation and tracking techniques are critical to position medical instruments precisely within the three-dimensional surgical space. For instance, optical stereotactic systems are being developed for brain surgery, and flexible micronavigation devices are being engineered for medical laser ablation treatments.

With the completion of the sequencing of the human genome, one of the greatest impacts of genomics and proteomics is the establishment of an entirely new approach to biomedical research. With whole-genome sequences and new automated, high-throughput systems, photonic technologies such as biochips and microarrays can address biological and medical problems systematically and on a large scale in a massively parallel manner. They provide the tools to study how tens of thousands of genes and proteins work together in interconnected networks to orchestrate the chemistry of life. Specific genes have been deciphered and linked to numerous diseases and disorders, including breast cancer, muscle disease, deafness, and blindness. Furthermore, advanced biophotonics has contributed dramatically to the field of diagnostics, therapy, and drug discovery in the postgenomic area. Genomics and proteomics present the drug discovery community with a wealth of new potential targets. Biomedical photonics can provide tools capable of identifying specific subsets of genes encoded within the human genome that can cause the development of diseases. Photonic techniques based on molecular probes are being developed to identify the molecular alterations that distinguish a diseased cell from a normal cell. Such technologies will ultimately aid in characterizing and predicting the pathologic behavior of that diseased cell, as well as the cell's responsiveness to drug treatment. Information from the human genome project will one day make personal, molecular medicine an exciting reality.

The second edition of this handbook is intended to present the most recent scientific and technological advances in biomedical photonics, as well as their practical applications, in a single source. The three-book handbook represents the collective work of over 150 scientists, engineers, and clinicians. It includes many new topics and chapters such as fiber-optics probes design, laser and optical radiation safety, photothermal detection, multidimensional fluorescence imaging, surface plasmon resonance imaging, molecular contrast optical coherence tomography, multiscale photoacoustics, polarized light for medical diagnostics, quantitative diffuse reflectance imaging, interferometric light scattering, nonlinear interferometric vibrational imaging, nanoscintillator-based therapy, SERS molecular sentinel nanoprobes, and plasmonic coupling interference nanoprobes.

The handbook includes 71 chapters grouped in 8 sections:

1. Volume I: *Biomedical Photonics Handbook*, Second Edition: *Fundamentals, Devices, and Techniques*
2. Volume II: *Biomedical Photonics Handbook*, Second Edition: *Biomedical Diagnostics*
3. Volume III: *Biomedical Photonics Handbook*, Second Edition: *Therapeutics and Advanced Biophotonics*

In Volume I, Section I (Photonics and Tissue Optics) contains introductory chapters on the fundamental optical properties of tissue, light–tissue interactions, and theoretical models for optical imaging. Section II (Basic Instrumentation) deals with basic instrumentation and hardware systems and contains chapters on lasers and excitation sources, basic optical instrumentation, optical fibers, probe designs, laser use, and optical radiation safety. Section III (Photonic Detection and Imaging Techniques) deals with methodologies and contains chapters on various detection techniques and systems (such as lifetime imaging, microscopy, two-photon detection, photothermal detection, interferometry, Doppler imaging, light scattering, and thermal imaging). Finally, Section IV (Spectroscopic Data) provides a

comprehensive compilation of useful information on spectroscopic data of biologically and medically relevant species for over 1000 compounds and systems.

In Volume II, Section I (Biomedical Analysis, Sensing, and Imaging) contains chapters describing in vitro diagnostics (e.g., glucose diagnostics, in vitro instrumentation, biosensors, surface plasmon resonance, and flow cytometry) and in vivo diagnostics (optical coherence tomography, polarized light diagnostics, functional imaging and photon migration spectroscopy, and multiscale photoacoustics). Section II (Biomedical Diagnostics and Optical Biopsy) is mainly devoted to novel optical techniques for cancer diagnostics, often referred to as *optical biopsy* (such as fluorescence, scattering, reflectance, interferometric light scattering, optoacoustics, and ultrasonically modulated optical imaging).

In Volume III, Section I (Therapeutic and Interventional Techniques) covers photodynamic therapy as well as various laser-based treatment techniques that are applied to different organs and disease endpoints (dermatology, pulmonology, neurosurgery, ophthalmology, otolaryngology, gastroenterology, and dentistry). There are several chapters dealing with nanotechnology for theranostics, that is, the modality combining diagnostics and therapy. Section II (Advanced Biophotonics and Nanophotonics) is devoted to the most recent advances in methods and instrumentation for biomedical and biotechnology applications. This section contains chapters on emerging photonic technologies (e.g., biochips, nanosensors, quantum dots, molecular probes, molecular beacons, molecular sentinels, plasmonic coupling nanoprobes, bioluminescent reporters, optical tweezers) that are being developed for gene expression research, gene diagnostics, protein profiling, and molecular biology investigations as well as for early diagnostics of disease biomarkers for the *new medicine*.

The goal of the second edition of this handbook is to provide a comprehensive forum that integrates interdisciplinary research and development of interest to scientists, engineers, manufacturers, teachers, students, and clinical providers. Each chapter provides introductory material with an overview of the topic of interest as well as a collection of published data with an extensive list of references for further details. The handbook is designed to present the most recent advances in instrumentation and methods as well as clinical applications in important areas of biomedical photonics. Because light is rapidly becoming an important diagnostic tool and a powerful weapon in the armory of the modern physician, it is our hope that this handbook will stimulate a greater appreciation of the usefulness, efficiency, and potential of photonics in medicine.

Tuan Vo-Dinh
Duke University
Durham, North Carolina

Acknowledgments

The completion of this work has been made possible with the assistance of many friends and colleagues. I wish to express my gratitude to members of the Scientific Advisory Board of the first edition. Their thoughtful suggestions and useful advice in the planning phase of the first edition have been important in achieving the breadth and depth of this handbook. It is a great pleasure for me to acknowledge, with deep gratitude, the contribution of over 150 contributors for the 71 chapters in this handbook. I wish to thank my coworkers at Duke University and the Oak Ridge National Laboratory, and many colleagues in academia, federal laboratories, and industry, for their kind help in reading and commenting on various chapters of the manuscript. My gratitude is extended to all my present and past students, postdoctoral associates, colleagues, and collaborators, who have been traveling with me on this exciting journey of discovery with the ultimate vision of bringing research at the intersection of photonics and medicine to the service of society.

I gratefully acknowledge the support of the US Department of Energy Office of Biological and Environmental Research, the National Institutes of Health, the Defense Advanced Research Projects Agency, the Department of the Army, the Army Medical Research and Materiel Command, the Department of Justice, the Federal Bureau of Investigation, the Office of Naval Research, the Environmental Protection Agency, the Fitzpatrick Foundation, the R. Eugene and Susie E. Goodson Endowment Fund, and the Wallace Coulter Foundation.

The completion of this work has been made possible with the love, encouragement, and inspiration of my wife, Kim-Chi, and my daughter, Jade.

Editor

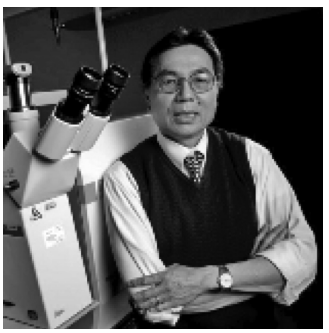

Tuan Vo-Dinh is R. Eugene and Susie E. Goodson Distinguished Professor of Biomedical Engineering, professor of chemistry, and director of the Fitzpatrick Institute for Photonics at Duke University. A native of Vietnam and a naturalized US citizen, he completed high school education in Saigon (now Ho Chi Minh City). He continued his studies in Europe, where he received his BS in physics in 1970 from EPFL (Ecole Polytechnique Federal de Lausanne) in Lausanne and his PhD in physical chemistry in 1975 from ETH (Swiss Federal Institute of Technology) in Zurich, Switzerland. Before joining Duke University in 2006, Dr. Vo-Dinh was director of the Center for Advanced Biomedical Photonics, group leader of Advanced Biomedical Science and Technology Group, and a corporate fellow, one of the highest honors for distinguished scientists at Oak Ridge National Laboratory (ORNL). His research has focused on the development of advanced technologies for the protection of the environment and the improvement of human health. His research activities involve biophotonics, plasmonics, nanobiotechnology, laser spectroscopy, molecular imaging, medical theranostics, cancer detection, nanosensors, chemical sensors, biosensors, and biochips.

Dr. Vo-Dinh has authored over 350 publications in peer-reviewed scientific journals. He is the author of a textbook on spectroscopy and the editor of six books. He holds over 37 US and international patents, 5 of which have been licensed to private companies for commercial development. Dr. Vo-Dinh has presented over 200 invited lectures at international meetings in universities and research institutions. He has chaired over 30 international conferences in his field of research and served on various national and international scientific committees. He also serves the scientific community through his participation in a wide range of governmental and industrial boards and advisory committees.

Dr. Vo-Dinh has received seven R&D 100 Awards for Most Technologically Significant Advance in Research and Development for his pioneering research and inventions of innovative technologies. He has received the Gold Medal Award, Society for Applied Spectroscopy (1988); the Languedoc–Roussillon Award, France (1989); the Scientist of the Year Award, ORNL (1992); the Thomas Jefferson Award, Martin Marietta Corporation (1992); two Awards for Excellence in Technology Transfer, Federal Laboratory Consortium (1995, 1986); the Inventor of the Year Award, Tennessee Inventors Association (1996); the Lockheed Martin Technology Commercialization Award (1998); the Distinguished Inventors Award, UT-Battelle (2003); and the Distinguished Scientist of the Year Award, ORNL (2003). In 1997, he was presented the Exceptional Services Award for distinguished contribution to a healthy citizenry from the US Department of Energy. In 2011, he received the Award for Spectrochemical Analysis from the American Chemical Society (ACS) Division of Analytical Chemistry.

Contributors

R. Rox Anderson
Harvard Medical School
and
Department of Dermatology
Massachusetts General Hospital
Boston, Massachusetts

Terry Beck
TriLink BioTechnologies, Inc.
San Diego, California

Wladimir Benalcazar
Beckman Institute for Advanced Science and Technology
University of Illinois at Urbana–Champaign
Urbana, Illinois

Stephen A. Boppart
Beckman Institute for Advanced Science and Technology
University of Illinois at Urbana–Champaign
Urbana, Illinois

Darryl J. Bornhop
Department of Chemistry
Vanderbilt University
Nashville, Tennessee

David Boyer
The Retina Vitreous Associates Medical Group
Doheny Eye Institute
and
Keck School of Medicine
University of Southern California
Los Angeles, California

Murphy Brasuel
Chemistry & Biochemistry Department
Colorado College
Colorado Springs, Colorado

Richard D. Bucholz
Department of Neurosurgery
Saint Louis University
Saint Louis, Missouri

Eric J. Chaney
Beckman Institute for Advanced Science and Technology
University of Illinois at Urbana–Champaign
Urbana, Illinois

Bernard Choi
Department of Surgery
and
Department of Biomedical Engineering
University of California, Irvine
Irvine, California

Praveen D. Chowdary
Beckman Institute for Advanced Science and Technology
University of Illinois at Urbana–Champaign
Urbana, Illinois

Thomas G. Chu
The Retina Vitreous Associates Medical Group
Doheny Eye Institute
and
Keck School of Medicine
University of Southern California
Los Angeles, California

Christopher H. Contag
Department of Pediatrics
and
Department of Radiology
and
Department of Microbiology and Immunology
Stanford University Medical Center
Stanford, California

Pamela R. Contag
ConcentRx Inc.
San Jose, California

Georgeta Crivat
Department of Chemistry
University of New Orleans
New Orleans, Louisiana

Brian M. Cullum
Department of Chemistry and Biochemistry
University of Maryland, Baltimore County
Baltimore, Maryland

Sandra M. Da Silva
Biochemical Science Division
National Institute of Standards and Technology
Gaithersburg, Maryland

Andrew M. Fales
Department of Biomedical Engineering
Duke University
Durham, North Carolina

Xiaohong Fang
Institute of Chemistry
Chinese Academy of Science
Beijing, People's Republic of China

Daniel Fried
University of California, San Francisco
San Francisco, California

Lilit Garibyan
Harvard Medical School
and
Department of Dermatology
Massachusetts General Hospital
Boston, Massachusetts

Sandra O. Gollnick
Photodynamic Therapy Center
Roswell Park Cancer Institute
Buffalo, New York

Molly K. Gregas
Department of Biomedical Engineering
Duke University
Durham, North Carolina

Guy D. Griffin
Department of Biomedical Engineering
Duke University
Durham, North Carolina

Martin Gruebele
Beckman Institute for Advanced Science and Technology
University of Illinois at Urbana–Champaign
Urbana, Illinois

Barbara W. Henderson
Photodynamic Therapy Center
Roswell Park Cancer Institute
Buffalo, New York

Henry Hirschberg
Beckman Laser Institute and Medical Clinic
University of California, Irvine
Irvine, California

Richard Hogrefe
TriLink BioTechnologies, Inc.
San Diego, California

H. Ray Jalian
Department of Dermatology
Massachusetts General Hospital
Boston, Massachusetts

Zhi Jiang
Beckman Institute for Advanced Science and Technology
University of Illinois at Urbana–Champaign
Urbana, Illinois

Penny Joshi
Photodynamic Therapy Center
Roswell Park Cancer Institute
Buffalo, New York

Brad A. Kairdolf
Department of Biomedical Engineering
Georgia Institute of Technology
and
Emory University
Atlanta, Georgia

Tiina I. Karu
Institute of Laser and Information Technologies
Russian Academy of Sciences
Moscow, Russian Federation

Venkata R. Kethineedi
Department of Chemistry
University of New Orleans
New Orleans, Louisiana

Charles K. Klutse
Ghana Atomic Energy Commission
Accra, Ghana

Yong-Eun Koo Lee
Department of Chemistry
Hanyang University
Seoul, Korea

Raoul Kopelman
Department of Chemistry
University of Michigan
Ann Arbor, Michigan

Suzanne J. Lassiter
Louisiana State University
Baton Rouge, Louisiana

B. Lauly
Department of Chemistry and Biochemistry
Miami University
Oxford, Ohio

Keith A. Laycock
Department of Neurosurgery
Saint Louis University
Saint Louis, Missouri

Kai Licha
Mivenion GmbH
and
Free University
Berlin, Germany

Steen J. Madsen
Department of Health Physics and Diagnostic Sciences
University of Nevada, Las Vegas
Las Vegas, Nevada

Ezra Maguen
Ophthalmology Research Laboratories
Cedars-Sinai Medical Center
and
Geffen School of Medicine
University of California, Los Angeles
Los Angeles, California

Daniel L. Marks
Beckman Institute for Advanced Science and Technology
University of Illinois at Urbana–Champaign
Urbana, Illinois

Anubhav N. Mathur
Department of Dermatology
Indiana University Medical School
Indianapolis, Indiana

Praveen N. Mathur
Department of Medicine
Indiana University Medical School
Indianapolis, Indiana

Timothy E. McKnight
Oak Ridge National Laboratory
Oak Ridge, Tennessee

Eric Monson
Art, Art History and Visual Studies
Duke University
Raleigh, North Carolina

Hoan Thanh Ngo
Department of Biomedical Engineering
and
Department of Chemistry
Duke University
Durham, North Carolina

Shuming Nie
Department of Biomedical Engineering
Georgia Institute of Technology
and
Emory University
Atlanta, Georgia

Stephen J. Norton
Department of Biomedical Engineering
Duke University
Durham, North Carolina

Bergein F. Overholt
Fort Sanders Regional Medical Center
Thompson Cancer Survival Center
Knoxville, Tennessee

Clyde V. Owens
Louisiana State University
Baton Rouge, Louisiana

Ravindra K. Pandey
Photodynamic Therapy Center
Roswell Park Cancer Institute
Buffalo, New York

Masoud Panjehpour
Fort Sanders Regional Medical Center
Thompson Cancer Survival Center
Knoxville, Tennessee

Martin A. Philbert
Department of Environmental Health Sciences
University of Michigan
Ann Arbor, Michigan

Ashley D. Quach
Department of Chemistry
University of New Orleans
New Orleans, Louisiana

Lou Reinisch
School of Arts and Sciences
Farmingdale State College
Farmingdale, New York

Zeev Rosenzweig
Department of Chemistry and Biochemistry
University of Maryland, Baltimore County
Baltimore, Maryland

Lynn E. Samuelson
Department of Cancer Biology
Vanderbilt University
Nashville, Tennessee

John P. Scaffidi
Department of Biomedical Engineering
Duke University
Durham, North Carolina

Steven A. Soper
Louisiana State University
Baton Rouge, Louisiana

Dimitra N. Stratis-Cullum
Electro-Optics and Photonics Division
US Army Research Laboratory
Adelphi, Maryland

Kittisak Suthamjariya
Faculty of Medicine
Mahidol University
Bangkok, Thailand

Weihong Tan
Department of Chemistry
and
Department of Physiology and Functional Genomics
University of Florida
Gainesville, Florida

and

Hunan University
Changsha, People's Republic of China

Matthew A. Tarr
Department of Chemistry
University of New Orleans
New Orleans, Louisiana

Haohua Tu
Beckman Institute for Advanced Science and Technology
University of Illinois at Urbana–Champaign
Urbana, Illinois

Pierre M. Viallet
Laboratory of Physicochemical Biology of Integrated Systems
University of Perpignan
Perpignan, France

Tuan Vo-Dinh
Department of Biomedical Engineering
and
Department of Chemistry
Duke University
Durham, North Carolina

Emanuel Waddell
Louisiana State University
Baton Rouge, Louisiana

Hsin-Neng Wang
Department of Biomedical Engineering
and
Department of Chemistry
Duke University
Durham, North Carolina

Kemin Wang
College of Biology
and
College of Chemistry and Chemical Engineering
Hunan University
Changsha, People's Republic of China

M. Wendy Williams (Retired)
Advanced Biomedical Science and Technology Group
Oak Ridge National Laboratory
Oak Ridge, Tennessee

Cuichen Wu
Department of Chemistry
and
Department of Physiology and Functional Genomics
University of Florida
Gainesville, Florida

Yichuan Xu
Louisiana State University
Baton Rouge, Louisiana

Chaoyong James Yang
Department of Chemical Biology
Xiamen University
Xiamen, People's Republic of China

Kenji Yasuda
Department of Biomedical Information
Tokyo Medical and Dental University
Tokyo, Japan

Hsiangkuo Yuan
Department of Biomedical Engineering
Duke University
Durham, North Carolina

Y. Zhang
Nanometrics Incorporated
Hillsboro, Oregon

I

Therapeutic and Interventional Techniques

1

Mechanistic Principles of Photodynamic Therapy

Barbara W. Henderson
Roswell Park Cancer Institute

Sandra O. Gollnick
Roswell Park Cancer Institute

1.1 Introduction

Photodynamic therapy (PDT) exploits the biological consequences of localized oxidative damage inflicted by photodynamic processes. A schematic outline of the major steps that lead to tumor destruction by PDT is given in Figure 1.1. Three critical elements are required for the initial photodynamic processes to occur: a drug that can be activated by a photosensitizer, light, and oxygen. Interaction of light at the appropriate wavelength with a photosensitizer produces an excited triplet state photosensitizer that can interact with ground state oxygen via two different pathways, designated as type I and type II. The individual steps of these pathways are shown in Figure 1.2. The type II reaction that gives rise to singlet oxygen ($^1O_2$) is believed to be the dominant pathway since the elimination of oxygen or scavenging of $^1O_2$ from the system essentially eliminates the cytocidal effects of PDT.[1–3] Type I reactions, however, may become important under hypoxic conditions or where photosensitizers are highly concentrated.[1] The highly reactive $^1O_2$ has a short lifetime (<0.04 μs) in the biological milieu and therefore a short radius of action (<0.02 μm).[4] Consequently, $^1O_2$-mediated oxidative damage will occur in the immediate vicinity of the subcellular site of photosensitizer localization. Depending on photosensitizer pharmacokinetics, these sites can be varied and numerous, resulting in a large and complex array of cellular effects. Similarly, on a tissue level, tumor cells as well as various normal cells can take up photosensitizer, which, upon activation by light, can lead to effects upon such targets as the tumor cells, the tumor and normal microvasculature, and the inflammatory and immune host system. PDT effects

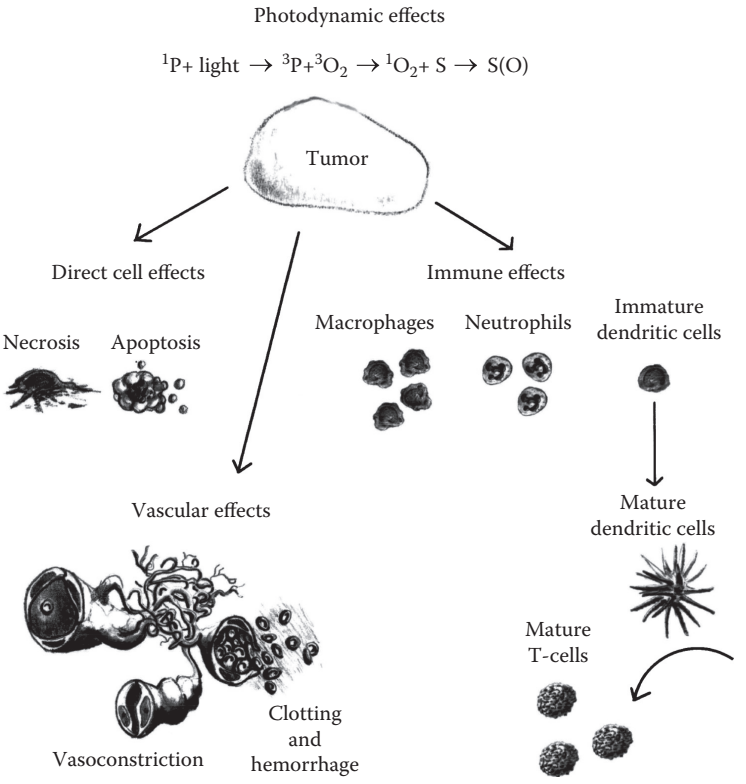

FIGURE 1.1 Illustration of the three major tissue targets affected by the photodynamic effect. Tumor cells can be damaged and/or killed directly by the effects of singlet oxygen generated within them, they can succumb to oxygen and nutrient deprivation due to vascular damage inflicted by PDT, or they can be attacked by the inflammatory/immune system activated by PDT.

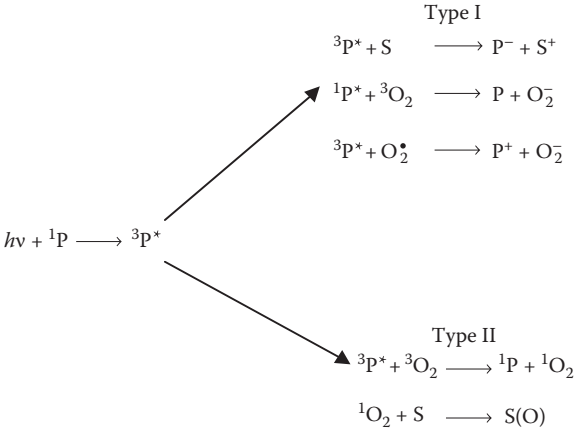

FIGURE 1.2 Photoreaction pathways emanating from the interaction of a photosensitizer with light where ^1P is a photosensitizer in a singlet ground state, $^3P^*$ is a photosensitizer in a triplet excited state, S is a substrate molecule, P^- is a reduced photosensitizer molecule, S^+ is an oxidized substrate molecule, $^3O_2$ is molecular oxygen (triplet ground state), O_2^- is the superoxide anion, $_1O_2^\bullet$ is the superoxide radical, P^+ is the oxidized photosensitizer, $^1O_2$ is oxygen in a singlet excited state, and S(O) is an oxygen adduct of a substrate. (Adapted from MacDonald, I.J. and Dougherty, T.J., *J. Porphyrins Phthalocyanines*, 5, 105, 2001. With permission.)

on all these targets may influence each other, producing a plethora of responses; the relative importance of each has yet to be fully defined. It seems clear, however, that the combination of all these components is required for long-term tumor control.

1.2 Subcellular Targets for Photosensitization

The potential cellular targets of PDT are shown schematically in Figure 1.3. They depend on the specific photosensitizer structure and pharmacokinetic characteristics, such as lipophilicity, amphiphilicity, aggregation, and serum protein interactions, and therefore the localization of the photosensitizer, but appear to be largely independent of cell type (Table 1.1). Localization studies have generally been carried out in in vitro cell systems where exposure conditions to the photosensitizer can be easily controlled or varied. Alternative drug uptake mechanisms determine cellular photosensitizer accumulation: Diffusion results in predominantly mitochondrial accumulation, while endocytosis of surface-bound agents leads to deposition in the endosomal/lysosomal compartments.[5] Studies have also revealed that cellular photosensitizer distribution can be a dynamic process, influenced by such parameters as length of exposure and drug concentration.[6–8] Photosensitizers may even relocalize after photodamage to an initial site of accumulation, such as from lysosomes to other, possibly more sensitive, cellular locations where they will then be available for activation.[9] That subcellular localization of a photosensitizer, and consequently the target of PDT, may influence in vivo treatment outcome was demonstrated in a series of studies that could relate structure and activity of a congeneric series of photosensitizing compounds to their subcellular localization (Figure 1.4).[10] Pyropheophorbide-a ether derivatives, designed to possess progressively increasing degrees of lipophilicity, exhibited drug uptake in tumor cells that increased linearly with lipophilicity, while PDT activity tested in an vivo murine tumor system showed a parabolic quantitative structure–activity relationship (QSAR). Comparison of the subcellular localization of the most and least active compounds in this series revealed mitochondrial localization for the former and lysosomal localization for the latter.

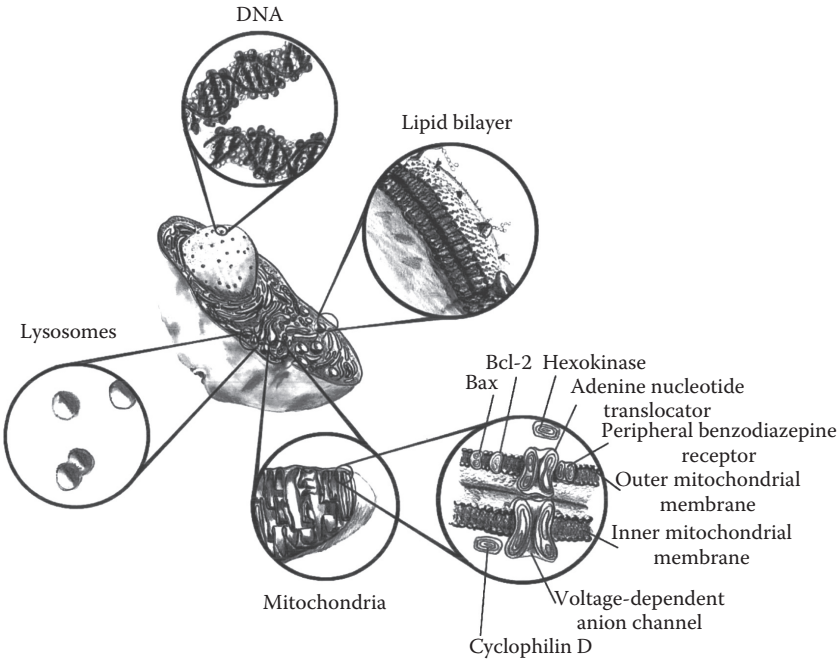

FIGURE 1.3 Illustration of the major cellular targets affected by PDT.

TABLE 1.1 Intracellular Localization Sites of Major Photosensitizers in Cells In Vitro

Photosensitizer	Cell Line	Localization Site	References
BPD-MA (Verteporfin®[a])	NHIK3025	ER/Golgi	[36]
Phthalocyanines	NHIK3025, RIF, LOX, V79	Lysosomes Cytoplasm	[23,226–228]
Hematoporphyrin/ Photofrin®	V79, L1210	Plasma membrane Mitochondria	[229,230]
Lutex	EMT6	Lysosomes	[231,232]
mTHPC	V79	Cytoplasm, diffuse	[233]
Npe_6 and analogs	CHO, L1210	Lysosomes Mitochondria Plasma membrane	[16,234,235]
PpIX from ALA	WiDr, NHIK3025, V79 FaDu, RIF	Mitochondria	[15,236]
Pyropheophorbide derivatives	FaDu, RIF	Mitochondria Lysosomes	[10]
TPPS analogs	NHIK3025	Lysosomes Mitochondria Perinuclear	[37,237–239]
Purpurin analogs $SnEt_2$	P388, OVCAR5	Lysosomes	[49]

[a] Registered trademark of QLT Inc., Vancouver, British Columbia, Canada.

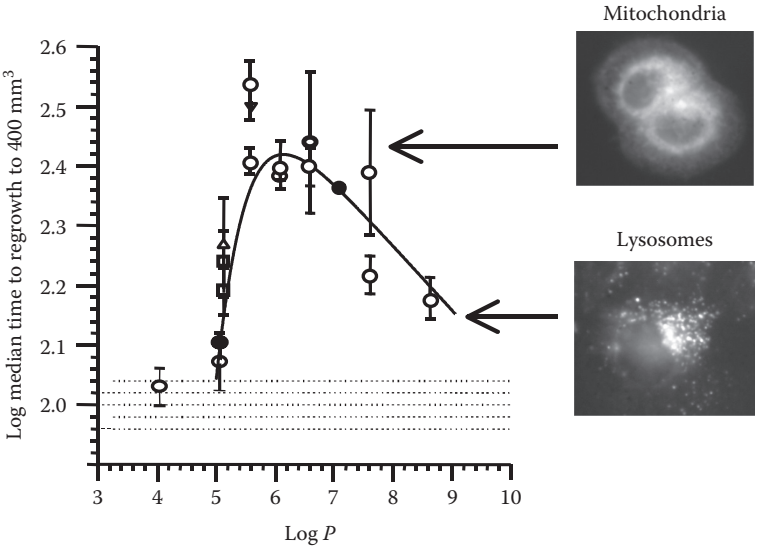

FIGURE 1.4 Relationship of the log median time of tumor regrowth to 400 mm^3 tumor volume to log *P* for a series of congeneric pyropheophorbide photosensitizers and to their subcellular distribution. Optimal compounds accumulate in mitochondria and suboptimal compounds in lysosomes. (Adapted from Henderson, B.W. et al., *Cancer Res*., 57, 4000, 1997. With permission.)

An important discovery was the realization that the adenosine triphosphate (ATPase)-dependent transporter ABCG2, a multidrug-resistant pump expressed to varying degrees in cancer cells and cancer stem cells, can bind and efflux certain photosensitizers, greatly affecting photosensitizer retention.[11,12] Substrates for ABCG2 include certain porphyrins, chlorins, and hypericin. Tyrosine kinase inhibitors, such as imatinib mesylate (Gleevec), can block ABCG2-mediated photosensitizer efflux and thus affect PDT efficacy for agents that are ABCG2 substrates.[5,13]

All cellular sites that accumulate photosensitizer can be effective targets for cell destruction. Mitochondria have long been known to be sensitive sites for PDT (also see Table 1.1).[14–17] Especially the mitochondrial permeability transition pore, a protein complex consisting of hexokinase, peripheral benzodiazepine receptor, voltage-dependent anion channel, creatine kinase, adenine nucleotide translocator (ANT), and cyclophilin D, has been implicated as PDT target.[18–21] PDT-induced rupture of lysosomes can lead to cell death through the release of damaging hydrolytic enzymes into the cytoplasm.[22] Selective lysosomal photodamage that was associated with the release of cathepsin B was found to be followed by a gradual loss of mitochondrial membrane potential, release of cytochrome c into the cytosol, caspase 3 activation, and a limited apoptotic response. Thus, lysosomal damage may secondarily mediate mitochondrial damage. It has also been suggested that lysosomes might serve as reservoirs, from which photosensitizers might be released after vesicle rupture and migrate to more sensitive sites.[23] All these studies assume that initial sensitizer accumulation is restricted to the lysosomes, but the possibility cannot be entirely excluded that high lysosomal concentration may mask small but highly effective sensitizer accumulations at other sites.[24]

When photosensitizers are confined to or specifically targeted to the plasma membrane, it can become a highly lethal PDT target.[25] Membrane damage manifests itself rapidly through blebbing,[26,27] as well as leakage of cytosolic enzymes[28,29] and chromium.[30] Leakage of lactate dehydrogenase showed the same kinetics as generation of prostaglandin E_2 from tumor cells in vitro, directly relating membrane disruption to production of eicosanoids.[29] The biosynthesis of eicosanoids, which play an important role in mediating the PDT tissue response (discussed in the succeeding texts), is set in motion when phospholipases catalyze the liberation of free fatty acids from membrane phospholipids. Unsaturated phospholipids and cholesterol are important membrane targets of photodamage, and lipid peroxidation by PDT has been extensively studied and linked with cell lethality.[31,32] Oxidation of intrinsic membrane proteins has also been observed.[33] PDT can inhibit the plasma membrane enzymes Na^+K^+-ATPase and Mg^{2+}-ATPase.[34] Ca^{2+} flux may be affected and the plasma membrane may become depolarized.[35] Certain membrane-localized photosensitizers, such as sulfonatedtetraphenylporphines (TPPS), can destroy microtubules in interphase cells and lead to arrest of cells in mitosis.[36,37]

While protein cross-linking has been reported by Moan and Vistnes in 1986,[38] it has taken on new emphasis with the discovery that cross-linking of the signal transducer and activator of transcription 3 (STAT3) correlates strongly with the strength of the local PDT reaction and thus can be used as a molecular reporter for that reaction in tissue, including in human biopsy samples collected immediately following PDT.[39]

Photosensitizers used in PDT generally do not accumulate in the cell nucleus, and therefore frank DNA damage such as strand breaks, sister chromatid exchanges, and chromatid aberrations are much less frequently observed in PDT than in ionizing or UV irradiation.[40–42] Consistent with these findings, the mutation potential of PDT was found to be significantly less than that of ionizing radiation or UV.[43]

1.3 Pathways to Cell Death and Survival

Three cell death pathways can be induced by PDT—apoptotic, autophagic, and necrotic (reviewed in Ref. 44). The apoptotic pathway is an intrinsic physiological process that is dependent upon active cellular metabolism and is characterized by chromatin condensation, DNA fragmentation, and the formation of apoptotic bodies.[45] Autophagy is a lysosomal pathway of self-degradation of damaged cellular proteins and organelles, including those damaged by oxidative stress insults.[46–48] (Macro) autophagy, found to be relevant in PDT, is marked by the formation of double-membrane vesicles that sequester and transport materials from the cytoplasm to the lysosomal system.[44,47,48] Necrosis is mainly metabolism independent and a result of a massive insult, especially to the plasma membrane, characterized by vacuolization of the cytoplasm, swelling, and breakdown of the plasma membrane.[44] Recent evidence suggests that under certain circumstances necrosis may be actively induced through signaling pathways.[44] The dominant mode of cell death is dependent upon the photosensitizer used, the localization of the photosensitizer, and the treatment protocol. Studies by

Kessel and Luo[16] demonstrated that photosensitizers that localize to the mitochondria resulted in apoptotic cell death while those that localize to the lysosome or cell membrane did not. Kessel et al. also demonstrated that photodamage of the cell membrane can inhibit the induction of apoptosis by photodamage to the mitochondria and that the mode of cell death shifts in response to the photodynamic dose, such that high doses result in a necrotic cell death, while lower doses result in an apoptotic mode of death.[49,50]

The rapid induction of apoptosis suggests that PDT triggers late-stage apoptotic processes directly. Release of cytochrome c from the mitochondria triggers caspase 3 activation and results in initiation of apoptosis at a late stage in the pathway.[51] Cytochrome c release is associated with a loss of mitochondrial potential. PDT results in the loss of mitochondrial potential and the rapid release of cytochrome.[52–55] Several studies have demonstrated that PDT also induces rapid activation of caspases 3, 6, 7, and 8 and cleavage of poly(ADP-ribose) polymerase (PARP).[52,56] Kessel and Luo have shown that PDT-induced release of cytochrome c is sufficient to directly initiate a caspase-dependent apoptotic cell death.[57] However, while caspase 3 is required for the late stages of apoptosis, it is not the critical lethal event in PDT-induced apoptosis.[58]

Bcl-2, the antiapoptotic member of the Bcl-2 family, has been shown to block the release of cytochrome c from the mitochondria and thus prevent apoptosis.[51] Several groups have altered the expression of bcl-2, through overexpression or antisense technology, and demonstrated that increasing the levels of bcl-2 enhances cellular resistance to PDT-induced apoptotic cell death.[59–61] Xue et al. have demonstrated that bcl-2 is a target for photochemical destruction.[62,63] Interestingly, a study by Kim et al.[63] reported that overexpression of bcl-2 enhanced the apoptotic response. In these studies, overexpression of bcl-2 was accompanied by an increase in bax, a proapoptotic member of the bcl-2 family. PDT resulted in the selective destruction of bcl-2 but had no effect on bax. The greater apoptotic response in the cells overexpressing bcl-2 was attributed to a higher bax–bcl-2 ratio after PDT. A PDT-induced shift in the bax–bcl-2 ratio toward apoptosis has also been reported by others.[59,64]

PDT also affects other proteins implicated in apoptosis. Phospholipases C and A_2, which are involved in the transient increases in intracellular calcium levels and DNA fragmentation, are activated by Photofrin® PDT.[65] Ceramide, which has been linked to apoptosis in several malignant cell lines, accumulates following PDT and has been associated with PDT-induced apoptosis and cytotoxicity.[66] Gupta et al.[67] have demonstrated that Pc 4-PDT induces expression of nitric oxide and have suggested that it may be involved in PDT-induced apoptosis.

Autophagy was first recognized by Kessel and Arroyo[68] as a prominent PDT-induced cell death pathway that occurs in many normal and transformed cell types and that can precede, concur with, or follow the development of apoptosis.[47] Autophagy can contribute to cell survival through sequestration and removal of damaged cellular material but may also have a role in stress-induced cell death.[48] Moreover, extensive cross talk between apoptosis and autophagy exists as they share the same stimuli and similar effectors and regulators.[48] Thus, in apoptosis-deficient cells, such as cells without Bcl-2, autophagy was increased,[68] while overexpression of Bcl-2 only stimulated apoptosis without affecting autophagy.[69] Conversely, silencing of essential autophagy genes, such as *Atg5* and *Atg7*, promotes apoptotic photokilling.[48]

Numerous other signaling pathways are engaged in the cellular response to PDT that can either promote cell death or survival and proliferation. Foremost among these is the stress MAPK pathway, with the activation of JNK and p38 the most consistently observed immediate reaction to PDT.[70–74] PDT has been shown to stimulate stress kinase signaling pathways (SAPK/JNK, p38/HOG1)[70,75] and HS1 phosphorylation[76] as well as stress response transcriptional activators. Hypoxia-inducible factor-1 (HIF-1) is a key regulator of the cellular response to hypoxia and is induced in response to PDT.[77,78] PDT also enhanced the expression of the HIF-1 target gene, vascular endothelial growth factor (VEGF),[78] and it has been proposed that HIF-1 expression may act as a predictor of PDT responsiveness.[77] Finally, PDT also activates the heat shock protein (HSP) family promoters[79] and induces

the expression of HSPs and the related glucose-regulated proteins,[80–84] as well as heme oxygenase (HSP 32).[84]

PDT has been shown to alter the expression of the redox-regulated transcription factor, AP-1.[85,86] AP-1 is induced by changes in the redox potential[87] and hypoxia.[88] It is composed of homodimers of the products of the c-jun gene family or heterodimeric combinations of c-jun and c-fos family members. PDT induces prolonged expression of both c-fos and c-jun as a result of oxidative stress.[89,90] Therefore, modulation of AP-1 activity by PDT might be mediated by changes in oxidative potential as a result of the generation of singlet oxygen or PDT-induced hypoxia.

NF-κB plays a critical role in the expression of immunomodulatory and proinflammatory genes.[91] Activated NF-κB is a heterodimeric protein most commonly comprised of the p50 and p65 (Rel A) species and is activated in response to cellular oxidative stress.[92] NF-κB is sequestered in the cytoplasm by IκB proteins; phosphorylation of IκB results in its proteasomal degradation and release of NF-κB.[93,94] NF-κB binding activity was found to be induced by PDT[95–97] and has been proposed to play a role in determining the cellular response to PDT.[98] Granville et al.[95] demonstrated that cellular levels of IκB were transiently depressed following Verteporfin® PDT. Pyropheophorbide-a methyl ester PDT also leads to IκB degradation.[97] In contrast to these studies, other groups have failed to demonstrate NF-κB activation following Photofrin PDT.[85,86] Thus, NF-κB activation may be photosensitizer specific. It has also been suggested that activation is related to PDT dose in that higher doses do not result in decreases in IκB.[95]

1.4 Tissue Targets of Photosensitization

1.4.1 Tumor Cells

The capacity of PDT to eliminate tumor cells through direct photodamage has been most effectively studied by in vivo–in vitro tumor explant methodology.[99] Such in-depth analysis has revealed that the full potential of direct photodynamic tumor cell kill, provided by the gross tumor photosensitizer concentration and absorbed light dose, is generally not realized by in vivo PDT treatment.[100] Clonogenic assays carried out with a number of different photosensitizers and tumor systems immediately after potentially curative PDT exposures in vivo have revealed that at most 1–2 logs of direct tumor cell kill have been achieved,[101–106] far less than the 7–8 logs required for tumor cure. Clearly, limitations to direct tumor cell kill exist in vivo, the most important of which may be (1) inhomogeneous photosensitizer distribution within the tumor, including a gradual decrease of photosensitizer concentration with distance from blood vessels,[107] (2) insufficient light penetration through the tissue (light is attenuated exponentially with depth of tissue penetration),[108,109] and (3) insufficient oxygen availability (discussed in the following under separate heading). That intrinsic tumor cell sensitivity contributes to the overall PDT response was suggested by studies using tumor cells selected to be resistant to PDT.[110] Tumors of resistant phenotype were less responsive to PDT than sensitive tumors while exhibiting equal vascular responses. The studies did not exclude the possibility, however, that tumor immunogenicity might have differed in the two tumor lines, thus affecting the response. On the other hand, tumors expressing a multidrug resistance phenotype that prevented the uptake of a cationic photosensitizer were nevertheless found responsive to PDT carried out with that agent, the antitumor effect being attributed to vascular disruption.[111] Studies like these illustrate the capacity of PDT to exert its antitumor action through several different tissue targets.

Initial studies trying to establish a pattern of selectivity of photosensitizer uptake in malignant versus normal cells in vitro were largely unsuccessful.[112] Recent studies employing a coculture system of primary human lung epithelial tumor cells and corresponding stromal fibroblasts revealed cell-type-specific retention of the pyropheophorbide-a derivative hexyl pyropheophorbide ether (HPPH), which was both independent and dependent on the ABCG2 transporter and could be exploited for highly

selective killing of either tumor cells or fibroblasts.[5] In vivo, moderately favorable tumor to normal tissue ratios can be found for almost all photosensitizers, with establishment of these ratios depending on the specific pharmacokinetics of the compound as well as the pathophysiology of the tumor (for detailed reviews, see Refs. 113,114). Mechanisms invoked for this *selectivity* range from leaky vasculature and impaired lymphatic drainage in tumors to low tumor pH and an increase in low-density lipoprotein and/or other membrane receptors on tumor cells.[115,116] Carrier systems, such as antibody conjugates, have been designed to direct the photosensitizer directly to the tumor cells. Such immunoconjugates have been directed against epitopes on ovarian[117] and colon cancer cells[118] as well as against the epidermal growth factor receptor (EGFR) that is overexpressed in many cancers.[119]

1.4.2 Microvasculature

The microvasculature was one of the earliest tissue targets identified because vascular PDT effects are rapid and dramatic, especially with the use of the sensitizer Photofrin and its forerunners. Reduction and/or cessation of tumor microcirculation following in vivo PDT exposure employing a variety of photosensitizers has been demonstrated in preclinical models through numerous different techniques, summarized in Table 1.2. Since the kinetics of vascular shutdown and tumor cell death have been found to coincide[102,120] and inhibition of shutdown retards tumor response,[121] it has been argued that disruption of the tumor microcirculation is a major factor contributing to tumor control by PDT. Differences in response between tumor and normal microvasculature are subtle and difficult to discern.[122] Careful dose-ranging studies have revealed that the tumor vasculature is slightly more susceptible to shutdown than its normal counterpart.[123,124] It has also been demonstrated that Photofrin PDT at high fluence rate can protect the normal skin microvasculature, but the same treatment fails to protect tumor vessels.[106,125] Occlusion of the tumor-surrounding vasculature can contribute to tumor control, at least in preclinical models, presumably by adding to the nutrient deprivation and retardation of vascular resupply of the tumor.[123,126] Another approach toward retardation of vessel regrowth after PDT is the use of anti-angiogenic agents in combination with PDT, which has been shown to enhance long-term tumor control.[78,127]

The acute manifestations of PDT-induced vascular damage greatly depend on the type and dose of photosensitizer used. On the microscopic level, vascular changes in a rat cremaster muscle preparation after Photofrin PDT included vessel constriction; occlusive platelet thrombi in arteries, arterioles, vein, and venules; edema; and neutrophil margination and migration.[128,129] Ultrastructural features included damage to numerous endothelial cell organelles, as well as perivascular changes such as degranulation of perivascular mast cells and damage to myocytes.[128] Npe6 (mono-L-aspartyl chlorin e6) PDT in a rat chondrosarcoma model resulted in obstructive platelet thrombi but no vasoconstriction.[130] PDT with variously substituted zinc Pcs, tested in the same tumor model, showed a spectrum of effects, including vessel constriction and leakage, with one compound (disulfonated zinc Pc) exhibiting no apparent effects.[131] In preclinical studies, PDT-induced vascular leakage has been exploited to enhance the uptake in tumors of the liposomally formulated chemotherapeutic agent doxorubicin.[132]

Numerous vascular response mediators seem to be involved in these processes, summarized in Table 1.3. Most studied and prominent among them are the eicosanoids. They are products of the release from the cell membrane of arachidonic acid that is subsequently metabolized by cyclooxygenase to generate prostaglandins and thromboxanes and by lipoxygenase to form leukotrienes and hydroxy acids. The generation of a wide spectrum of arachidonic acid metabolites by PDT has been described in mast cells, macrophages, endothelial cells, platelets, and tumor cells, as well as in animals. Interestingly, in vitro PDT exposure of platelets blocks their capacity to aggregate[133,134] and in vitro exposure of endothelial cells is dominated by the release of prostacyclin (PGI_2) that inhibits platelet aggregation.[134] These in vitro findings contradict the well-established, proaggregating mechanisms observed in vivo and demonstrate the difficulty of translating in vitro data to the

TABLE 1.2 Tumor Perfusion and Oxygenation Following PDT

Photosensitizer	Tumor Model	Technique	References
Hematoporphyrin derivative	RMA rat mammary tumor	Window chamber observation	[240]
Photofrin®	Cremaster muscle, rat	Window chamber observation	[129]
Phthalocyanine analogs	Chondrosarcoma, rat	Window chamber observation	[131]
Npe6	Chondrosarcoma, rat	Window chamber observation	[130]
Photofrin	RIF-1 mouse fibrosarcoma	Radiobiological assay	[241]
Hematoporphyrin derivative	AY-27 rat urothelial tumor	^{103}Ru, ^{141}Ca	[242]
Photofrin	RIF-1 mouse fibrosarcoma	^{86}Rb extraction Hoechst 33342	[243]
Polyhematoporphyrin ALA	$LSBD_1$ rat fibrosarcoma	Microspheres ^{86}Rb extraction	[244]
HpD	T50 80 mouse mammary tumor	NMR imaging	[245]
Photofrin	R3230A rat mammary tumor	NMR imaging	[246]
Bacteriochlorophyll–serine	M2R melanotic melanoma xenograft	Contrast-enhanced MRI	[247]
Photofrin	Chondrosarcoma, rat	Oxygen microelectrode	[248]
Photofrin	VX-2 rabbit skin carcinoma	Transcutaneous oxygen electrodes	[149]
Photofrin	Mammary carcinoma, mouse	Oxygen microelectrode	[150]
Photofrin	RIF-1 mouse fibrosarcoma	Oxygen microelectrode, ^{86}Rb extraction, fluorescein	[125]
Photofrin	A673 sarcoma, human xenograft	Laser Doppler	[136]
Photofrin	RIF-1 mouse fibrosarcoma	Hypoxia marker	[157]
HPPH	Colo-26 mouse colon carcinoma	Fluorescent microspheres	[132]
HPPH	Ward rat colon carcinoma	MRI	[169]

TABLE 1.3 Vascular Response Mediators Generated/Affected by PDT

Photosensitizer	Cell/Tumor Type	Mediator	References
Hematoporphyrin derivative	Mast cells, rat	Histamine	[249]
Protoporphyrin	Mast cells, rat	PGD_2, PGE_2, PGI_2	[250]
Hematoporphyrin	Platelets, human	Serotonin	[251]
Phthalocyanine (ClAl-S)	Endothelial cells, bovine	Clotting factors	[252]
Photofrin®	Endothelial cells, human	Von Willebrand factor	[253]
Photofrin	EMT6 mammary tumor, mouse; RIF fibrosarcoma, mouse	PGE_2	[29]
Photofrin	Macrophages, mouse	PGE_2	[29]
Photofrin Phthalocyanine (ZnS)	Endothelial cells, bovine; human	PGI_2, AA, $F_2\alpha$, HETES	[134]
Photofrin	Mouse serum	Thromboxane B_2	[135]

in vivo situation. The latter represents a much more complex interplay of mechanistic components that likely involves platelets, endothelial cells, leukocytes, macrophages, and other stromal cells. Thromboxane appears to play a major role in mediating the observed vascular effects, at least in rat models.[135] Anti-inflammatory drugs, such as indomethacin or aspirin, can block the release of eicosanoids in vitro[29,134] and in vivo.[131,135–137] Rats made thrombocytopenic and thus deprived of a source for thromboxane generation also show a diminished vascular response.[138] Eicosanoids, as well as serotonin, appear to also be involved in changes of tumor interstitial pressure observed after Photofrin PDT, a consequence of fluid leakage from the vasculature and possibly contributing to occlusion of the tumor microvasculature.[139]

1.5 Tumor Oxygenation and PDT

Any restriction of tissue oxygen supply *during* PDT light delivery will reduce $^1O_2$ production and therefore have negative consequences for treatment outcome. Such restrictions can arise from numerous sources, including preexisting tumor hypoxia, acute vascular damage, and photochemical oxygen depletion. All of these can interact, and the dynamics of these interactions may determine treatment success.

1.5.1 Preexisting Tumor Hypoxia

Preexisting tumor hypoxia, a therapeutic problem still grappled with by radiation oncologists because of the oxygen dependence of sparsely ionizing radiation treatment, may limit the oxygen supply for PDT as well. Solid tumors are prone to develop hypoxic tumor regions due to deteriorating diffusion geometry, structural abnormalities of tumor microvessels, and disturbed microcirculation.[140] Hypoxic, but viable, tumor cells located in these areas may be protected from PDT-induced photodamage. In a preclinical study, Fingar et al.[141] manipulated tumors pharmacologically and physically to induce a wide range of hypoxic tumor fractions (~2% to ~40%) and followed this by aggressive Photofrin PDT. It was found that hypoxic fractions below 5% did not adversely affect tumor control, hypoxic fractions of ~10% slightly diminished tumor control, and hypoxic fractions of ~40% totally blocked tumor control. Vascular shutdown and nutrient deprivation following PDT were believed to be responsible for the elimination of small numbers of initially surviving hypoxic tumor cells. Early preclinical attempts to raise tumor oxygenation prior to PDT through the administration of a perfluorochemical emulsion and carbogen breathing were highly successful in increasing tumor oxygen levels (~10-fold) up to 1 h after PDT. The intervention did not alter long-term tumor control,[142] probably because the vascular damage induced by the aggressive PDT regime overwhelmed any subtle improvement in treatment outcome that might have been attributed to increased tumor oxygenation. Other studies, both preclinical and clinical, have demonstrated significantly improved PDT efficiency with adjuvant administration of hyperbaric oxygen or carbogen.[143–145]

The factor, however, that probably influences preexisting tumor hypoxia most profoundly is one that accompanies most PDT treatments, namely, changes in tumor temperature. Temperature increases due to PDT light delivery have been analyzed by Svaasand et al.[146] and have been recorded in preclinical models[147] and in patient's tumors.[148] Measurements of baseline intratumoral temperature and pO_2 in nodular basal cell carcinomas have demonstrated a linear relationship between increasing tumor pO_2 and lesion temperature in the ranges between 0–20 mm Hg and 30°C–35°C.[156] Upon laser illumination during Photofrin PDT, the temperature in these lesions increased further in a fluence rate–dependent manner. Surprisingly, even low fluence rate light produced significant temperature rises (150 mW/cm^2, median temperature change +1.9°C [range 1.0–6.2]; 30 mW/cm^2, median temperature change +1.5°C [range –1.3–3.6]), and these correlated with increased tumor pO_2. It remains to be seen whether these relationships hold true for tumors other than skin tumors.

1.5.2 Oxygen Limitation through Vascular Damage

With photosensitizers that can acutely constrict and/or occlude vessels, blood flow obstruction can be marked, very rapidly limiting the oxygen supply to the tumor. Photofrin PDT in mouse models, for example, rendered up to 10% of tumor cells hypoxic within a very moderate light exposure (45 J/cm^2, 10 min).[10] This hypoxia was persistent and progressive with time, 50% of tumor cells being hypoxic within 1 h of such light exposure. Similar observations were reported for a rabbit skin tumor model, where a series of brief light exposures resulted in induction of irreversible tumor hypoxia that was cumulative with the number of exposures, that is, fluence.[149] Hypoxia induction by PDT depends greatly on the vascular supply of a given tumor and even on the site of tumor implantation in rodent models.[150] Transient reoxygenation may occur, depending on PDT dose.[150] With certain second-generation sensitizers, many of which exert less severe acute effects on the vasculature than Photofrin,[131] and a tendency toward the use of lower drug doses, such acute vascular effects are less likely to occur. As discussed earlier, the extent and timing of vascular damage, and therefore induction of tumor hypoxia, is of significant importance for treatment outcome. Vascular occlusion can be detrimental when occurring *during* treatment but beneficial when occurring *after* completion of the PDT tumor treatment.

1.5.3 Oxygen Limitation through Photochemical Oxygen Depletion

Photochemical oxygen depletion is roughly characterized by instantaneous or near instantaneous development of tumor hypoxia upon light exposure of a photosensitized tumor/tissue and equally rapid reoxygenation upon cessation of light. The theoretical basis for this phenomenon has been provided through mathematical modeling of the dynamic changes to be expected in tissue when oxygen is consumed in the process of $^1O_2$ generation.[151] Photochemical oxygen depletion will occur in tissue if the rate of photodynamic oxygen consumption is faster than the rate of oxygen resupply from the vasculature. The major parameters that determine whether or not photochemical oxygen depletion will occur are (1) the absorption coefficient of the photosensitizer, (2) the tissue concentration of the photosensitizer, (3) the fluence rate of light, and (4) the vascular supply of the tissue.[151–153] If the first three parameters are high, $^1O_2$ production will be rapid and oxygen depletion will be favored; if the vascular supply of the tissue is poor, oxygen depletion will also be favored. The mathematical predictions have been validated in tightly defined in vitro systems[154,155] in tumor models[125,149,156,157] and in humans.[148] Light fluence rate is the most easily controlled parameter, one that can be readily modulated during light delivery. Therefore, much attention has been paid to the effects of fluence rate on PDT oxygen consumption. It is clear that lowering of the fluence rate can diminish or eliminate photochemical oxygen consumption through lowering the $^1O_2$ generation rate. However, the optimal fluence rate will depend on the other parameters listed earlier and therefore vary from situation to situation. In human tumors, the variability is great, both among patients and among lesions in the same patient.[148]

1.5.4 Role of Photobleaching in Photochemical Oxygen Depletion

Photobleaching is the destruction of the photosensitizer by light-mediated processes.[158–161] Since photosensitizer concentration is one of the major determinants for photochemical oxygen depletion, it stands to reason that the destruction of photosensitizer through photobleaching during PDT will reduce the likelihood that oxygen depletion will occur. The most detailed studies of photobleaching have been carried out in an in vitro multicell tumor spheroid model.[162] It was shown that sustained illumination of Photofrin-photosensitized spheroids led to a progressive decrease of photochemical oxygen depletion, implying reduction of photosensitizer levels, and consistent with a theoretical model in which bleaching occurs via a self-sensitized singlet oxygen reaction with the photosensitizer ground state. Similarly, protoporphyrin IX (PpIX) was degraded by $^1O_2$-mediated mechanisms, while another photosensitizer (Nile blue selenium) was degraded by $^1O_2$-independent mechanisms.[163] Oxygen measurements in rodent

tumor models and human basal cell carcinomas also implicated photobleaching in influencing photochemical oxygen depletion.[125,148] In these studies, significant oxygen depletion was observed during the early time periods of illumination at high fluence rates of Photofrin-photosensitized lesions, but less or no oxygen depletion was detected toward the end of illumination, implying that the Photofrin concentration had been reduced through photobleaching below the threshold needed for oxygen depletion. Noninvasive devices have been developed that can monitor photobleaching in patients during PDT light delivery, allowing correlation of photobleaching kinetics and hemodynamic responses.[164]

1.5.5 Enhancement of PDT Efficiency through Modified Light Delivery Schemes

It is evident that any means by which the well-oxygenated tumor volume can be increased during light exposure should have beneficial effects on treatment outcome. Downward adjustment of treatment fluence rate is one such means, and fractionation of light delivery is another.[125,165–167] While the former allows for continuous maintenance of oxygen levels sufficient for $^1O_2$ production, the latter facilitates reoxygenation of the tissue between light exposures. Significant enhancements of tumor response have been observed with either of these alternatives for PDT with Photofrin, 5-aminolevulinic acid (ALA)/PpIX, and meso-tetra-hydroxyphenyl-chlorin (mTHPC). In part, this may be due to a significant but moderate increase in direct photodamage to tumor cells. Direct tumor cell death increased with low fluence rate PDT by ~1/2–1 log in the RIF mouse model.[168] However, the microvasculature, especially the normal, tumor-surrounding microvasculature, can also be affected by modification of fluence rate.[106] One practical drawback of low fluence rate treatment, as compared to high fluence rate, is the increase in exposure time required to deliver a given fluence. Due to the higher treatment efficiency, this can be somewhat, but not entirely, compensated for by a reduction of the total fluence delivered. In fact, a reduction of the total fluence may be necessary with low fluence rate treatment since the PDT efficiency for causing vascular and normal tissue effects will also increase, thus decreasing treatment selectivity.[106,167,169]

Enhanced responses to light dose fractionation in ALA PDT of murine tumors and normal rat colon may involve relocalization and/or resupply of PpIX during dark periods, in addition to reoxygenation.[170,171]

A two-step irradiance protocol has recently been developed for ALA PDT of nonmelanoma skin cancers that minimizes the severe pain experienced by patients during PDT light delivery.[172,173] It involves an initial short period of illumination at low fluence rate to photobleach 80%–90% of PpIX, followed by high fluence rate for the remainder of the total prescribed fluence. This approach achieves alleviation of pain and excellent results while only minimally prolonging the treatment time.

1.6 Immune Effects of PDT

1.6.1 Immune Suppression

Immune suppressive effects are largely confined to cutaneous and transdermal PDT. Cutaneous PDT can suppress allograft rejection[174–177] and contact hypersensitivity (CHS) reactions.[178–182] The mechanism of PDT-induced immune suppression appears to be associated with the induction of immunosuppressive cytokines. PDT induces tumor necrosis factor (TNF)-α,[183,184] which is involved in some aspects of UV-mediated immunosuppression.[185] However, it is not responsible for PDT-induced CHS suppression.[183] PDT also induces interleukin (IL)-10,[178,186,187] which has been shown to inhibit cell-mediated immune responses, including CHS.[186,188] Gollnick et al. have shown that in vitro PDT induces IL-10 expression from keratinocytes as a result of activation of the IL-10 gene promoter by enhanced expression of AP-1 and prolonged IL-10 mRNA half-life.[86] Direct mechanistic studies of the role of IL-10 in PDT-induced suppression of CHS have yielded contradictory results that can be explained, at least

in part, by the treatment regime and dose of PDT. Treatment with cutaneous PDT, using Photofrin and blue light centered at 430 nm, results in irradiation that is mostly limited to the skin. In contrast, transdermal PDT, with benzoporphyrin derivative monoacid ring A (BPD-MA) and illumination with 690 nm light, involves whole body illumination. Also, due to the greater depth of light penetration of this wavelength, some light exposure of internal sites may occur. Simkin et al.[186] implicated IL-10 as the active mediator in transdermal PDT-induced suppression of CHS by demonstrating that IL-10 knockout (KO) mice did not undergo transdermal PDT-induced CHS suppression. In contrast, cutaneous PDT treatment of IL-10 KO mice did induce CHS suppression.[178] The lack of involvement of IL-10 in suppression of CHS by cutaneous PDT was further confirmed when studies using neutralizing anti-IL-10 antibodies failed to inhibit cutaneous PDT-induced CHS suppression.[178,182] Thus, it appears as though the mechanism of PDT-induced suppression of CHS is dependent upon the treatment regime. Regimes that result in large treatment fields and internal exposure, that is, transdermal and potentially peritoneal PDT, mediate CHS suppression via IL-10. PDT regimes that employ lower doses and superficial cutaneous exposure suppress CHS reactions via an IL-10-independent mechanism.

Interestingly, CHS suppression by both transdermal and cutaneous PDT was reversed by administration of exogenous IL-12,[178,186] suggesting that these processes share a common regulatory point, perhaps in the development of Th1 and/or Tc1 cells.

In addition to the effects of cytokines on PDT-induced suppression of immune responses, it is important to consider the effect of PDT on the expression of immune molecules critical to immune system activation. Transdermal PDT has been shown to inhibit the ability of Langerhans cells (LC) to stimulate alloreactive T cells, and LC treated ex vivo expressed lower levels of major histocompatibility complex (MHC) antigens and CD80 and CD86 costimulatory molecules, which are needed for T cell activation.[189] Additionally, in vitro PDT-treated murine dendritic cells (DC) had a reduced ability to stimulate alloreactive T cells and exhibited lower levels of MHC molecules, costimulatory molecules, and adhesion molecules.[190] Thus, in addition to altering the function of antigen presenting cells (APCs), PDT has the ability to disrupt the APC–T cell cognate, which is needed for T cell activation.

Immune suppression has also been reported following topical PDT in humans.[191] In this study, both MAL PDT and ALA PDT significantly suppressed delayed-type hypersensitivity responses. In a follow-up study, Frost et al.[192] showed that the degree of immune suppression was decreased when low flounce rates were used to deliver equivalent light doses. These findings support the hypothesis that the immune effects of PDT are highly dependent upon the treatment regimen employed.

1.6.2 Immune Potentiation

Tumor-directed PDT represents a confined sterile injury that leads to a local inflammatory reaction, the latter usually being the first sign of the PDT tissue response.

The initiation of the inflammatory process has been ascribed to alarmins, molecules that preexist in cells and are released upon cell dissociation.[193] They include damage-associated molecular pattern molecules (DAMPs), cytokines, and metabolites. Several abundant cellular proteins serve as DAMPs, such as HSPs, peroxiredoxin-1, S100 proteins, and high-mobility group protein B1 (HMGB1).[193–196] In addition, intracellular cytokines, released from dying cells, can commence signaling functions via their receptors on neighboring cells. A recent study in a coculture system of primary human epithelial tumor cells and their stromal fibroblast counterparts has identified IL-1α, released from PDT exposed tumor cells, as the major alarmin activating fibroblasts to generate inflammatory mediators such as IL-6.[25]

The first manifestation of the inflammatory response is a rapid influx of neutrophils, which appear to be critical to long-term tumor control.[197–200] The influx of neutrophils into the treatment site is preceded by an induction of chemokines and adhesion molecules critical to neutrophil migrations, and blocking their function retards the PDT response.[200] Neutrophilic infiltration is followed by mast cells and macrophages.[187,201] The PDT regimen can strongly influence the inflammatory response—high PDT doses, while locally curative through mainly vascular mechanisms, suppress inflammation, while

oxygen-conserving, low PDT doses enhance it.[202,203] A treatment protocol is currently being developed that combines the two PDT approaches, first inducing the inflammatory reaction to maximize stimulation of the adaptive antitumor immune response, followed by the locally curative treatment (Gollnick, unpublished data).

PDT enhances macrophage tumoricidal activity[204,205] and stimulates macrophage release of TNF-α.[89] It has been suggested that nonspecific killing of tumor cells by inflammatory cells, potentially through the release of reactive oxygen species, contributes to the overall tumor kill by PDT.[201] This hypothesis is supported by studies showing that if the PDT-induced inflammatory response is further stimulated by addition of adjuvants or macrophage activating factors, the overall tumor response to PDT is greater.[206–208] The role of the innate immune response in overall tumor kill by PDT was also shown to involve natural killer (NK) cells. Depletion of NK cells reduced the long-term tumor control by PDT[209] and augmentation of NK activity enhanced PDT tumor control.[210] The ability of cytolytic T lymphocytes (CTLs) and NK cells to destroy tumor cells depends on their recognition of MHC class 1 and MHC class 1–related molecules. PDT induced the MHC class 1–related molecules MICA and increased expression of NKG2DL in human tumor cells and increased their lysis by NK cells.[211]

A plethora of important immune modulators is generated via activation of stress response factors such as AP-1 and NF-κB,[85,89,187] including IL-6, TNF-α, IL-1β, IL-2, and granulocyte macrophage colony-stimulating factor (GM-CSF).[183,184,187,212,213] The role played by IL-6 has been unclear, but a recent study showed that the elimination of IL-6 had no effect on innate cell mobilization into the tumor bed and did not affect primary antitumor T cell activation but did negatively regulate antitumor immune memory.[214]

Taken together, PDT creates a tumor milieu that is conducive to the antitumor immune modulation[215] that has been documented in both preclinical and clinical studies. Tumor draining lymph node cells isolated from PDT-treated mice are able to suppress subsequent tumor challenges when transferred to a naïve host.[216,217] Canti et al.[217] have shown that PDT-treated mice that remain tumor free for 100 days post-PDT are resistant to subsequent tumor challenges, suggesting the presence of immune memory cells. The importance of the immune response in PDT was definitively shown by a series of experiments in severe combined immunodeficient (SCID) and nude mice.[197,209] PDT treatment, at a dose that was curative in immunocompetent BALB/c mice, provided only short-term cures of EMT6 tumors in SCID and nude mice. The ability to provide long-term cures was restored when immunodeficient animals were reconstituted with bone marrow cells from BALB/c mice. Depletion studies showed that the critical cells involved in the PDT-induced immune response were $CD8^+$ cells, with NK cells playing a supportive role.[205,218] Clinical studies have demonstrated an infiltration of $CD8^+$ cells into PDT-treated tumor tissue.[219,220] Kabingu et al.[221] demonstrated in basal cell carcinoma patients that ALA PDT enhanced recognition of MHC-1–antigen complexes by immune cells and activation of tumor-specific $CD8^+$ cells. As in the inflammatory response,[202,203] PDT treatment parameters (fluence rate, fluence) influence the adaptive antitumor immune response.[218,220]

The knowledge gained by these preclinical and clinical studies has raised the hope and possibility that the benefit of PDT, so far restricted to local tumor treatment, might be expanded to attack distant disease. To support this goal, effective antitumor vaccines have been generated by in vitro PDT treatment of tumor cells, which are able to stimulate the maturation and activation of DC as well as activation of tumor-specific $CD8^+$ T cells.[222–225]

1.7 Conclusion

The scientific effort that supports this new cancer therapy has led to numerous significant advances. The development of new photosensitizers is essentially eliminating the problem of prolonged cutaneous photosensitivity and is extending treatment depth, an issue dealt with in detail elsewhere in this volume. The complex dynamics of tumor oxygenation in response to PDT are now largely understood. The oxidative stress effects of PDT on redox-sensitive transcription factors and the genes they control are

being uncovered. The complex interplay of biological mechanisms governing the PDT tumor response has been realized. Given these accomplishments, it remains for them to be translated into actual patient benefit. Noninvasive probes need to be perfected that will allow the monitoring of photosensitizer levels, of oxygen status, or, ideally directly, of singlet oxygen, the cytotoxic agent. New light delivery regimes need to be devised for clinical use that will minimize oxygen limitations. The ways in which such regimes might influence redox-sensitive gene regulation and how these genes might affect treatment outcome need to be explored. Finally, our expanding understanding of the complex effects of PDT on host immunity needs to be exploited to modulate the PDT response.

Abbreviations

ALA	5-aminolevulinic acid
APC	antigen presenting cells
BPD-MA	benzoporphyrin derivative, monoacid ring A
CHS	contact hypersensitivity
DC	dendritic cells
HpD	hematoporphyrin derivative
HPPH	hexyl pyropheophorbide ether
LC	Langerhans cells
Lutex	lutetium texaphyrin
mTHPC	meso-tetra-hydroxyphenyl-chlorin
MHC	major histocompatibility complex
NPe6	mono-L-aspartyl chlorin e6
Pc	phthalocyanine
PDT	photodynamic therapy
PpIX	protoporphyrin IX
$SnEt_2$	tin etiopurpurin
Tc	T cells
Th cells	T helper cells
TPPS	sulfonated tetraphenylporphines

Acknowledgment

The authors thank Ian MacDonald for the creation and preparation of figures presented in this chapter.

References

1. Foote CS. Mechanisms of photooxygenation. *Prog Clin Biol Res* 1984;170:3–18.
2. Henderson BW, Miller AC. Effects of scavengers of reactive oxygen and radical species on cell survival following photodynamic treatment in vitro: Comparison to ionizing radiation. *Radiat Res* 1986;108:196–205.
3. Moan J, Sommer S. Oxygen dependence of the photosensitizing effect of hematoporphyrin derivative in NHIK 3025 cells. *Cancer Res* 1985;45:1608–1610.
4. Moan J, Berg K. The photodegradation of porphyrins in cells can be used to estimate the lifetime of singlet oxygen. *Photochem Photobiol* 1991;53:549–553.
5. Tracy EC, Bowman MJ, Pandey RK, Henderson BW, Baumann H. Cell-type selective phototoxicity achieved with chlorophyll-a derived photosensitizers in a co-culture system of primary human tumor and normal lung cells. *Photochem Photobiol* 2011;87:1405–1418.
6. MacDonald IJ, Dougherty TJ. Basic principles of photodynamic therapy. *J Porphyrins Phthalocyanines* 2001;5:105–129.

7. Kessel D, Chang CK, Musselman B. Chemical, biologic and biophysical studies on 'hematoporphyrin derivative'. *Adv Exp Med Biol* 1985;193:213–227.
8. Zheng X, Morgan J, Pandey SK, Chen Y, Tracy E, Baumann H et al. Conjugation of 2-(1′-hexyloxyethyl)-2-devinylpyropheophorbide-a (HPPH) to carbohydrates changes its subcellular distribution and enhances photodynamic activity in vivo. *J Med Chem* 2009;52:4306–4318.
9. Berg K, Madslien K, Bommer JC, Oftebro R, Winkelman JW, Moan J. Light induced relocalization of sulfonated meso-tetraphenylporphines in NHIK 3025 cells and effects of dose fractionation. *Photochem Photobiol* 1991;53:203–210.
10. Henderson BW, Bellnier DA, Greco WR, Sharma A, Pandey RK, Vaughan LA et al. An in vivo quantitative structure-activity relationship for a congeneric series of pyropheophorbide derivatives as photosensitizers for photodynamic therapy. *Cancer Res* 1997;57:4000–4007.
11. Robey RW, Steadman K, Polgar O, Bates SE. ABCG2-mediated transport of photosensitizers: Potential impact on photodynamic therapy. *Cancer Biol Ther* 2005;4:187–194.
12. Morgan J, Jackson JD, Zheng X, Pandey SK, Pandey RK. Substrate affinity of photosensitizers derived from chlorophyll-a: The ABCG2 transporter affects the phototoxic response of side population stem cell-like cancer cells to photodynamic therapy. *Mol Pharm* 2010;7:1789–1804.
13. Liu W, Baer MR, Bowman MJ, Pera P, Zheng X, Morgan J et al. The tyrosine kinase inhibitor imatinib mesylate enhances the efficacy of photodynamic therapy by inhibiting ABCG2. *Clin Cancer Res* 2007;13:2463–2470.
14. Kennedy JC, Pottier RH, Pross DC. Photodynamic therapy with endogenous protoporphyrin IX: Basic principles and present clinical experience. *J Photochem Photobiol B* 1990;6:143–148.
15. Peng Q, Berg K, Moan J, Kongshaug M, Nesland JM. 5-Aminolevulinic acid-based photodynamic therapy: Principles and experimental research. *Photochem Photobiol* 1997;65:235–251.
16. Kessel D, Luo Y. Mitochondrial photodamage and PDT-induced apoptosis. *J Photochem Photobiol B* 1998;42:89–95.
17. Morgan J, Potter WR, Oseroff AR. Comparison of photodynamic targets in a carcinoma cell line and its mitochondrial DNA-deficient derivative. *Photochem Photobiol* 2000;71:747–757.
18. Verma A, Focchina SL, Hirsch S, Dillahey L, Williams J, Snyder SH. Photodynamic tumor therapy: Mitochondrial benzodiazepine receptors as a therapeutic target. *Mol Med* 1998;4:40–45.
19. Miccoli L, Beurdeley-Thomas A, DePinieux G, Sureau F, Oudard S, Dutrillaux B et al. Light induced photoactivation of hypericin affects the energy metabolism of human glioma cells by inhibiting hexokinase bound to mitochondria. *Cancer Res* 1998;58:5777–5786.
20. Perlin DS, Murant RS, Gibson SL, Hilf R. Effects of photosensitization by hematoporphyrin derivative on mitochondrial adenosine triphosphatase-mediated proton transport and membrane integrity of R3230AC mammary adenocarcinoma. *Cancer Res* 1985;45:653–658.
21. Morgan J, Oseroff AR. Mitochondria-based photodynamic anti-cancer therapy. *Adv Drug Deliv Rev* 2001;49:71–86.
22. Geze M, Morliere P, Maziere JC, Smith KM, Santus R. Lysosomes, a key target of hydrophobic photosensitizers proposed for chemotherapeutic applications. *J Photochem Photobiol B* 1993;20:23–25.
23. Moan J, Berg K, Anholt A, Madslien K. Sulfonated aluminum phthalocyanines as sensitizers for photochemotherapy. Effects of small doses on localization, dye fluorescence and photosensitivity in V79 cells. *Int J Cancer* 1994;58:865–870.
24. MacDonald IJ, Morgan J, Bellnier DA, Paszkiewicz G, Whitaker JE, Litchfield DJ et al. Subcellular localization patterns and their relationship to photodynamic activity of pyropheophorbide-a derivatives. *Photochem Photobiol* 1999;70:789–797.
25. Tracy EC, Bowman MJ, Henderson BW, Baumann H. Interleukin-1alpha is the major alarmin of lung epithelial cells released during photodynamic therapy to induce inflammatory mediators in fibroblasts. *Br J Cancer* 2012;107:1534–1546.
26. Kessel D, Woodburn K, Henderson BW, Chang CK. Sites of photodamage in vivo and in vitro by a cationic porphyrin. *Photochem Photobiol* 1995;62(5):875–881.

27. Moan J, Pettersen EO, Christensen T. The mechanism of photodynamic inactivation of human cells in vitro in the presence of haematoporphyrin. *Br J Cancer* 1979;39:398–407.
28. Christensen T, Volden G, Moan J, Sandquist T. Release of lysosomal enzymes and lactate dehydrogenase due to hematoporphyrin derivative and light irradiation of NHIK 3025 cells in vitro. *Ann Clin Res* 1982;14:46–52.
29. Henderson BW, Donovan JM. Release of prostaglandin E2 from cells by photodynamic treatment in vitro. *Cancer Res* 1989;49:6896–6900.
30. Bellnier DA, Dougherty TJ. Membrane lysis in Chinese hamster ovary cells treated with hematoporphyrin derivative plus light. *Photochem Photobiol* 1982;36:43–47.
31. Thomas JP, Girotti AW. Role of lipid peroxidation in hematoporphyrin derivative-sensitized photokilling of tumor cells: Protective effects of glutathione peroxidase. *Cancer Res* 1989;49:1682–1686.
32. Girotti AW. Photodynamic lipid peroxidation in biological systems. *Photochem Photobiol* 1990;51:497–509.
33. Deuticke B, Henseleit U, Haest CW, Heller KB, Dubbelman TM. Enhancement of transbilayer mobility of a membrane lipid probe accompanies formation of membrane leaks during photodynamic treatment of erythrocytes. *Biochim Biophys Acta* 1989;982:53–61.
34. Gibson SL, Murant RS, Hilf R. Photosensitizing effects of hematoporphyrin derivative and photofrin II on the plasma membrane enzymes 5′-nucleotidase, Na^+K^+-ATPase, and Mg^{2+}-ATPase in R3230AC mammary adenocarcinomas. *Cancer Res* 1988;48:3360–3366.
35. Specht KG, Rodgers MA. Plasma membrane depolarization and calcium influx during cell injury by photodynamic action. *Biochim Biophys Acta* 1991;1070:60–68.
36. Berg K, Moan J. Lysosomes and microtubules as targets for photochemotherapy of cancer. *Photochem Photobiol* 1997;65:403–409.
37. Berg K, Steen HB, Winkelman JW, Moan J. Synergistic effects of photoactivated tetra(4-sulfonatophenyl)porphine and nocodazole on microtubule assembly, accumulation of cells in mitosis and cell survival. *J Photochem Photobiol B* 1992;13:59–70.
38. Moan J, Vistnes AI. Porphyrin photosensitization of proteins in cell membranes as studied by spin-labelling and by quantification of DTNB-reactive SH-groups. *Photochem Photobiol* 1986;44:15–19.
39. Liu W, Oseroff AR, Baumann H. Photodynamic therapy causes cross-linking of signal transducer and activator of transcription proteins and attenuation of interleukin-6 cytokine responsiveness in epithelial cells. *Cancer Res* 2004;64:6579–6587.
40. Gomer CJ, Rucker N, Banerjee A, Benedict WF. Comparison of mutagenicity and induction of sister chromatid exchange in Chinese hamster cells exposed to hematoporphyrin derivative photoradiation, ionizing radiation, or ultraviolet radiation. *Cancer Res* 1983;43:2622–2627.
41. Evensen JF, Moan J. Photodynamic action and chromosomal damage: A comparison of haematoporphyrin derivative (HpD) and light with x-irradiation. *Br J Cancer* 1982;45:456–465.
42. McNair FL, Marples B, West CML, Moore JV. A comet assay of DNA damage and repair in K562 cells after photodynamic therapy using hematoporphyrin derivative, methylene blue and *meso*-tetrahydroxyphenylchlorin. *Br J Cancer* 1997;75:1721–1729.
43. Evans HH, Horng M-F, Ricanati M, Deahl JT, Oleinick NL. Mutagenicity of photodynamic therapy as compared to UVC and ionizing radiation in human and murine lymphoblast cell lines. *Photochem Photobiol* 1997;66:690–696.
44. Buytaert E, Dewaele M, Agostinis P. Molecular effectors of multiple cell death pathways initiated by photodynamic therapy. *Biochim Biophys Acta* 2007;1776:86–107.
45. Henkel T. Apoptosis: Corralling the corpses. *Cell* 2001;104:325–328.
46. Agostinis P, Berg K, Cengel KA, Foster TH, Girotti AW, Gollnick SO et al. Photodynamic therapy of cancer: An update. *CA Cancer J Clin* 2011;61:250–281.
47. Reiners JJ Jr., Agostinis P, Berg K, Oleinick NL, Kessel D. Assessing autophagy in the context of photodynamic therapy. *Autophagy* 2010;6:7–18.

48. Dewaele M, Maes H, Agostinis P. ROS-mediated mechanisms of autophagy stimulation and their relevance in cancer therapy. *Autophagy* 2010;6:838–854.
49. Kessel D, Luo Y, Deng Y, Chang CK. The role of subcellular localization in the initiation of apoptosis by photodynamic therapy. *Photochem Photobiol* 1997;65:422–426.
50. Luo Y, Kessel D. Initiation of apoptosis versus necrosis by photodynamic therapy with chloroaluminum phthalocyanine. *Photochem Photobiol* 1997;66:479–483.
51. Yang J, Bhalla K, Kim CN, Ibrado AM, Peng TI, Jones DP et al. Prevention of apoptosis by Bcl-2: Release of cytochrome c from mitochondria blocked. *Science* 1997;275:1129–1132.
52. Granville DJ, Carthy CM, Jiang H, Shore GC, McManus BM, Hunt DWC. Rapid cytochrome c release, activation of caspases 3, 6, 7 and 8 followed by Bap31 cleavage in HeLa cells treated with photodynamic therapy. *FEBS Lett* 1998;437:5–10.
53. Chiu SM, Evans HH, Lam M, Nieminen A, Oleinick NL. Phthalocyanine 4 photodynamic therapy-induced apoptosis of mouse L5178Y-R cells results from a delayed but extensive release of cytochrome c from mitochondria. *Cancer Lett* 2001;165:51–58.
54. Chiu SM, Oleinick NL. Dissociation of mitochondrial depolarization from cytochrome c release during apoptosis induced by photodynamic therapy. *Br J Cancer* 2001;84:1099–1106.
55. Vantieghem A, Xu Y, Declercq W, Vandenabeele P, Denecker G, Vandenheede JR et al. Different pathways mediate cytochrome c release after photodynamic therapy with hypericin. *Photochem Photobiol* 2001;74:133–142.
56. Granville DJ, Levy JG, Hunt DWC. Photodynamic therapy induces caspase-3 activation in HL-60 cells. *Cell Death Differ* 1997;4:623–628.
57. Kessel D, Luo Y. Photodynamic therapy: A mitochondrial inducer of apoptosis. *Cell Death Differ* 1999;6:28–35.
58. Xue LY, Chiu SM, Oleinick NL. Photodynamic therapy-induced death of MCF-7 human breast cancer cells: A role for caspase-3 in the late steps of apoptosis but not for the critical lethal event. *Exp Cell Res* 2001;263:145–155.
59. Srivastava M, Ahmad N, Gupta S, Mukhtar H. Involvement of bcl-2 and bax in photodynamic therapy-mediated apoptosis. *J Biol Chem* 2001;276:15481–15488.
60. Granville DJ, Jiang H, An MT, Levy JG, McManus BM, Hunt DWC. Bcl-2 overexpression blocks caspase activation and downstream apoptotic events instigated by photodynamic therapy. *Br J Cancer* 1999;79:95–100.
61. He J, Agarwal ML, Larkin HE, Friedman LR, Xue LY, Oleinick NL. The induction of partial resistance to photodynamic therapy by the protooncogene bcl-2. *Photochem Photobiol* 1996;64:845–852.
62. Xue LY, Chiu SM, Oleinick NL. Photochemical destruction of the Bcl-2 oncoprotein during photodynamic therapy with the phthalocyanine photosensitizer Pc 4. *Oncogene* 2001;20:3420–3427.
63. Kim H, Luo Y, Li G, Kessel D. Enhanced apoptotic response to photodynamic therapy after bcl-2 transfection. *Cancer Res* 1999;59:3429–3432.
64. Usuda J, Okunaka T, Furukawa K, Tsuchida T, Kuroiwa Y, Ohe Y et al. Increased cytotoxic effects of photodynamic therapy in IL-6 gene transfected cells via enhanced apoptosis. *Int J Cancer* 2001;93:475–480.
65. Agarwal ML, Larkin HE, Zaidi SIA, Mukhtar H, Oleinick NL. Phospholipase activation triggers apoptosis in photosensitized mouse lymphoma cells. *Cancer Res* 1993;53:5897–5902.
66. Separovic D, Mann KJ, Oleinick NL. Association of ceramide accumulation with photodynamic treatment-induced cell death. *Photochem Photobiol* 1998;68:101–109.
67. Gupta S, Ahmad N, Mukhtar H. Involvement of nitric oxide during phthalocyanine (Pc4) photodynamic therapy-mediated apoptosis. *Cancer Res* 1998;58:1785–1788.
68. Kessel D, Arroyo AS. Apoptotic and autophagic responses to Bcl-2 inhibition and photodamage. *Photochem Photobiol Sci* 2007;6:1290–1295.
69. Xue LY, Chiu SM, Azizuddin K, Joseph S, Oleinick NL. Protection by Bcl-2 against apoptotic but not autophagic cell death after photodynamic therapy. *Autophagy* 2008;4:125–127.

70. Tao J-S, Sanghera S, Pelech SL, Wong G, Levy JG. Stimulation of stress-activated protein kinase and p38 HOG1 kinase in murine keratinocytes following photodynamic therapy with benzoporphyrin derivative. *J Biol Chem* 1996;271:27107–27115.
71. Klotz L-O, Fritsch C, Briviba K, Tsacmacidis N, Schliess F, Sies H. Activation of JNK and p38 but not ERK MAP kinases in human skin cells by 5-aminolevulinate-photodynamic therapy. *Cancer Res* 1998;58:4297–4300.
72. Assefa Z, Vantieghem A, Declercq W, Vandenabelle P, Vandenheede JR, Merlevede W et al. The activation of the c-jun N-terminal kinase and p38 mitogen-activated protein kinase signaling pathways protects HeLa cells from apoptosis following photodynamic therapy with hypericin. *J Biol Chem* 1999;274:8788–8796.
73. Wong TW, Tracy E, Oseroff A, Baumann H. Photodynamic therapy mediates immediate loss of cellular responsiveness to cytokines and growth factors. *Can Res* 2003;63:3812–3818.
74. Klotz LO, Kroncke KD, Sies H. Singlet oxygen-induced signaling effects in mammalian cells. *Photochem Photobiol Sci* 2003;2:88–94.
75. Oleinick NL, He J, Xue LY, Separovic D. Stress-activated signalling responses leading to apoptosis following photodynamic therapy. *Optical Methods for Tumor Treatment and Detection: Mechanisms and Techniques in Photodynamic Therapy VII*, San Jose, CA, January 24–25, 1998, pp. 82–88.
76. Xue LY, He J, Oleinick NL. Rapid tyrosine phosphorylation of HS1 in the response of mouse lymphoma L5178Y-R cells to photodynamic treatment sensitized by the phthalocyanine Pc4. *Photochem Photobiol* 1997;66:105–113.
77. Koukourakis MI, Giatromanolaki A, Skarlatos J, Corti L, Blandamura S, Piazza M et al. Hypoxia inducible factor (HIF-1a and HIF-2a) expression in early esophageal cancer and response to photodynamic therapy and radiotherapy. *Cancer Res* 2001;61:1830–1832.
78. Ferrario A, von Tiehl KF, Rucker N, Schwarz MA, Gill PS, Gomer CJ. Antiangiogenic treatment enhances photodynamic therapy responsiveness in a mouse mammary carcinoma. *Cancer Res* 2000;60(15):4066–4069.
79. Luna MC, Ferrario A, Wong S, Fisher AMR, Gomer CJ. Photodynamic therapy-mediated oxidative stress as a molecular switch for the temporal expression of genes ligated to the human heat shock promoter. *Cancer Res* 2000;60:1637–1644.
80. Gomer CJ, Ryter SW, Ferrario A, Rucker N, Wong S, Fisher AMR. Photodynamic therapy-mediated oxidative stress can induce expression of heat shock proteins. *Cancer Res* 1996;56:2355–2360.
81. Curry PM, Levy JG. Stress protein expression in murine tumor cells following photodynamic therapy with benzoporphyrin derivative. *Photochem Photobiol* 1993;58:374–379.
82. Gomer CJ, Ferrario A, Rucker N, Wong S, Lee AS. Glucose regulated protein induction and cellular resistance to oxidative stress mediated by porphyrin photosensitization. *Cancer Res* 1991;51:6574–6579.
83. Xue LY, Agarwal ML, Varnes ME. Elevation of GRP-78 and loss of HSP-70 following photodynamic treatment of V79 cells: Sensitization by nigericin. *Photochem Photobiol* 1995;62:135–143.
84. Gomer CJ, Luna M, Ferrario A, Rucker N. Increased transcription and translation of heme oxygenase in Chinese hamster fibroblasts following photodynamic stress or Photofrin II incubation. *Photochem Photobiol* 1991;53:275–279.
85. Kick G, Messer G, Goetz A, Plewig G, Kind P. Photodynamic therapy induces expression of interleukin 6 by activation of AP-1 but not NF-kB DNA binding. *Cancer Res* 1995;55:2373–2379.
86. Gollnick SO, Lee BY, Vaughan L, Owczarczak B, Henderson BW. Activation of the IL-10 gene promoter following photodynamic therapy of murine keratinocytes. *Photochem Photobiol* 2001;73:170–177.
87. Abate C, Patel L, Rauscher FJ, Curran T. Redox regulation of fos and jun DNA-binding activity *in vitro*. *Science* 1990;249:1157–1161.
88. Yao K-S, Zanthoudakis S, Curran T, O'Dwyer PJ. Activation of AP-1 and of nuclear redox factor, Ref1, in the response of HT29 colon cancer cells to hypoxia. *Mol Cell Biol* 1994;14:5997–6003.

89. Kick G, Messer G, Plewig G, Kind P, Goetz AE. Strong and prolonged injunction of c-*jun* and c-*fos* proto-oncogenes by photodynamic therapy. *Br J Cancer* 1996;74:30–36.
90. Luna MC, Wong S, Gomer CJ. Photodynamic therapy mediated induction of early response genes. *Cancer Res* 1994;54:1374–1380.
91. Baeuerle PA, Henkel T. Function and activation of NF-B in the immune system. *Annu Rev Immunol* 1994;12:141–179.
92. Schreck R, Albermann K, Baeuerle PA. Nuclear factor kB: An oxidative stress-responsive transcription factor of eukaryotic cells. *Free Radic Res Commun* 1992;17:221–237.
93. DiDonato JA, Mercurio R, Rosette C, Wu-Li J, Suyang H, Ghosh S et al. Mapping of the inducible IkB phosphorylation sites that signal its ubiquitination and degradation. *Mol Cell Biol* 1996;16:1295–1304.
94. DiDonato JA, Hayakawa M, Rothwarf DM, Zandi E, Karin M. A cytokine-responsive IkB kinase that activates the transcription factor NFkB. *Nature* 1997;388:548–554.
95. Granville DJ, Carthy CM, Jiang H, Levy JG, McManus BM, Matroule JY et al. Nuclear factor-kB activation by the photochemotherapeutic agent verteporfin. *Blood* 2000;95:256–262.
96. Ryter SW, Gomer CJ. Nuclear factor kB binding activity in mouse L1210 cells following Photofrin II-mediated photosensitization. *Photochem Photobiol* 1993;58:753–756.
97. Matroule JY, Bonizzi G, Morliere P, Paillous N, Santus R, Bours V et al. Pyropheophorbide-a methyl ester-mediated photosensitization activates transcription factor NF-kB through the interleukin-1 receptor-dependent signaling pathway. *J Biol Chem* 1999;270:2899–3000.
98. Legrand-Poels S, Schoonbroodts S, Matroule JY, Piette J. NF-kB: An important transcription factor in photobiology. *J Photochem Photobiol B* 1998;45:1–8.
99. Henderson BW. Probing the effects of photodynamic therapy through in vivo-in vitro methods. In: Kessel D, editor. *Photodynamic Therapy of Neoplastic Disease*, Vol. I. Boca Raton, FL: CRC Press, 1990, pp. 169–188.
100. Henderson BW, Fingar VH. Oxygen limitation of direct tumor cell kill during photodynamic treatment of a murine tumor model. *Photochem Photobiol* 1989;49:299–304.
101. Henderson BW, Waldow SM, Mang TS, Potter WR, Malone PB, Dougherty TJ. Tumor destruction and kinetics of tumor cell death in two experimental mouse tumors following photodynamic therapy. *Cancer Res* 1985;45:572–576.
102. Henderson BW, Sumlin AB, Owczarczak BL, Dougherty TJ. Bacteriochlorophyll-a as photosensitizer for photodynamic treatment of transplantable murine tumors. *J Photochem Photobiol B: Biol* 1991;10:303–313.
103. Henderson BW, Vaughan L, Bellnier DA, vanLeengoed H, Johnson PG, Oseroff AR. Photosensitization of murine tumor, vasculature and skin by 5-aminolevulinic acid-induced porphyrin. *Photochem Photobiol* 1995;62:780–789.
104. Cincotta L, Foley JW, Cincotta AH. Novel phenothiazinium photosensitizers for photodynamic therapy. In: Hasan T, editor. *Advances in Photochemotherapy*, Vol. 997. Washington, DC: SPIE, 1988, pp. 145–153.
105. Chan W-S, Brasseur N, La Madeleine C, van Lier JE. Evidence for different mechanisms of EMT-6 tumor necrosis by photodynamic therapy with disulfonated aluminum phthalocyanine or Photofrin: Tumor cell survival and blood flow. *Anticancer Res* 1996;16:1887–1892.
106. Sitnik T, Henderson BW. The effect of fluence rate on tumor and normal tissue responses to photodynamic therapy. *Photochem Photobiol* 1998;67:462–466.
107. Korbelik M, Krosl G. Cellular levels of photosensitisers in tumours: The role of proximity to the blood supply. *Br J Cancer* 1994;70:604–610.
108. Svaasand LO. Optical dosimetry for direct and interstitial photoradiation therapy of malignant tumors. *Prog Clin Biol Res* 1984;170:91–114.
109. Wilson BC, Jeeves WP, Lowe DM, Adam G. Light propagation in animal tissues in the wavelength range 375–825 nanometers. *Prog Clin Biol Res* 1984;170:115–132.

110. Adams K, Rainbow AJ, Wilson BC, Singh G. In vivo resistance to Photofrin-mediated photodynamic therapy in radiation-induced fibrosarcoma cells resistant to in vitro Photofrin-mediated photodynamic therapy. *J Photochem Photobiol B: Biol* 1999;49(2–3):136–141.
111. Kessel D, Hampton J, Fingar V, Morgan A. Tumor versus vascular photodamage in a rat tumor model. *J Photochem Photobiol B: Biol* 1998;45(1):25–27.
112. Pass HI, Evans S, Matthews WA, Perry R, Venzon D, Roth JA et al. Photodynamic therapy of oncogene-transformed cells. *J Thorac Cardiovasc Surg* 1991;101:795–799.
113. Henderson BW, Dougherty TJ. How does photodynamic therapy work? *Photochem Photobiol* 1992;55:145–157.
114. Dougherty TJ, Marcus SL. Photodynamic therapy. *Eur J Cancer* 1992;28A(10):1734–1742.
115. Hamblin MR, Newman EL. Photosensitizer targeting in photodynamic therapy II. Conjugates of hematoporphyrin with serum lipoproteins. *J Photochem Photobiol B: Biol* 1994;26:147–157.
116. Hamblin MR, Newman EL. Photosensitizer targeting in photodynamic therapy I. Conjugates of hematoporphyrin with albumin and transferrin. *J Photochem Photobiol B: Biol* 1994;26:45–56.
117. Molpus KL, Hamblin MR, Rizvi I, Hasan T. Intraperitoneal photoimmunotherapy of ovarian carcinoma xenografts in nude mice using charged photoimmunoconjugates. *Gynecol Oncol* 2000;76(3):397–404.
118. DelGovernatore M, Hamblin MR, Shea CR, Rizvi I, Hasan T. Experimental photoimmunotherapy of hepatic metastases of colorectal cancer with a 17.1A chlorin (e6) immunoconjugate. *Cancer Res* 2000;60(15):4200–4205.
119. Soukos NS, Hamblin MR, Keel S, Fabian RL, Deutsch TF, Hasan T. Epidermal growth factor receptor-targeted immunophotodiagnosis and photoimmunotherapy of oral precancer in vivo. *Cancer Res* 2001;61(11):4490–4496.
120. Henderson BW, Dougherty TJ, Malone PB. Studies on the mechanism of tumor destruction by photoradiation therapy. *Prog Clin Biol Res* 1984;170:601–612.
121. Fingar VH, Siegel KA, Wieman TJ, Doak KW. The effects of thromboxane inhibitors on the microvascular and tumor response to photodynamic therapy. *Photochem Photobiol* 1993;58(3):393–399.
122. Reed MWR, Wieman TJ, Schuschke DA, Tseng MT, Miller FN. A comparison of the effects of photodynamic therapy on normal and tumor blood vessels in the rat microcirculation. *Radiat Res* 1989;119:542–552.
123. Fingar VH, Potter WR, Henderson BW. Drug and light dose dependence of photodynamic therapy: A study of tumor cell clonogenicity and histologic changes. *Photochem Photobiol* 1987;45:643–650.
124. Fingar VH, Kik PK, Haydon PS, Cerrito PB, Tseng M, Abang E et al. Analysis of acute vascular damage after photodynamic therapy using benzoporphyrin derivative (BPD). *Br J Cancer* 1999;79:1702–1708.
125. Sitnik TM, Hampton JA, Henderson BW. Reduction of tumor oxygenation during and after photodynamic therapy *in vivo*: Effects of fluence rate. *Br J Cancer* 1998;77:1386–1394.
126. Henderson BW, Sitnik-Busch TM, Vaughan LA. Potentiation of PDT anti-tumor activity in mice by nitric oxide synthase inhibition is fluence rate dependent. *Photochem Photobiol* 1999;70:64–71.
127. Dimitroff CJ, Klohs W, Sharma A, Pera P, Driscoll D, Smith J et al. Anti-angiogenic activity of selected receptor tyrosine kinase inhibitors, PD166285 and PD173074: Implications for combination treatment with photodynamic therapy. *Invest New Drugs* 1999;17:121–135.
128. Tseng MT, Reed MW, Ackermann DM, Schuschke DA, Wieman TJ, Miller FN. Photodynamic therapy induced ultrastructural alterations in microvasculature of the rat cremaster muscle. *Photochem Photobiol* 1988;48:675–681.
129. Fingar VH, Wieman J, Wiehle SA, Cerrito PB. The role of microvascular damage in photodynamic therapy: The effect of treatment on vessel constriction, permeability, and leukocyte adhesion. *Cancer Res* 1992;53:4914–4921.
130. McMahon KS, Wieman TJ, Moore PH, Fingar VH. Effects of photodynamic therapy using mono-L-aspartyl chlorin e_6 on vessel constriction, vessel leakage, and tumor response. *Cancer Res* 1994;54:5374–5379.

131. Fingar VH, Wieman TJ, Karavolos PS, Doak KW, Ouellet R, van Lier JE. The effects of photodynamic therapy using differently substituted zinc phthalocyanines on vessel constriction, vessel leakage and tumor response. *Photochem Photobiol* 1993;58(2):251–258.
132. Snyder JW, Greco WR, Bellnier DA, Vaughan L, Henderson BW. Photodynamic therapy: A means to enhanced drug delivery to tumors. *Cancer Res* 2003;63:8126–8131.
133. Zieve PD, Solomon HM, Krevans JR. The effect of hematoporphyrin and light on human platelets. I. Morphologic, functional, and biochemical changes. *J Cell Physiol* 1966;67:271–279.
134. Henderson BW, Owczarczak B, Sweeney J, Gessner T. Effects of photodynamic treatment of platelets or endothelial cells in vitro on platelet aggregation. *Photochem Photobiol* 1992;56:513–521.
135. Fingar VH, Weiman TJ, Doak KW. Role of thromboxane and prostacyclin release on photodynamic therapy-induced tumor destruction. *Cancer Res* 1990;50:2599–2603.
136. Reed MW, Schuschke DA, Miller FN. Prostanoid antagonists inhibit the response of the microcirculation to "early" photodynamic therapy. *Radiat Res* 1991;127:292–296.
137. Fingar VH, Taber SW, Haydon PS, Harrison LT, Kempf SJ, Wieman TJ. Vascular damage after photodynamic therapy of solid tumors: A view and comparison of effect in pre-clinical and clinical models at the University of Louisville. *In Vivo* 2000;14:93–100.
138. Fingar VH, Wieman TJ, Haydon PS. The effects of thrombocytopenia on vessel stasis and macromolecular leakage after photodynamic therapy using Photofrin. *Photochem Photobiol* 1997;66:513–517.
139. Fingar VH, Wieman TJ, Doak KW. Changes in tumor interstitial pressure induced by photodynamic therapy. *Photochem Photobiol* 1991;53:763–768.
140. Hockel M, Vaupel P. Tumor hypoxia: Definitions and current clinical, biologic, and molecular aspects. *J Natl Cancer Inst* 2001;93:266–276.
141. Fingar VH, Wieman TJ, Park YJ, Henderson BW. Implications of a pre-existing tumor hypoxic fraction on photodynamic therapy. *J Surg Res* 1992;53:524–528.
142. Fingar VH, Mang TS, Henderson BW. Modification of photodynamic therapy-induced hypoxia by fluosol-DA (20%) and carbogen breathing in mice. *Cancer Res* 1988;48:3350–3354.
143. Schouwink H, Ruevekamp M, Oppelaar H., van Veen R, Bass P, Stewart FA. Photodynamic therapy for malignant mesothelioma: Preclinical studies for optimization of treatment protocols. *Photochem Photobiol* 2001;73:410–417.
144. Jirsa MJ, Pouckova P, Dolezal J, Pospisil J, Jirsa M. Hyperbaric oxygen and photodynamic therapy in tumour-bearing nude mice [letter]. *Eur J Cancer* 1991;27:109.
145. Maier A, Tomaselli F, Anegg U, Rehak P, Fell B, Luznik S et al. Combined photodynamic therapy and hyperbaric oxygenation in carcinoma of the esophagus and the esophago-gastric junction. *Eur J Cardiothorac Surg* 2001;18:649–654.
146. Svaasand LO, Doiron DR, Dougherty TJ. Temperature rise during photoradiation therapy of malignant tumors. *Med Phys* 1983;10:10–17.
147. Mattiello J, Hetzel F, Vandenheede L. Intratumor temperature measurements during photodynamic therapy. *Photochem Photobiol* 1987;46:873–879.
148. Henderson BW, Busch TM, Vaughan LA, Frawley NP, Babich D, Sosa TA et al. Photofrin photodynamic therapy can significantly deplete or preserve oxygenation in human basal cell carcinomas during treatment, depending on fluence rate. *Cancer Res* 2000;60:525–529.
149. Tromberg BJ, Orenstein A, Kimel S, Barker SJ, Hyatt J, Nelson JS et al. In vivo tumor oxygen tension measurements for the evaluation of the efficiency of photodynamic therapy. *Photochem Photobiol* 1990;52:375–385.
150. Chen Q, Chen H, Hetzel FW. Tumor oxygenation changes post-photodynamic therapy. *Photochem Photobiol* 1996;63:128–131.
151. Foster TH, Murant RS, Bryant RG, Knox RS, Gibson SL, Hilf R. Oxygen consumption and diffusion effects in photodynamic therapy. *Radiat Res* 1991;126:296–303.

152. Foster TH, Gao L. Dosimetry in photodynamic therapy: Oxygen and the critical importance of capillary density. *Radiat Res* 1992;130:379–383.
153. Pogue BW, Hasan T. A theoretical study of light fractionation and dose-rate effects in photodynamic therapy. *Radiat Res* 1997;147:551–559.
154 Foster TH, Hartley DF, Nichols MG, Hilf R. Fluence rate effects in photodynamic therapy of multicell tumor spheroids. *Cancer Res* 1993;53:1249–1254.
155. Mitra S, Finlay JC, McNeill D, Conover DL, Foster TH. Photochemical oxygen consumption, oxygen evolution and spectral changes during UVA irradiation of EMT6 spheroids. *Photochem Photobiol* 2001;73(6):703–708.
156. Zilberstein J, Bromberg A, Frantz A, Rosenbach-Belkin V, Kritzmann A, Pfefermann R et al. Light-dependent oxygen consumption in bacteriochlorophyll-serine-treated melanoma tumors: On-line determination using a tissue-inserted oxygen microsensor. *Photochem Photobiol* 1997;65:1012–1019.
157. Busch TM, Hahn SM, Evans SM, Koch CJ. Depletion of tumor oxygenation during photodynamic therapy: Detection by the hypoxia marker EF3. *Cancer Res* 2000;60:2636–2642.
158. Mang TS, Dougherty TJ, Potter WR, Boyle DG, Somer S, Moan J. Photobleaching of porphyrins used in photodynamic therapy and implications for therapy. *Photochem Photobiol* 1987;45:501–506.
159. Spikes JD. Quantum yields and kinetics of the photobleaching of hematoporphyrin, Photofrin II, tetra(4-sulfonatophenyl)porphine and uroporphyrin. *Photochem Photobiol* 1992;55(6):797–808.
160. Coutier S, Mitra S, Bezdetnaya LN, Parache RM, Georgakoudi I, Foster TH et al. Effects of fluence rate on cell survival and photobleaching in meta-tetra-(hydroxyphenyl)chlorin-photosensitized Colo 26 multicell tumor spheroids. *Photochem Photobiol* 2001;73:297–303.
161. Finlay JC, Conover DL, Hull EL, Foster TH. Porphyrin bleaching and pdt-induced spectral changes are irradiance dependent in ala-sensitized normal rat skin in vivo. *Photobiochem Photobiophys* 2001;73:54–63.
162. Georgakoudi I, Nichols MG, Foster TH. The mechanism of Photofrin photobleaching and its consequences for photodynamic dosimetry. *Photochem Photobiol* 1997;65:135–144.
163. Georgakoudi I, Foster TH. Singlet oxygen- *versus* nonsinglet oxygen-mediated mechanisms of sensitizer photobleaching and their effects on photodynamic dosimetry. *Photochem Photobiol* 1998;67:612–625.
164. Sunar U, Rohrbach D, Rigual N, Tracy E, Keymel KR, Cooper M et al. Monitoring photobleaching and hemodynamic responses to HPPH-mediated photodynamic therapy of head and neck cancer: A case report *Opt Express*. 2010;18(14):14969–14978.
165. Iinuma S, Schomacker KT, Wagnieres G, Rajadhyaksha M, Bamberg M, Momma T et al. In vivo fluence rate and fractionation effects on tumor response and photobleaching: Photodynamic therapy with two photosensitizers in an orthotopic rat tumor model. *Cancer Res* 1999;59(24):6164–6170.
166. van Geel IPJ, Oppelaar H, Marijnissen JPA, Stewart FA. Influence of fractionation and fluence rate in photodynamic therapy with Photofrin or mTHPC. *Radiat Res* 1996;145:602–609.
167. Blant SA, Woodtli A, Wagnieres G, Fontolliet C, Van den Bergh H, Monnier P. In vivo fluence rate effect in photodynamic therapy of early cancers with tetra(m-hydroxyphenyl)chlorin. *Photochem Photobiol* 1996;64:963–968.
168. Sitnik TM, Henderson BW. Effects of fluence rate on cytotoxicity during photodynamic therapy. *Proc SPIE* 1997;2972:95–102.
169. Seshadri M, Bellnier DA, Vaughan LA, Spernyak JA, Mazurchuk R, Foster TH et al. Light delivery over extended time periods enhances the effectiveness of photodynamic therapy. *Clin Cancer Res* 2008;14:2796–2805.
170. Curnow A, McIlroy BW, Postle-Hacon MJ, MacRobert AJ, Bown SG. Light dose fractionation to enhance photodynamic therapy using 5-aminolevulinic acid in the normal rat colon. *Photochem Photobiol* 1999;69:71–76.

171. DeBruijn HS, van der Veen N, Robinson DJ, Star WM. Improvement of systemic 5-aminolevulinic acid-based photodynamic therapy in vivo using light fractionation with a 75-minute interval. *Cancer Res* 1999;59:901–904.
172. Cottrell WJ, Paquette AD, Keymel KR, Foster TH, Oseroff AR. Irradiance-dependent photobleaching and pain in delta-aminolevulinic acid-photodynamic therapy of superficial basal cell carcinomas. *Clin Cancer Res* 2008;14:4475–4483.
173. Zeitouni NC, Paquette AD, Housel JP, Shi Y, Wilding GE, Foster TH et al. A retrospective review of pain control by a two-step irradiance schedule during topical ALA-photodynamic therapy of nonmelanoma skin cancer. *Lasers Surg Med* 2013;45:89–94.
174. Obochi MO, Ratkay LG, Levy JG. Prolonged skin allograft survival after photodynamic therapy associated with modification of donor skin antigenicity. *Transplantation* 1997;63:810–817.
175. Gruner S, Meffert H, Volk HD, Grunow R, Jahn S. The influence of haematoporphyrin derivative and visible light on murine skin graft survival, epidermal Langerhans cells and stimulation of the allogeneic mixed leucocyte reaction. *Scand J Immunol* 1985;21:267–273.
176. Qin B, Selman SH, Payne KM, Keck RW, Metzger DW. Enhanced allograft survival after photodynamic therapy: Association with lymphocyte inactivation and macrophage stimulation. *Transplantation* 1993;56:1481–1486.
177. Dragieva G, Hafner J, Dummer R, Schmid-Grendelmeier P, Roos M, Prinz BM et al. Topical photodynamic therapy in the treatment of actinic keratoses and Bowen's disease in transplant recipients. *Transplantation* 2004;77:115–121.
178. Gollnick SO, Musser DA, Oseroff AR, Vaughan LA, Owczarczak B, Henderson BW. IL-10 does not play a role in cutaneous Photofrin® photodynamic therapy-induced suppression of the contact hypersensitivity response. *Photochem Photobiol* 2001;74:811–816.
179. Elmets CA, Bowen KD. Immunological suppression in mice treated with hematoporphyrin derivative photoradiation. *Cancer Res* 1986;46:1608–1611.
180. Musser DA, Fiel RJ. Cutaneous photosensitizing and immunosuppressive effects of a series of tumor localizing porphyrins. *Photochem Photobiol* 1991;53:119–123.
181. Simkin G, Obochi M, Hunt DWC, Chan AH, Levy JG. Effect of photodynamic therapy using benzoporphyrin derivative on the cutaneous immune response. *Proc SPIE 2392, Optical Methods for Tumor Treatment and Detection: Mechanisms and Techniques in Photodynamic Therapy IV*, 1995, pp. 23–33.
182. Reddan JC, Anderson C, Xu H, Hrabovsky S, Freye K, Fairchild R et al. Immunosuppressive effects of silicon phthalocyanine photodynamic therapy. *Photochem Photobiol* 1999;70:72–77.
183. Anderson C, Hrabovsky S, McKinley Y, Tubesing K, Tang H-P, Dunbar R et al. Phthalocyanine photodynamic therapy: Disparate effects of pharmacologic inhibitors on cutaneous photosensitivity and on tumor regression. *Photochem Photobiol* 1997;65:895–901.
184. Ziolkowski P, Symonowicz K, Milach J, Szkudlarek T. In vivo tumor necrosis factor-alpha induction following chlorin e_6-photodynamic therapy in Buffalo rats. *Neoplasma* 1996;44:192–196.
185. Rivas JM, Ullrich SE. The role of IL-4, IL-10, and TNF-a in the immune suppression induced by ultraviolet radiation. *J Leukoc Biol* 1994;56:769–775.
186. Simkin G, Tao J-S, Levy JG, Hunt DWC. IL-10 contributes to the inhibition of contact hypersensitivity in mice treated with photodynamic therapy. *J Immunol* 2000;164:2457–2462.
187. Gollnick SO, Liu X, Owczarczak B, Musser DA, Henderson BW. Altered expression of interleukin 6 and interleukin 10 as a result of photodynamic therapy in vivo. *Cancer Res* 1997;57:3904–3909.
188. Moore KW, de Waal Malefyt R, Coffman RL, O'Garra A. Interleukin-10 and the interleukin-10 receptor. *Annu Rev Immunol* 2001;19:683–765.
189. Obochi MOK, Ratkay LG, Levy JG. Prolonged skin allograft survival after photodynamic therapy associated with modification of donor skin antigenicity. *Transplantation* 1997;63:810–817.
190. King DE, Jiang H, Simkin G, Obochi M, Levy JG, Hunt DWC. Photodynamic alteration of the surface receptor expression pattern of murine splenic dendritic cells. *Scand J Immunol* 1999;49:184–192.

191. Matthews YJ, Damian DL. Topical photodynamic therapy is immunosuppressive in humans. *Br J Dermatol* 2010;162:637–641.
192. Frost GA, Halliday GM, Damian DL. Photodynamic therapy-induced immunosuppression in humans is prevented by reducing the rate of light delivery. *J Invest Dermatol* 2011;131:962–968.
193. Gallucci S, Matzinger P. Danger signals: SOS to the immune system. *Curr Opin Immunol* 2001;13:114–119.
194. Moroz OV, Burkitt W, Wittkowski H, He W, Ianoul A, Novitskaya V et al. Both Ca^{2+} and Zn^{2+} are essential for S100A12 protein oligomerization and function. *BMC Biochem* 2009;10:11.
195. Levy RM, Mollen KP, Prince JM, Kaczorowski DJ, Vallabhaneni R, Liu S et al. Systemic inflammation and remote organ injury following trauma require HMGB1. *Am J Physiol Regul Integr Comp Physiol* 2007;293:R1538–R1544.
196. Riddell JR, Wang XY, Minderman H, Gollnick SO. Peroxiredoxin 1 stimulates secretion of proinflammatory cytokines by binding to TLR4. *J Immunol* 2010;184:1022–1030.
197. Korbelik M, Krosl G, Krosl J, Dougherty GJ. The role of host lymphoid populations in the response of mouse EMT6 tumor to photodynamic therapy. *Cancer Res* 1996;56:5647–5652.
198. deVree WJA, Essers MC, DeBruijn HS, Star WM, Koster JF, Sluiter W. Evidence for an important role of neutrophils in the efficacy of photodynamic therapy *in vivo*. *Cancer Res* 1996;56:2908–2911.
199. Korbelik M, Cecic I. Contribution of myeloid and lymphoid host cells to the curative outcome of mouse sarcoma treatment by photodynamic therapy. *Cancer Lett* 1999;137:91–98.
200. Gollnick S, Evans SS, Baumann H, Owczarczak B, Maier P, Vaughan L et al. Role of cytokines in photodynamic therapy-induced local and systemic inflammation. *Br J Cancer* 2003;88:1772–1779.
201. Krosl G, Korbelik M, Dougherty GJ. Induction of immune cell infiltration into murine SCCVII tumour by Photofrin-based photodynamic therapy. *Br J Cancer* 1995;71:549–555.
202. Henderson BW, Gollnick SO, Snyder JW, Busch TM, Kousis PC, Cheney RT et al. Choice of oxygen-conserving treatment regimen determines the inflammatory response and outcome of photodynamic therapy of tumors. *Cancer Res* 2004;64:2120–2126.
203. Kousis PC, Henderson BW, Maier PG, Gollnick SO. Photodynamic therapy enhancement of antitumor immunity is regulated by neutrophils. *Cancer Res* 2007;67:10501–10510.
204. Yamamoto N, Hoober JK, Yamamoto S. Tumoricidal capacities of macrophages photodynamically activated with hematoporphyrin derivative. *Photochem Photobiol* 1992;56:245–250.
205. Korbelik M, Krosl G. Enhanced macrophage cytotoxicity against tumor cells treated with photodynamic therapy. *Photochem Photobiol* 1994;60:497–502.
206. Korbelik M, Sun J, Posakony JJ. Interaction between photodynamic therapy and BCG immunotherapy responsible for the reduced recurrence of treated mouse tumors. *Photochem Photobiol* 2001;73:403–409.
207. Korbelik M, Naraparaju VR, Yamamoto N. Macrophage-directed immunotherapy as adjuvant therapy. *Br J Cancer* 1997;75:202–207.
208. Korbelik M, Cecic I. Enhancement of tumour response to photodynamic therapy by adjuvant mycobacterium cell-wall treatment. *J Photochem Photobiol B* 1998;44:151–158.
209. Korbelik M, Dougherty GJ. Photodynamic therapy-mediated immune response against subcutaneous mouse tumors. *Cancer Res* 1999;59:1941–1946.
210. Korbelik M, Sun J. Cancer treatment by photodynamic therapy combined with adoptive immunotherapy using genetically altered natural killer cell line. *Int J Cancer* 2001;93:269–274.
211. Belicha-Villanueva A, Riddell J, Bangia N, Gollnick SO. The effect of photodynamic therapy on tumor cell expression of major histocompatibility complex (MHC) class I and MHC class I-related molecules. *Lasers Surg Med* 2012;44:60–68.
212. Nseyo UO, Whalen RK, Duncan MR, Berman B, Lundahl SL. Urinary cytokines following photodynamic therapy for bladder cancer. A preliminary report. *Urology* 1990;36:167–171.
213. deVree WJ, Essers MC, Koster JF, Sluiter W. Role of interleukin 1 and granulocyte colony-stimulating factor in Photofrin-based photodynamic therapy of rat rhabdomyosarcoma tumors. *Cancer Res* 1997;57:2555–2558.

214. Brackett CM, Owczarczak B, Ramsey K, Maier PG, Gollnick SO. IL-6 potentiates tumor resistance to photodynamic therapy (PDT). *Lasers Surg Med* 2011;43:676–685.
215. Gollnick SO, Brackett CM. Enhancement of anti-tumor immunity by photodynamic therapy. *Immunol Res* 2010;46:216–226.
216. Curry PM, Levy JG. Tumor inhibitory lymphocytes derived from the lymph nodes of mice treated with photodynamic therapy. *Photochem Photobiol* 1995;61S–72S.
217. Canti G, Lattuada D, Nicolin A, Taroni P, Valentini G, Cubeddu R. Immunopharmacology studies on photosensitizers used in photodynamic therapy (PDT). *Proc SPIE 2078, Photodyn Ther Cancer* 1994;268–275.
218. Kabingu E, Vaughan L, Owczarczak B, Ramsey KD, Gollnick SO. $CD8^+$ T cell-mediated control of distant tumours following local photodynamic therapy is independent of $CD4^+$ T cells and dependent on natural killer cells. *Br J Cancer* 2007;96:1839–1848.
219. Abdel-Hady ES, Martin-Hirsch P, Duggan-Keen M, Stern PL, Moore JV, Corbitt G et al. Immunological and viral factors associated with the response of vulval intraepithelial neoplasia to photodynamic therapy. *Cancer Res* 2001;61:192–196.
220. Thong PS, Olivo M, Kho KW, Bhuvaneswari R, Chin WW, Ong KW et al. Immune response against angiosarcoma following lower fluence rate clinical photodynamic therapy. *J Environ Pathol Toxicol Oncol* 2008;27:35–42.
221. Kabingu E, Oseroff AR, Wilding GE, Gollnick SO. Enhanced systemic immune reactivity to a Basal cell carcinoma associated antigen following photodynamic therapy. *Clin Cancer Res* 2009;15:4460–4466.
222. Gollnick SO, Vaughan L, Henderson BW. Generation of effective anti-tumor vaccines using photodynamic therapy. *Cancer Res* 2002;62:1604–1608.
223. Korbelik M, Stott B, Sun J. Photodynamic therapy-generated vaccines: Relevance of tumour cell death expression. *Br J Cancer* 2007;97:1381–1387.
224. Zhang H, Ma W, Li Y. Generation of effective vaccines against liver cancer by using photodynamic therapy. *Lasers Med Sci* 2009;24:549–552.
225. Jalili A, Makowski M, Switaj T, Nowis D, Wilczynski GM, Wilczek E et al. Effective photoimmunotherapy of murine colon carcinoma induced by the combination of photodynamic therapy and dendritic cells. *Clin Cancer Res* 2004;10:4498–4508.
226. Peng Q, Farrants GW, Madslien K, Bommer JC, Moan J, Danielsen HE et al. Subcellular localization, redistribution and photobleaching of sulfonated aluminum phthalocyanines in a human melanoma cell line. *Int J Cancer* 1991;49:290–295.
227. Peng Q, Moan J, Farrants GW, Danielsen HE, Rimington C. Location of P-II and AlPCS4 in human tumor LOX in vitro and in vivo by means of computer-enhanced video fluorescence microscopy. *Cancer Lett* 1991;58:37–47.
228. Wood SR, Holroyd JA, Brown SB. The subcellular localization of Zn(II) phthalocyanines and their redistribution on exposure to light. *Photochem Photobiol* 1997;65:397–402.
229. Kessel D. Sites of photosensitization by derivatives of hematoporphyrin. *Photochem Photobiol* 1986;44:489–493.
230. Singh G, Jeeves WP, Wilson BC, Jang D. Mitochondrial photosensitization by Photofrin II. *Photochem Photobiol* 1987;46:645–649.
231. Woodburn KW, Fan Q, Miles DR, Kessel D, Luo Y, Young SW. Localization and efficacy analysis of the phototherapeutic lutetium texaphyrin (PCI-0123) in the murine EMT6 sarcoma model. *Photochem Photobiol* 1997;65:410–415.
232. Kessel D, Luo Y, Mathieu P, Reiners JJ Jr. Determinants of the apoptotic response to lysosomal photodamage. *Photochem Photobiol* 2000;71:196–200.
233. Ma L, Moan J, Berg K. Evaluation of a new photosensitizer, meso-tetra-hydroxyphenyl-chlorin, for use in photodynamic therapy: A comparison of its photobiological properties with those of two other photosensitizers. *Int J Cancer* 1994;87:883–888.

234. Kessel D, Woodburn K, Gomer CJ, Jagerovic N, Smith KM. Photosensitization with derivatives of chlorin p6. *J Photochem Photobiol B* 1995;28:13–18.
235. Kessel D. Determinants of photosensitization by mono-L-aspartyl chlorin e6 [published erratum appears in *Photochem Photobiol* Dec 1989;50(6):1]. *Photochem Photobiol* 1989;49:447–452.
236. Kennedy JC, Pottier RH. Endogenous protoporphyrin IX, A clinically useful photosensitizer for photodynamic therapy. *J Photochem Photobiol B: Biol* 1992;14:275–292.
237. Kessel D, Thompson P, Saatio K, Nantwi KD. Tumor localization and photosensitization by sulfonated derivatives of tetraphenylporphine. *Photochem Photobiol* 1987;45:787–790.
238. Berg K, Moan J, Bommer JC, Winkelman JW. Cellular inhibition of microtubule assembly by photoactivated sulphonated meso-tetraphenylporphines. *Int J Radiat Biol* 1990;58:475–487.
239. Berg K, Moan J. Lysosomes as photochemical targets. *Int J Biochem* 1994;59:814–822.
240. Star WM, Marijnissen HP, van den Berg Blok AE, Versteeg JA, Franken KA, Reinhold HS. Destruction of rat mammary tumor and normal tissue microcirculation by hematoporphyrin derivative photoradiation observed in vivo in sandwich observation chambers. *Cancer Res* 1986;46:2532–2540.
241. Henderson BW, Fingar VH. Relationship of tumor hypoxia and response to photodynamic treatment in an experimental mouse tumor. *Cancer Res* 1987;47:3110–3114.
242. Selman SH, Kreimer Birnbaum M, Klaunig JE, Goldblatt PJ, Keck RW, Britton SL. Blood flow in transplantable bladder tumors treated with hematoporphyrin derivative and light. *Cancer Res* 1984;44:1924–1927.
243. vanGeel IPJ, Oppelaar H, Rijken PFJW, Bernsen HJJA, Hagemeier NEM, van der Kogel AJ et al. Vascular perfusion and hypoxic areas in RIF-1 tumours after photodynamic therapy. *Br J Cancer* 1996;73:288–293.
244. Roberts DJH, Cairnduff F, Driver I, Dixon B, Brown SB. Tumour vascular shutdown following photodynamic therapy based on polyhaematoporphyrin or 5-aminolaevulinic acid. *Int J Oncol* 1994;5:763–768.
245. Dodd NFJ, Moore JV, Poppitt DG, Wood B. In vivo magnetic resonance imaging of the effects of photodynamic therapy. *Br J Cancer* 1989;60:164–167.
246. Chapman JD, McPhee MS, Walz N, Chetner MP, Stobbe CC, Soderlind K et al. Nuclear magnetic resonance spectroscopy and sensitizer-adduct measurements of photodynamic therapy-induced ischemia in solid tumors. *J Natl Cancer Inst* 1991;83:1650–1659.
247. Zilberstein J, Schreiber S, Bloemers MC, Bendel P, Neeman M, Schechtman E et al. Antivascular treatment of solid melanoma tumors with bacteriochlorophyll-serine-based photodynamic therapy. *Photochem Photobiol* 2001;73:257–266.
248. Reed MW, Mullins AP, Anderson GL, Miller FN, Wieman TJ. The effect of photodynamic therapy on tumor oxygenation. *Surgery* 1989;106:94–99.
249. Kerdel FA, Soter NA, Lim HW. In vivo mediator release and degranulation of mast cells in hematoporphyrin derivative-induced phototoxicity in mice. *J Invest Dermatol* 1987;88:277–280.
250. Lim HW. Effects of porphyrins on skin. *Photosensitizing Compounds: Their Chemistry, Biology and Clinical Use*. Chichester, England: John Wiley & Sons, 1989, pp. 148–153.
251. Zieve PD, Solomon HM. The effect of hematoporphyrin and light on human platelets. 3. Release of potassium and acid phosphatase. *J Cell Physiol* 1966;68:109–112.
252. Ben-Hur E, Heldman E, Crane SW, Rosenthal I. Release of clotting factors from photosensitized endothelial cells: A positive trigger for blood vessel occlusion by photodynamic therapy. *FEBS Lett* 1988;236:105–108.
253. Foster TH, Primavera MC, Marder VJ, Hilf R, Sporn LA. Photosensitized release of von Willebrand factor from cultured human endothelial cells. *Cancer Res* 1991;51:3261–3266.

2

Synthesis and Biological Significance of Porphyrin-Based Photosensitizers in Photodynamic Therapy

Penny Joshi
Roswell Park Cancer Institute

Ravindra K. Pandey
Roswell Park Cancer Institute

The porphyrins and related tetrapyrrolic systems are among the most widely studied compounds for their use as photosensitizers in photodynamic therapy (PDT).[1] Porphyrins are 18π-electron aromatic macrocycles that exhibit characteristic optical spectra with a strong π–π^* transition around 400 nm (Soret band) and usually four Q bands in the visible region. As can be seen in Figure 2.1, two of the peripheral double bonds in opposite pyrrolic rings are cross-conjugated and are not required to maintain aromaticity. Thus, the reduction of one or both of these cross-conjugated double bonds (to give chlorins and bacteriochlorins, respectively) maintains much of the aromaticity, but the change in symmetry results in bathochromically shifted Q bands with high extinction coefficients.[2] Nature uses these optical properties of the reduced porphyrins to harvest solar energy for photosynthesis with chlorophylls and bacteriochlorophylls as both antenna and reaction-center pigments.[3] The long-wavelength absorption of these natural chromophores led to explorations of their use as photosensitizers in PDT.

PDT is a promising cancer treatment that involves the combination of visible light and a photosensitizer.[4] Each factor is harmless by itself, but when combined with oxygen, they can produce lethal cytotoxic agents, initially singlet oxygen, that inactivate the tumor cells.[5] This enables greater selectivity

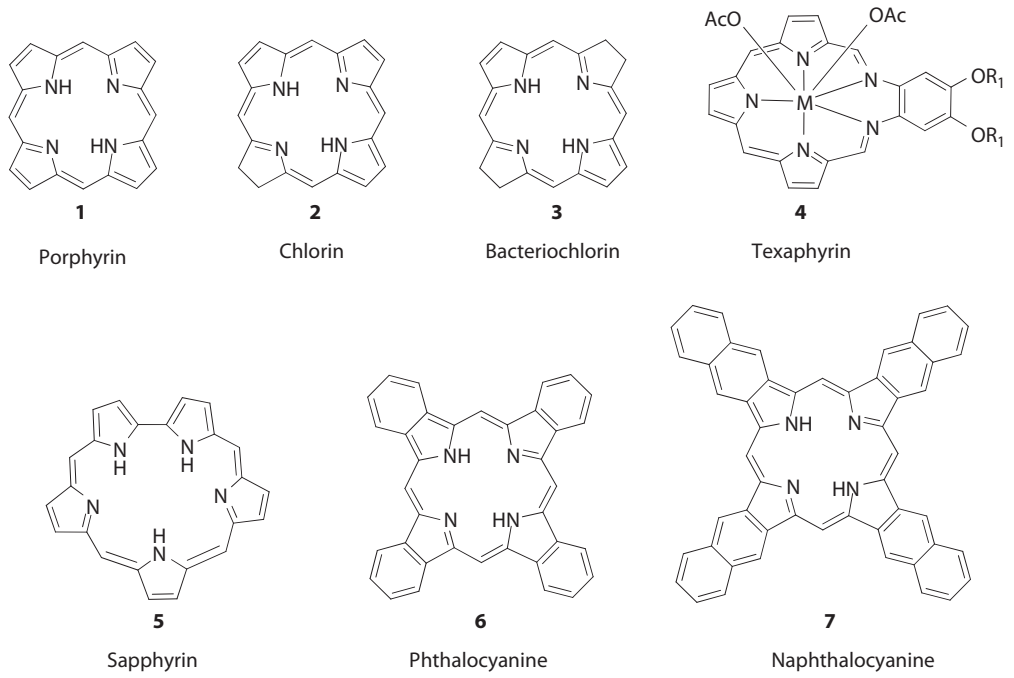

FIGURE 2.1 Basic structures of porphyrins and modified porphyrins.

toward diseased tissue, as only those cells that are simultaneously exposed to the photosensitizer, light, and oxygen are exposed to the cytotoxic effect. The dual selectivity of PDT is produced by both a preferential uptake of the photosensitizer by the diseased tissue and the ability to confine activation of the photosensitizer to this diseased tissue by restricting the illumination to the specific site (Figure 2.1).

As indicated previously, PDT is based on the interaction of a photosensitizer retained in tumors with photons of visible light, resulting in the formation of singlet oxygen ($^1O_2$), the putative lethal agent.[6] To achieve an effective destruction of tumor cells, a high quantum yield of singlet oxygen is required. Even in the absence of heavy atom substitution(s) and coordination of transition-metal ions, porphyrin systems generally satisfy these criteria and that is why most of the sensitizers currently under clinical evaluation for PDT are porphyrins or porphyrin-based molecules.

At present, Photofrin®,* a hematoporphyrin derivative,[7] is the only photosensitizer that has been approved worldwide for the treatment of various types of cancer by PDT. It fits some of the criteria for ideal photosensitizers, but it also suffers from several drawbacks. First, it is a complex mixture of various monomeric, dimeric, and oligomeric forms.[7b–e] Second, its long-wavelength absorption falls at 630 nm, which lies well below the wavelength necessary for the maximum tissue penetration. Finally, it induces prolonged cutaneous phototoxicity, a major adverse effect associated with most of the porphyrin-based photosensitizers.

It is well established that both absorption and scattering of light by tissue increases as the wavelength decreases and that most efficient sensitizers are those that have strong absorption bands from 700 to 800 nm.[8] Light transmission by tissues drops rapidly below 550 nm; however, it doubles from 550 to 630 nm and doubles again from 630 to 700 nm. This is followed by an additional 10% increase in tissue penetration as the wavelength increases toward 800 nm.[3] Another reason to set the ideal wavelength for PDT at 700–800 nm is due to the availability of easy-to-use diode lasers. Although diode lasers are now

* Registered trademark of Axcan Scandipharm Inc., Birmingham, AL.

available at 630 nm (where clinically approved Photofrin absorbs), photosensitizers with absorptions between 700 and 800 nm in conjunction with diode lasers are still desirable for treating deeply seated tumors. Therefore, in recent years, a variety of photosensitizers related to chlorins, bacteriochlorins, porphycenes, phthalocyanines, naphthalocyanines, and expanded porphyrins have been synthesized and evaluated for PDT efficacy. However, for designing improved photosensitizers for PDT, it becomes necessary to consider several other factors such as overall lipophilicity (i.e., a proper balance between hydrophilicit and hydrophobicity), pH, lymphatic drainage, and lipoprotein binding, which could influence the biodistribution and localization of sensitizers in tissue and tumors.[9]

The main focus of this review article is to summarize the various synthetic strategies followed by several research groups in designing long-wavelength absorbing photosensitizers related to chlorins, bacteriochlorins, expanded porphyrins, and phthalocyanines. An ongoing interest on developing target-specific photosensitizers has also been briefly reviewed. The majority of chlorins and bacteriochlorins have been generated through three different approaches. One method involves the modification of a preformed porphyrin. The second approach utilizes the use of chlorophyll *a* as the starting material for the synthesis of other chlorins and bacteriochlorins. The third approach utilizes the unstable bacteriochlorophyll *a* as a substrate for the synthesis of stable bacteriochlorins. Each procedure has been used successfully for the preparation of sensitizers that show promise in PDT and is discussed in terms of synthetic methodology and biological significance.

2.1 Chlorins and Bacteriochlorins from Porphyrins

2.1.1 Chlorins and Bacteriochlorins by Diimide Reduction

Almost 30 years ago, Whitlock et al.[10] developed an efficient diimide-reduction method for the synthesis of bacteriochlorins and isobacteriochlorins from porphyrins. Diimide reduction of metal-free tetraphenyl chlorin afforded tetraphenyl bacteriochlorin, while the reduction of the corresponding zinc analog produced the related tetraphenylisobacteriochlorin. It is now accepted that the reduced double bond in chlorins induces a pathway for the delocalized π electrons that *isolates* the diagonal crossing-conjugated pyrrolic double bond, such that the reduction of this double bond is favored due to minimal loss of π energy over the double bond present in the adjacent ring. The presence of a metal changes the delocalization of the π electrons, which makes the adjacent pyrrolic ring more reactive, and diimide reduction produces mainly the corresponding isobacteriochlorin. In order to avoid the formation of an isomeric mixture, this approach is useful only for reduction of symmetrical porphyrins. This diimide-reduction approach was later employed by Bonnett[11] for preparing the *meso*-tetra (*m*-hydroxyphenyl)-chlorin (*m*-THPC) (**9**) (650 nm) and the bacteriochlorin (*m*-THPBC) (**10**). The formation of these components was found to depend on the amount of the reductant used.

Although the formation of a bacteriochlorin resulted in further red shift in the electronic absorption spectrum with long-wavelength absorption near 750 nm, these molecules were generally found to be air sensitive. Among various chlorin analogs, *m*-THPC (Foscan®) (**9**) (Scheme **2.1**) appears to be quite effective and is currently under phase III human clinical trials.

2.1.2 Chlorins and Bacteriochlorins by Diels–Alder Reaction

Cycloaddition reactions are among the most powerful reactions available to the organic chemists.[12] The ability to simultaneously form and break several bonds, with a wide variety of atomic substitution patterns and often with high degree of stereocontrol, has made cycloaddition reactions the subject of intense study. In porphyrin chemistry, the [4+2] Diels–Alder reactions have been used by various investigators for converting porphyrins into chlorin systems. Callot et al. were the first to show that protoporphyrin IX dimethyl ester (**11**) can undergo cycloaddition reactions with various dienophiles[13] (Scheme **2.2**). A few years later, Dolphin and coworkers discovered the utility of one of such analogs

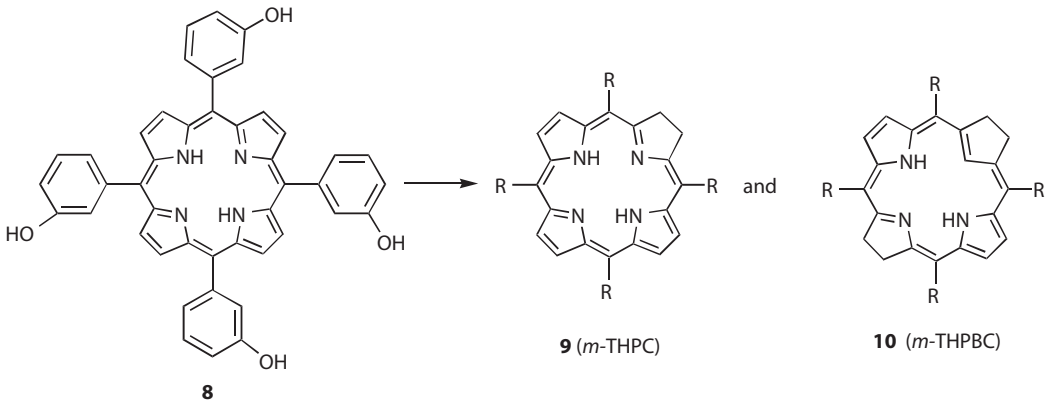

SCHEME 2.1 Conversion of meso-substituted porphyrin to corresponding chlorin and bacteriochlorin.

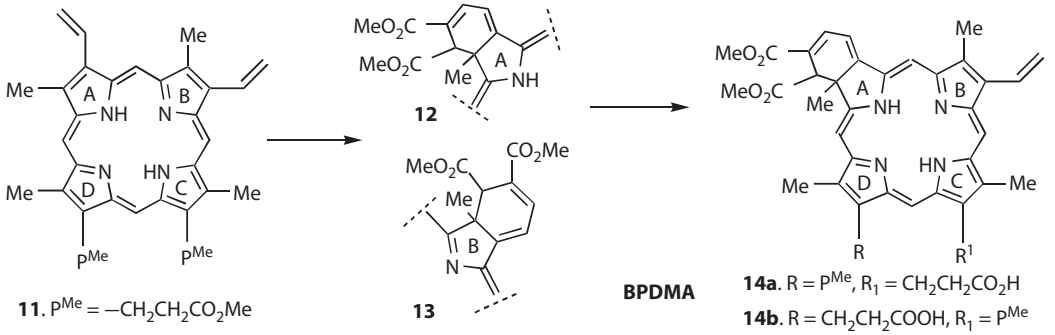

SCHEME 2.2 Conversion of Protoporphyrin IX dimethyl ester to benzoporphyrin derivatives.

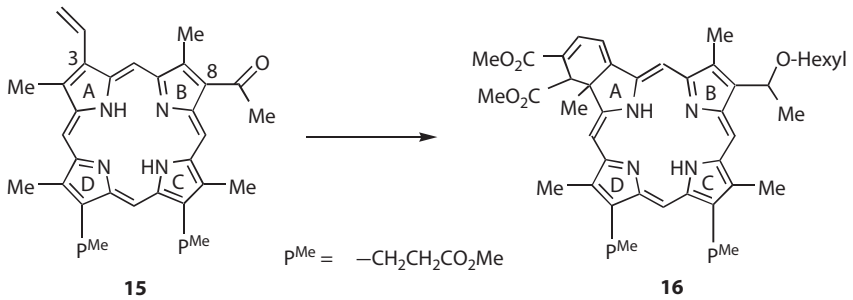

SCHEME 2.3 Synthesis of 8-(1′-hexyloxy)ethylbenzoporphyrin derivative dimethyl ester.

named as benzoporphyrin derivative monocarboxylic acid (BPDMA) **14a** and **14b** for treating age-related macular degeneration (AMD) when activated with light at 690 nm.[14] This treatment has already received approval worldwide. BPDMA has also been used for the treatment of cancer by PDT. However, due to its rapid clearance, it was found to be effective only if the tumors were treated with light at 3 h postinjection of the drug. Pandey et al.[15] developed another approach for preparing these analogs starting from 8-acetyl-3-vinyl deuteroporphyrin IX dimethyl ester (Scheme **2.3**).

The vinyl group was replaced with various alkyl ether functionalities. Among these analogs, the related 8-(1′-hexyloxy)ethyl derivative (**16**) was found to be more effective than BPDMA in eradicating tumors in mice bearing SMT-F tumors.[15a–c]

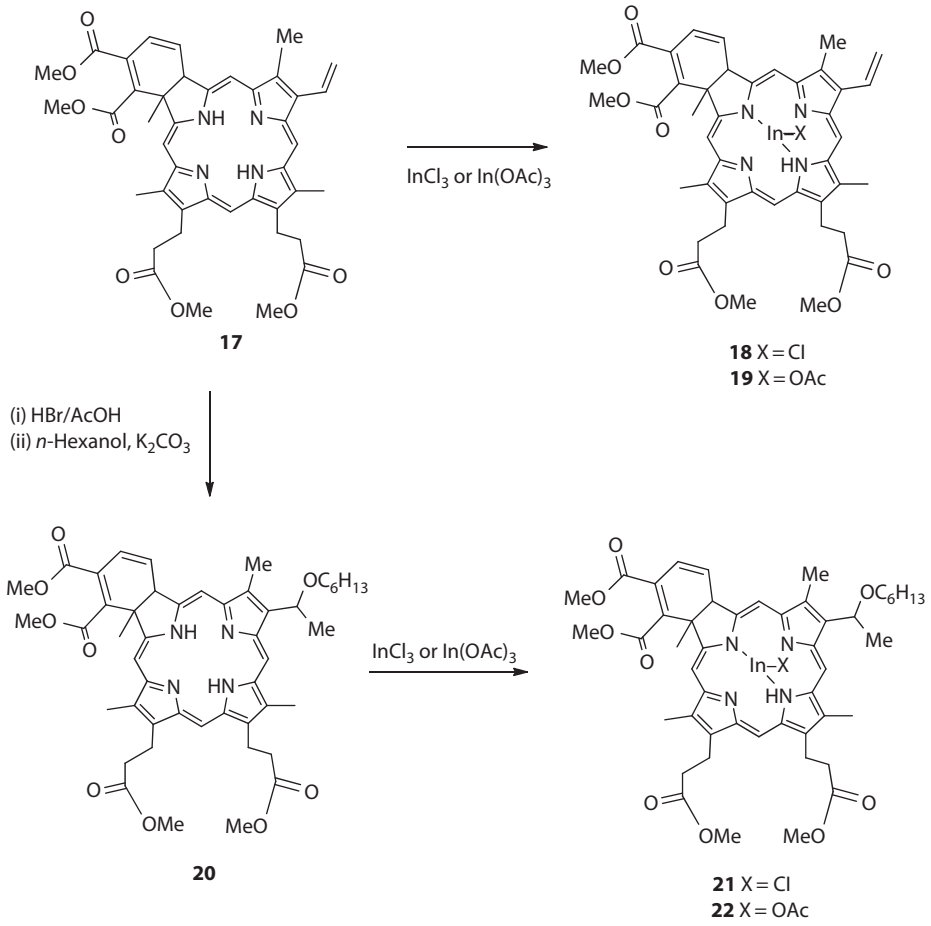

SCHEME 2.4 Synthesis of In(III) complex of 8-(1′-hexyloxy)ethyl benzoporphyrin derivative dimethyl ester.

To investigate the impact of indium as a central metal atom, recently Pandey et al. synthesized In (III) complex of benzoporphyrin dimethyl ester (**18**, **19**) and its 8-(1[1]-hexyloxy)ethyl analog (**21**, **22**), which showed enhanced in vitro photosensitizing ability[15d] (Scheme **2.4**).

The methodology mentioned earlier was further extended independently by Pandey et al.[16] and Yon-Hin et al.[17] for the synthesis of novel bacteriochlorins, which involved a double Diels–Alder reaction on divinylporphyrins **23** and **25** (Scheme **2.5**). These bacteriochlorins **24** and **26** exhibit long-wavelength absorption maxima near 800 nm with PDT efficacy.

Morgan et al.[18] have shown that bacteriochlorin-like macrocycles can also be generated by cyclization of either 5,10- or 5,15-bis[(ethoxycarbonyl)vinyl]-porphyrins. However, the resulting products rapidly decomposed upon exposure to air, thus precluding their use as photosensitizers for PDT. For developing a general synthesis of stable bacteriochlorins, the same authors[19] followed the pinacol–pinacolone approach in preparing ketochlorins **30** and **31**. In brief, dehydration of **27** produced a mixture of **28** and **29**, which on reaction with dimethyl acetylenedicarboxylate (DMAD) produced the corresponding bacteriochlorins **30** and **31** as an isomeric mixture. This isomeric mixture showed some photodynamic activity in a mouse tumor model; 75% of the mice treated at a dose of 1 mg/kg were found to be free from palpable tumor 12 days after the light treatment. However, in this class of compounds, the spectroscopic properties of **30** and **31** resemble those of porphyrinones (long-wavelength absorption near 700 nm) rather than bacteriochlorins (Scheme **2.6**).

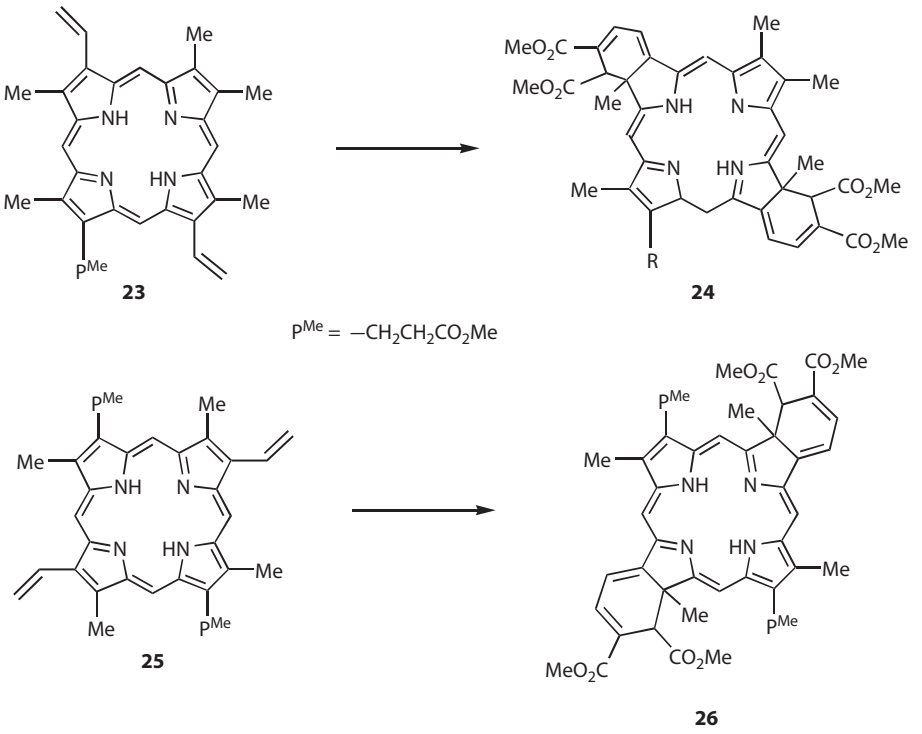

SCHEME 2.5 Synthesis of bacteriochlorins via Diels–Alder reaction.

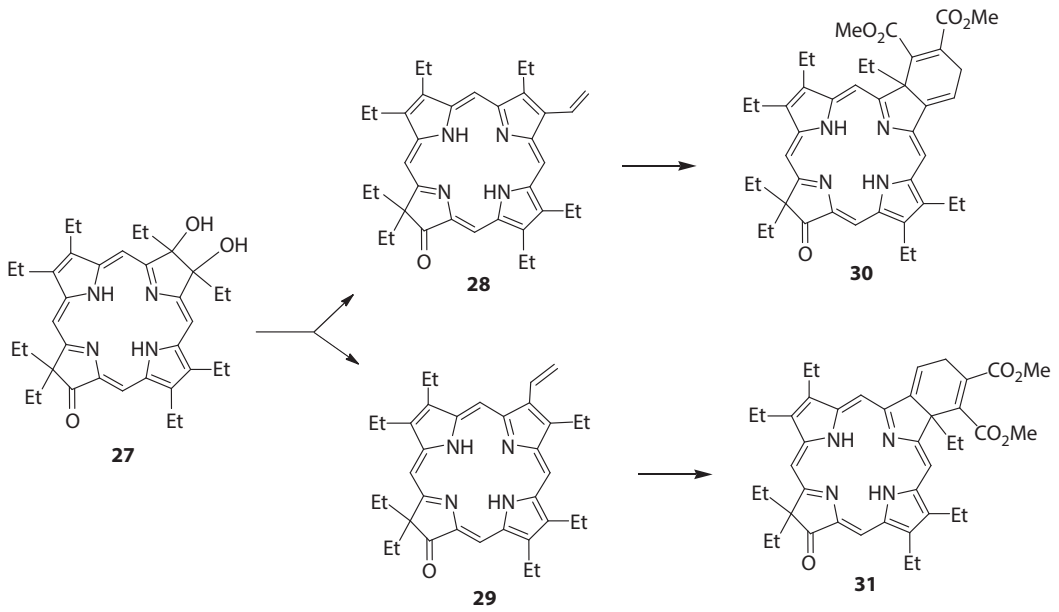

SCHEME 2.6 Synthesis of 17-ketobacteriochlorins from 7,8-di-hydroxy-1-keto-octaethylchlorin.

2.1.3 Benzochlorins and Benzobacteriochlorins

Benzochlorin consists of a benzene ring fused between the *meso*- and the adjacent β-position of the pyrrole ring. In a sequence of reactions, this class of compounds was first reported by Arnold et al. from octaethylporphyrin.[20] Morgan et al.[21] were the first to demonstrate the photosensitizing efficacy of these analogs (e.g., **36**). One of the major problems associated with this preparation is the difficulty in demetalation at the final step of the synthesis, and it is also difficult to chemically modify these benzochlorins. Therefore, this procedure has limited application in preparing a series of analogs with variable lipophilicity. This problem can be avoided by following the method recently reported by Li et al.[22,23] (Scheme **2.7**) In their approach, Ni(II)meso-(2-formylvinyl)octaethylporphyrin (**34**) was reacted with the Grignard's reagent of various fluorinated or nonfluorinated alkyl halides and/or Ruppert's reagent. The corresponding intermediates via intramolecular cyclization under acidic conditions afforded the related free-base benzochlorins (**42**). In this series of compounds, compared to the free-base analogs, the related Zn(II) complexes (671–677 nm) were found to be more effective both in vitro and in vivo. In preliminary screening, the fluorinated analogs showed better efficacy than the corresponding nonfluorinated derivatives.[22b]

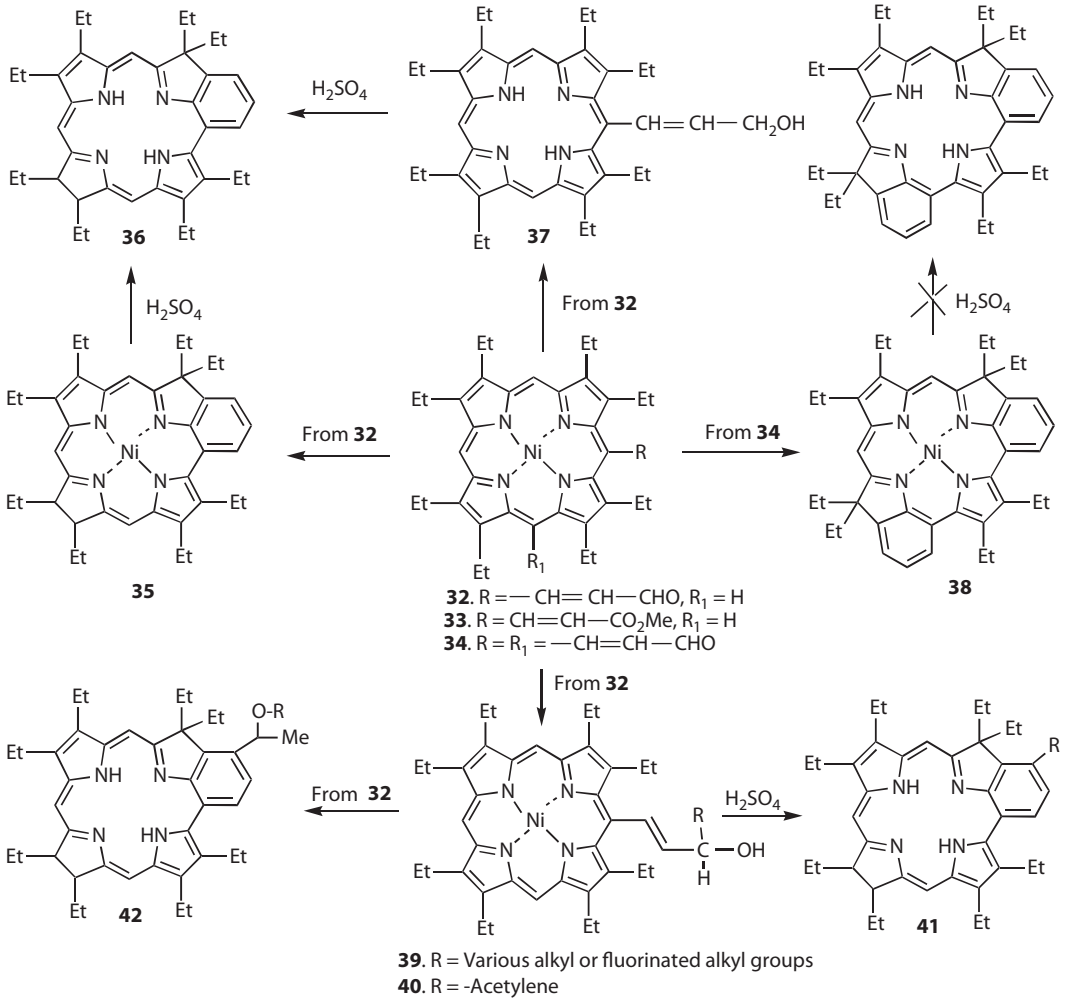

SCHEME 2.7 Synthesis of octaethyl-based benzochlorins.

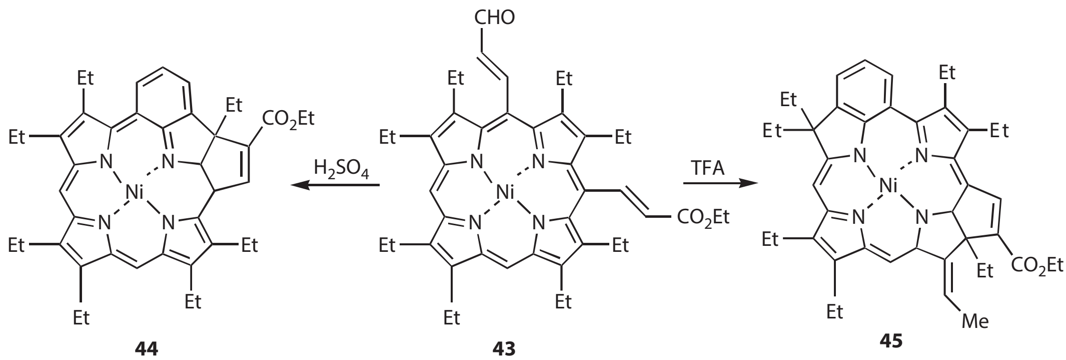

SCHEME 2.8 Synthesis of chlorins and bacteriochlorins with fused ring systems.

This methodology was later extended by Vicente and Smith[24] for the preparation of octaethylporphyrin-based benzochlorin (**38**) by intramolecular cyclization, of Ni(II)5,10 bis-(2-formylvinyl) porphyrin (**34**) (Scheme **2.8**). Unfortunately, attempts to remove the Ni(II) metal were unsuccessful. When Ni(II)5-(2-formyl-vinyl)-10-(2-ethoxycarbonyl-vinyl)octaethyl porphyrin was used as a substrate, the formation of the reaction product was found to depend on the strength of the acid used.[25] For example, reaction of **43** with sulfuric acid produced a chlorin containing both six- and five-member rings fused at the same pyrrole unit (**44**). Replacing sulfuric acid with trifluoroacetic acid (TFA) produced **45**, the Ni (II) complex of bacteriochlorin containing an ethylidene group at the peripheral position (λ_{max} 895 nm). Attempts to prepare the desired free-base analogs for investigating their application as photosensitizers were unsuccessful.

2.1.4 Purpurins (Tin Etiopurpurin Dichloride)

Purpurins have been known as degradation products of chlorophyll for quite some time.

The first synthesis of this class of compounds was reported by Woodward[26] during the synthesis of chlorophyll *a* by intramolecular cyclization of a *meso*acrylate functionality to a β-pyrrolic position. This methodology was later followed by Morgan et al.[27] and others[28] to synthesize a series of octaethylporphyrin, etioporphyrin, and 5,10-diphenyl- and 5,10-dipyridylporphyrin-based purpurin analogs. Among all the purpurins evaluated for PDT efficacy, the Sn etiopurpurin ($SnEt_2$) (**48**) (Scheme **2.9**) is considered to be the most effective in vivo (Scheme **2.9**).[27] Its long-wavelength absorption falls at 650 nm and produces a high singlet oxygen quantum yield. This product is currently in phase III clinical trials for the treatment of AMD, a major cause of blindness among people over 50 years of age.

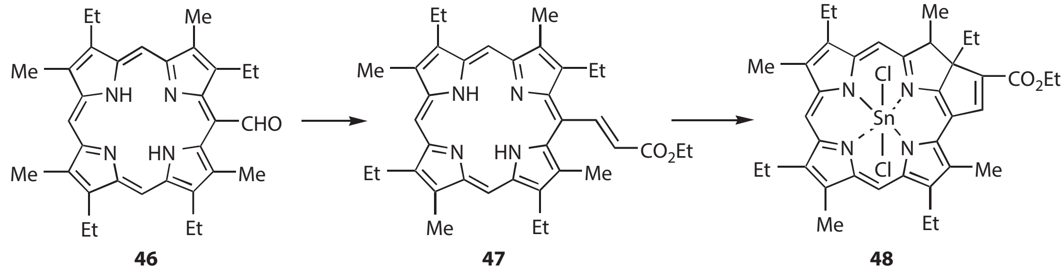

SCHEME 2.9 Synthesis of Sn(II) etiopurpurin.

2.2 Chlorins and Bacteriochlorins from Chlorophyll

Chlorophyll *a*, the green photosynthetic pigment, is one of the prototypes of the chlorin class of natural product. Because of its ready availability, a large amount of work has been done by several investigators to modify and to synthesize other chlorin-like chromophores. The photosensitizers derived from chlorophyll *a* can be divided into three categories in which the five-member isocyclic ring was either cleaved or kept intact or replaced with other ring system(s). Some of the photosensitizers in these series have attracted enormous attention; their description follows.

2.2.1 Aspartic Acid Derivative of Chlorin e_6 (Npe$_6$)

Chlorophyllin, a water-soluble degradation product of chlorophyll *a*, can be obtained by the cleavage of the isocyclic ring of chlorophyll.[29] The removal of magnesium resulted in chlorin e_6 with limited in vivo photosensitizing efficacy. It has been shown that replacing the vinyl group with alkyl ether groups of variable carbon units generally enhances the photosensitizing efficacy.[30] However, in this series, better results were obtained with the monoaspartyl derivative known as Npe$_6$.[31] This photosensitizer appears to clear rapidly from skin, and good tumor response was obtained only after irradiation within 3–4 h of sensitizer administration. Npe$_6$ is in human clinical trials in Japan for treatment of endobronchial lung cancer. The recent extensive NMR studies of Npe$_6$ confirmed that in Npe$_6$, the aspartic acid functionality is linked with an amide bond at position 15 (**49**) of chlorin e_6,[32] instead of at position 17 (**50**) as reported in several publications[33] (Scheme **2.10**).

2.2.2 Alkyl Ether Derivatives of Pyropheophorbide *a*

To understand the effect of various substituents on photosensitizing efficacy, the Roswell Park group synthesized and evaluated a series of pyropheophorbide *a* analogs with variable lipophilicity. In their effort to establish a structure–activity relationship (quantitative structure activity relationship [QSAR]), a congeneric series of the primary and secondary alkyl ether derivatives of pyropheophorbide *a* were synthesized (the isocyclic ring was kept intact). For the preparation of these analogs, methylpheophorbide *a* obtained from *Spirulina Pacifica* was converted into more stable pyropheophorbide *a* (**51**), which on reacting with HBr/AcOH and then the appropriate alcohol(s) produced the corresponding ether analogs in excellent yield[34] (Scheme **2.11**). At the final step, the methyl ester functionality was hydrolyzed into the corresponding carboxylic acid (**52**) (hexyl ether derivative of pyropheophorbide-a

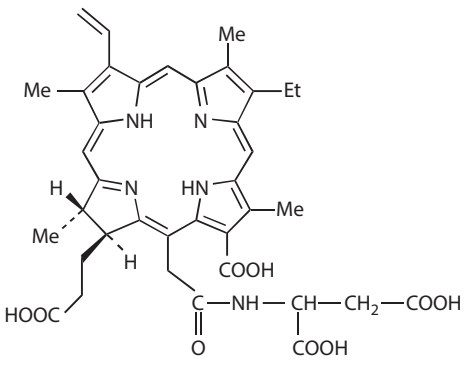

(Correct structure)

49

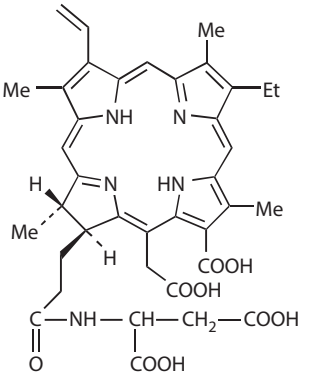

(Incorrect structure)

50

SCHEME 2.10 Structures of the aspartic acid derivative of chlorin e_6.

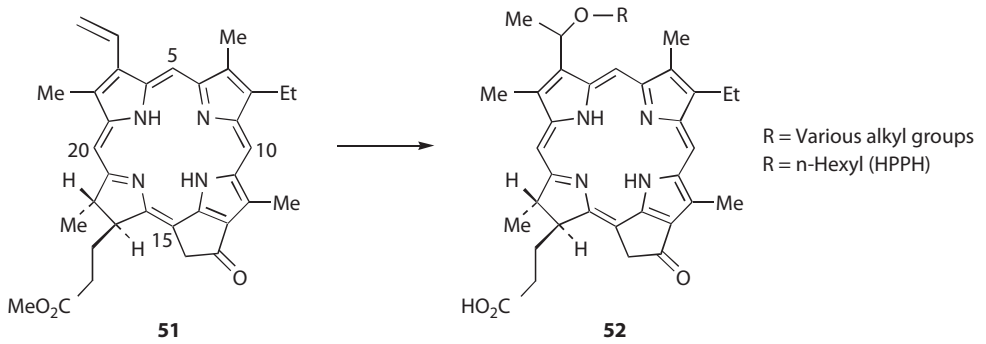

SCHEME 2.11 Synthesis of alkyl ether analogs of pyropheophorbide-a.

[HPPH]: R = *n*-hexyl). These analogs exhibit long-wavelength absorption near 665 nm (in vivo) and showed excellent singlet oxygen-producing efficiency (45%). The results obtained from the in vivo studies in mice demonstrated that the photodynamic efficacy of these photosensitizers increased by increasing the length of the carbon chain, reaching a maximum in compounds with *n*-hexyl and *n*-heptyl chains at position 3. Interestingly, the PDT efficacy decreased by further increasing the length of alkylether carbon units. When compensated for differences in tumor photosensitizer concentration, the *n*-hexyl derivative (HPPH) (optimal lipophilicity) was fivefold more potent than the *n*-dodecyl derivative (more lipophilic) and threefold more potent than the *n*-pentyl analog (less lipophilic). Interestingly, the introduction of the hexyl ether side chain at other positions of the macrocycle (position 8 or position 20) significantly reduced the in vivo efficacy.[35] These data suggest that besides the lipophilicity, the presence and position of the substituent possibly play an important role in drug efficacy. HPPH is currently at phase I/II human clinical trials for the treatment of a variety of cancers. Among the patients treated so far, no long-term skin phototoxicity has been observed.[36a]

To investigate the effect of central metal in PDT, Pandey et al. synthesized and investigated a series of pyropheophorbide and their metal complexes. They converted pyropheophorbide *a* (**53**) into the corresponding Zn (II), In(III), and Ni (II) complexes.[36b] Among these analogs, In(III) complexes showed the best PDT efficacy. The Ni (II) complexes because of its inability to produce any singlet oxygen didn't show any PDT efficacy.[36c] Also to look into the effect of lipophilicity, a series of In (III) analogs of methyl pyropheophorbide with variable lipophilicity were synthesized in which the vinyl group at position 3 was replaced with hexyl ether (**55**) and di- and mono-PEG substituents **61** and **63**, respectively (Scheme **2.12**).[36b]

It was seen that the presence of metals had a significant effect in the peripheral benzodiazepine receptor (PBR) binding and photosensitizing efficacy. On the basis of in vitro screening, indium complexes were found to be the most efficacious, which could be due to its higher singlet oxygen. Out of all the metal analogs, only HPPH (**54**) and its and indium complex (**55**) were tested for their in vivo PDT efficacy in C3H mice bearing RIF tumors. The indium complex of HPPH (**55**) was found to be more potent than the free-base HPPH, and with compound at a dose of 0.2 μmol/kg, 80% of mice were tumor-free after day 90 at a light 135 J/cm^2, 75 mW/cm^2.[36b]

2.2.3 Alkyl Ether Analogs of Purpurinimides

Having developed a QSAR for the alkyl ether analogs of pyropheophorbide series, the Roswell Park group extended their approach to photosensitizers with longer-wavelength absorption. For this study, the purpurin-18 methyl ester obtained from methylpheophorbide *a*[37] was converted into purpurin-18-*N*-alkyl imides (**65**).[38] The vinyl group at position 3 was then replaced with a variety of alkyl ether analogs (**66**) (Scheme **2.13**) with variable carbon units with log *P* values ranging from 5.32 to 16.44 and exhibiting long-wavelength absorption near 700 nm.[39]

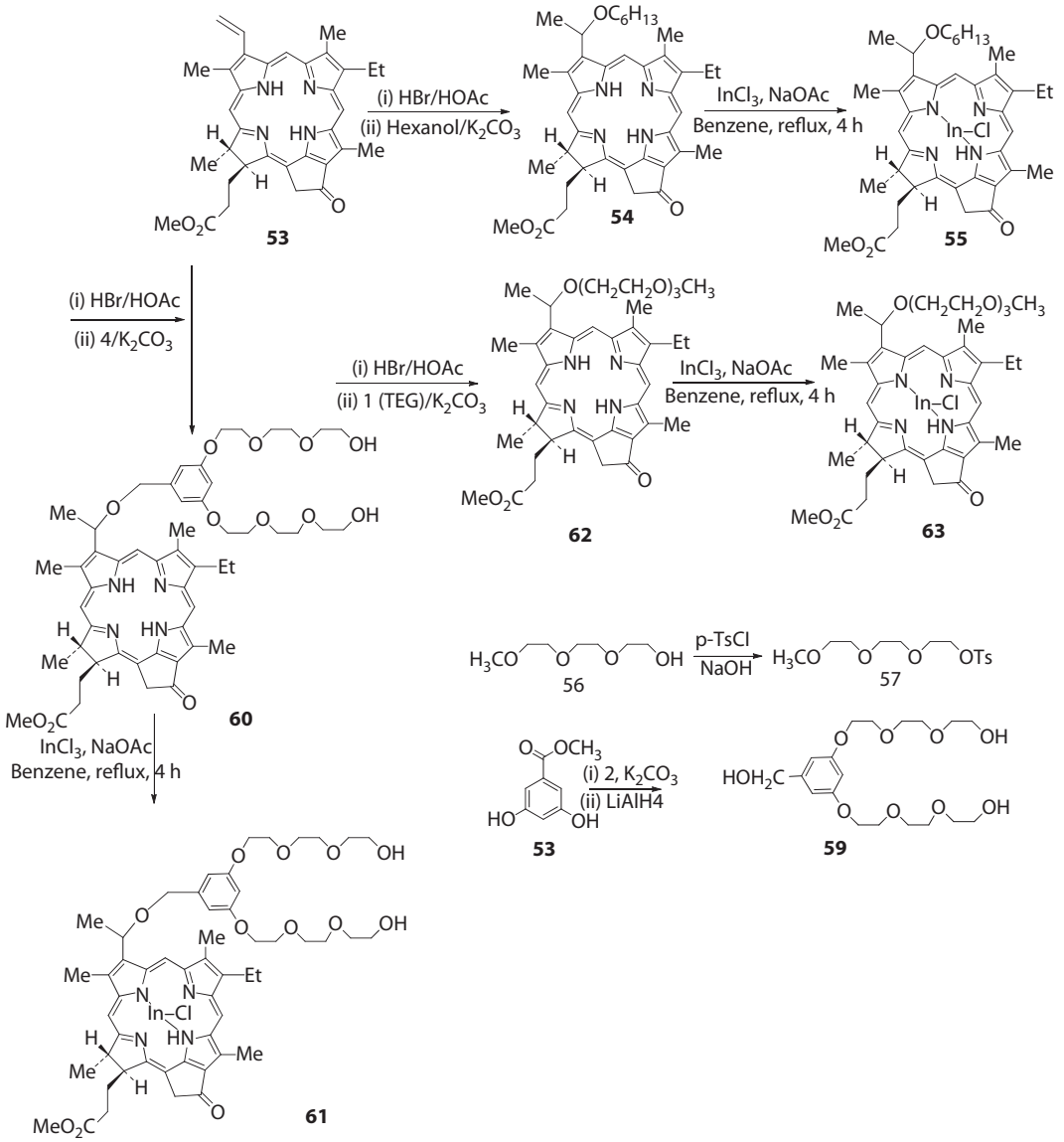

SCHEME 2.12 Synthesis of In(III)3-substituted methyl pyropheophorbide-a.

In animal studies, this class of compounds was found to be quite effective in vivo. The results obtained from a set of photosensitizers with similar lipophilicity (log *P* 10.68–10.88) indicate that similar to the pyropheophorbide series, in addition to the overall lipophilicity, the presence and position of the alkyl groups (*O*-alkyl vs. *N*-alkyl) in a molecule also play an important role in tumor uptake, tumor selectivity, and in vivo PDT efficacy.[39,40a,b]

The importance of fluorine in medicinal chemistry is well known.[40c,d] Fluorine substitutions are known to increase lipid solubility, which could result in increasing the rate of transportation of biologically active compounds across the lipid membrane.[40e] Gryshuk et al. synthesized a series of fluorinated and corresponding nonfluorinated purpurin-based photosensitizer (**70**, **71**, **73**, **74**), and it was observed that fluorinated analogs bearing trifluoromethyl substituents (**71**) showed enhanced photodynamic efficacy[40f] (Scheme **2.14**).

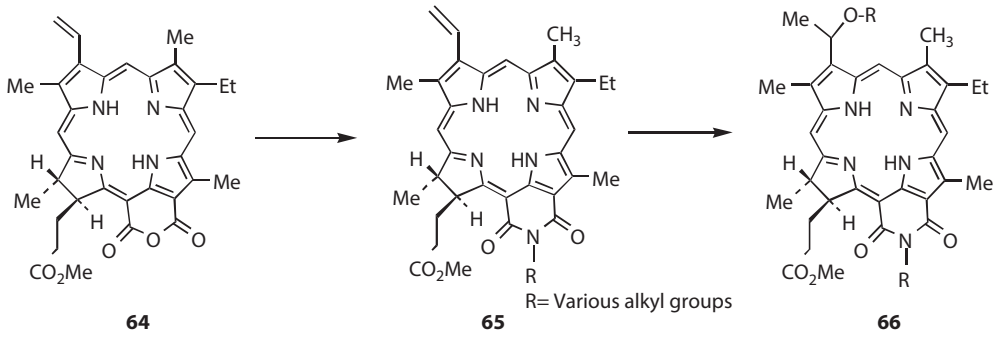

SCHEME 2.13 Synthesis of alkyl ether analogs of N-alkyl substituted purpurinimides.

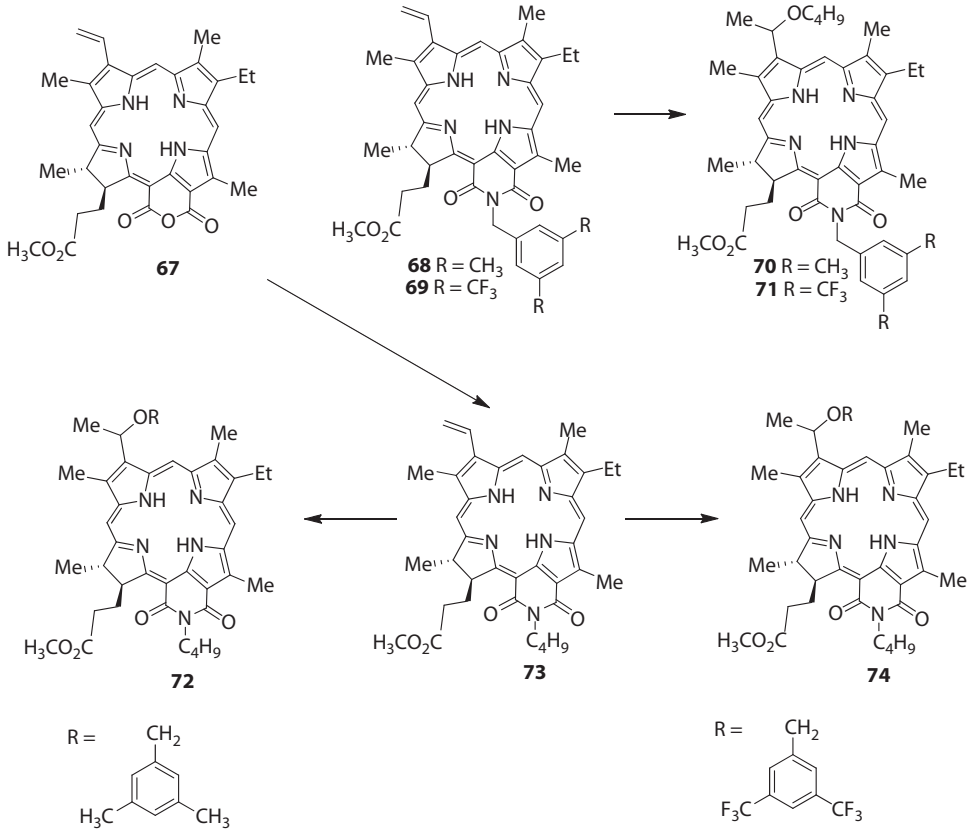

SCHEME 2.14 Synthesis of aryl ether analogs of N-aryl substituted purpurinimides.

2.2.4 Benzoporphyrin Derivatives Derived from Pyropheophorbide *a* and Purpurinimides

One of the main synthetic problems associated with PP-IX-based benzoporphyrin derivatives is to isolate the most effective analog (ring A reduced, monocarboxylic acid) from the complex reaction mixture. In order to solve this problem, the Roswell Park and Vancouver groups[41,42] have reported the preparation of various BPD analogs (e.g., **76**) from phylloerythrin and methyl 9-deoxypyropheophorbide (Scheme **2.15**).

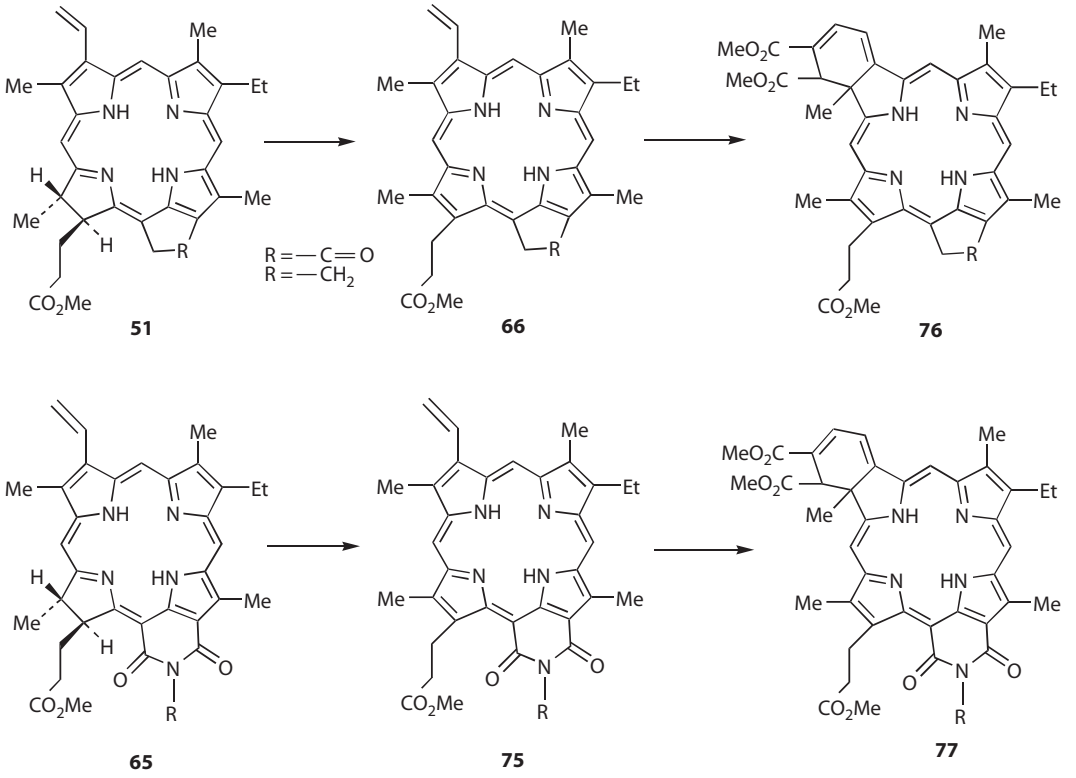

SCHEME 2.15 Benzoporphyrin derivatives derived from pyropheophorbide-a and purpurinimide.

Among these compounds, the benzoporphyrin derivative (*cis*-isomer) obtained from rhodoporphyrin XV di-*tert*-butyl aspartate was found to have PDT efficacy similar to BPDMA. This methodology was also extended in the purpurinimide series, and the lipophilicity was altered by introducing *N*-alkyl groups with variable carbon units at the imide ring system (**77**).[43] In preliminary in vivo testing, the corresponding *N*-hexyl and *N*-dodecyl analogs were found to be quite effective at a dose of 0.5 μM/kg when treated with light (135 J/cm^2, 75 mW/cm^2) at 728 nm and 24 h postinjection. Under similar treatment conditions (treated with light at 690 nm), the BPDMA obtained from protoporphyrin IX dimethyl ester did not produce any photosensitizing efficacy.[44] Therefore, the Diels–Alder approach in purpurinimide system provides a simple approach for generating effective photosensitizers with variable lipophilicity.

2.2.5 *Vic*-Dihydroxy- and Ketobacteriochlorins

Osmium tetroxide has very frequently been used for the conversion of porphyrins to the corresponding *vic*-dihydroxy chlorins and tetrahydroxy bacteriochlorins as a mixture of isomers.[45] The overall lipophilicity of these analogs can be altered by subjecting them to pinacol–pinacolone reaction conditions. The formation of the corresponding ketoanalog is not straightforward and depends not only on the intrinsic nature of the migratory group but also of the electronic and steric factors elsewhere on the porphyrin nuclues.[46] Therefore, the concept of designing chlorin and bacteriochlorin analogs from porphyrins by following this approach was not successful. A few years ago, Chang et al.[47] showed that chlorins under certain conditions can be converted into *vic*-dihydroxybacteriochlorins upon reaction with osmium tetroxide. The Roswell Park group extended this methodology to the pheophorbide and chlorin e_6, and a series of *vic*-hydroxy- and ketobacteriochlorins were synthesized. The stable ketobacteriochlorins had strong absorptions in the range of 710–760 nm region, but did not show any significant photosensitizing

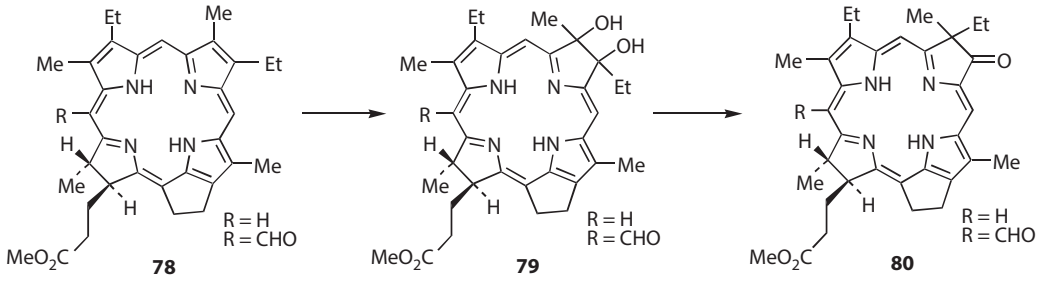

SCHEME 2.16 Synthesis of 8-keto methyl bacterio-pyropheophorbide-a analogs.

activity in mice (DBA/2) transplanted with SMT-F tumors.[48] However, the ketobacteriochlorins obtained from 9-deoxypyropheophorbide *a* (**78**) and the related *meso*formyl derivative with long-wavelength absorption showed long-wavelength absorptions at 734 and 758 nm, respectively (Scheme **2.16**). Among these bacteriochlorins, the triplet states were quenched by ground-state molecular oxygen in a relatively similar manner, yielding comparative singlet oxygen quantum yields. In preliminary in vivo screening, the ketochlorins (**80**) (R = CHO) were found to be more photodynamically active than the related *vic*-dihydroxy analogs. Replacement of the methyl ester functionalities with di-*tert*-butylaspartic acids enhanced the in vivo efficacy.[49a] It appears to be cleared rapidly from skin and good tumor responses can be obtained only after irradiation within 3–4 h of the sensitizer administration.

Joshi et al. synthesized a series of ketobacteriochlorins from ring B and ring D reduced chlorins (Schemes **2.17** and **2.18**).These newly synthesized compounds (**83**, **86**, **91**, **92**) show strong long-wavelength absorption and produce significant in vitro (Colon 26 cells) photosensitizing ability. Among all the compounds, the one containing a ketogroup at position 7 of ring B and bearing a cleaved five-member isocyclic ring (**92**) showed the best efficacy.[49b]

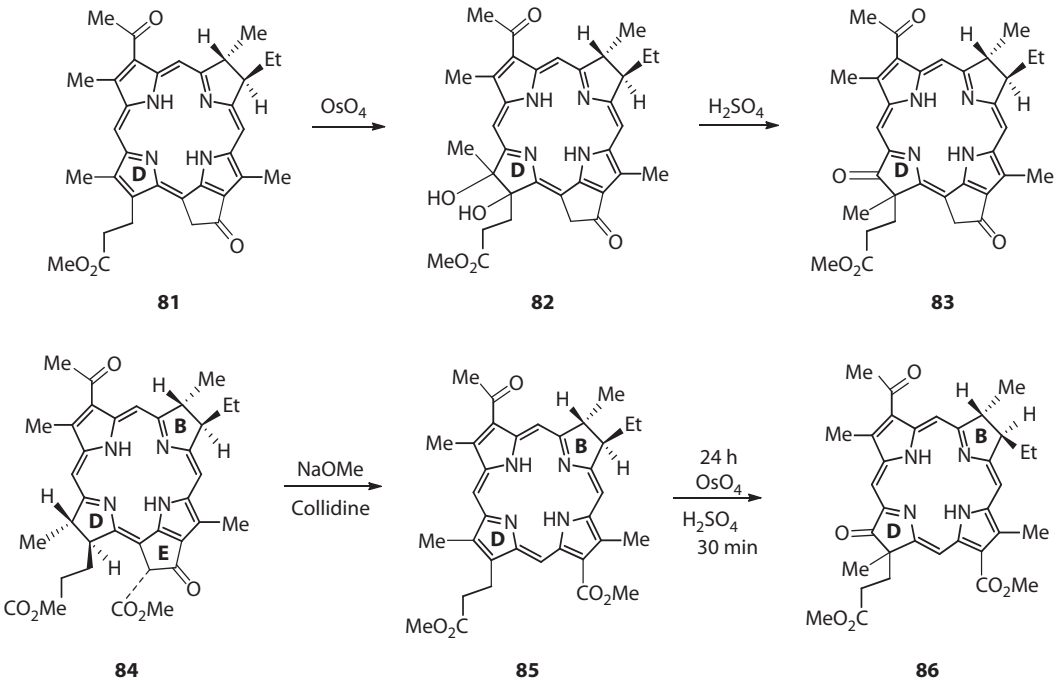

SCHEME 2.17 Synthesis of 18-keto-bacteriopyropheophorbide and bacteriorhodo-bacteriochlorins.

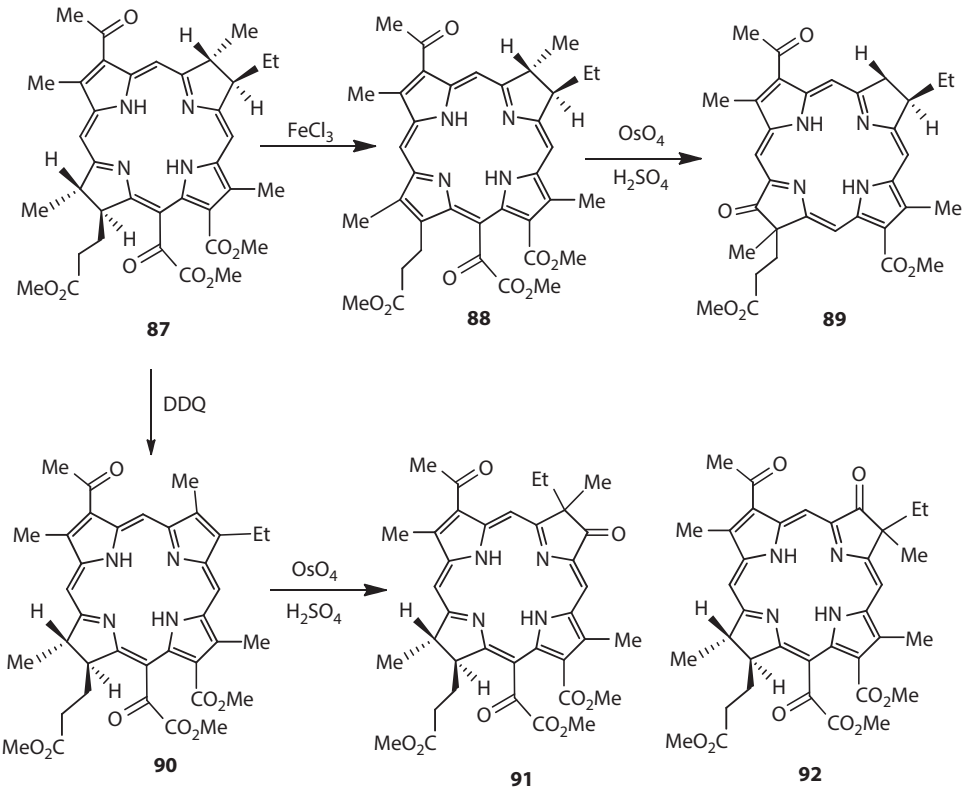

SCHEME 2.18 Synthesis of 3-acetyl-18-keto and 3-acetyl-8-ketobacteriochlorins.

2.2.6 Bacteriochlorins Derived from 8-Vinyl Chlorins

The Roswell Park group combined the use of osmium tetroxide and Diels–Alder approach for the construction of stable bacteriochlorins. In their approach, mesopurpurin-18 methyl ester (**93**) obtained from methylpheophorbide *a* was reacted with osmium tetroxide. The resulting *vic*-dihydroxy bacteriochlorin on reacting with *p*-toluenesulfonic acid in refluxing benzene produced the 8-vinyl derivative (**94**), which on reacting with DMAD under Diels–Alder reaction conditions produced bacteriochlorin (**95**) with long-wavelength absorption near 800 nm.[50] Unfortunately, the utility of this compound for the use in PDT was diminished due to the unstable nature of the six-member anhydride ring system (Scheme **2.19**). In another approach, the anhydride ring is replaced with an *N*-hexyl-imide ring system, and these compounds were found to be quite stable in vivo.[51] This system also possesses a unique opportunity to prepare a series of *N*-alkyl ether derivatives with variable carbon units and to establish the structure/activity relationship in a particular series of compounds.

2.2.7 Bacteriochlorins from Bacteriochlorophyll

Most of the naturally occurring bacteriochlorins have absorptions between 760 and 780 nm and have been studied by various investigators for their use as photosensitizers for PDT.[52] They were found to be extremely sensitive to oxidation, resulting in a rapid transformation into the chlorin state that generally has an absorption maxima at or below 660 nm.[53] Furthermore, if a laser is used to excite the bacteriochlorin in vivo, oxidation may result in the formation of a new chromophore absorbing outside the laser window, reducing the photodynamic efficacy. Due to the desirable photophysical properties and

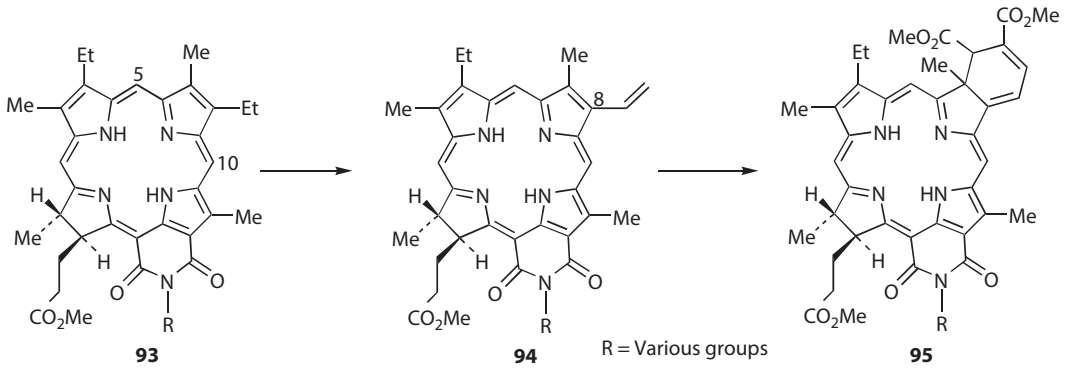

SCHEME 2.19 Synthesis of bacteriopurpurinimides.

promising in vitro/in vivo photosensitizing efficacy of bacteriochlorins, there has been increasing interest in the synthesis of stable bacteriochlorins either from bacteriochlorophyll *a* or from the other related tetrapyrrolic systems.

In general, for designing improved photosensitizers, overall lipophilicity has been proven to be one of the important factors. For example, among porphyrin-based photosensitizers, the hydrophobic porphyrins are preferentially accumulated and partitioned into corresponding hydrophobic loci in vivo. Moan and coworkers[54] have shown that among diether derivatives of hematoporphyrin, retention in cells increases with decreasing polarity. The Roswell Park group have studied the uptake of a series of alkyl ether derivatives of pyropheophorbide *a* and found that a strong correlation exists between uptake and hydrophobicity, although each correlation cannot be extended to the in vivo PDT efficacy. On the other hand, photosensitizers with high partition coefficient values (increased hydrophobicity) induce sensitizer insolubility, thus preventing drugs from entering the circulation. Therefore, a proper balance between hydrophobicity and hydrophilicity is probably the most important factor that influences tumor localization of sensitizers.

A simple approach used by the Roswell Park group was to vary the overall lipophilicity of various types of photosensitizers such as pyropheophorbide *a*, benzoporphyrin derivatives, benzochlorins, and purpurinimides by altering the length of carbon units in alkyl ether substituents, an approach which has been quite successful. It was demonstrated that replacing an anhydride ring system in purpurin-18 (a chlorophyll *a* analog) with a six-member imide ring substantially enhanced its in vivo stability and retained effective in vivo photodynamic activity.[55] Therefore, in order to investigate the effect of such substitutions in the bacteriochlorin series, bacteriochlorophyll *a*, present in *Rhodobacter sphaeroides*, was first converted (in situ) into bacteriopurpurin-18 (**96**),[56] which in a sequence of reactions was transformed into a series of related *N*-alkyl derivatives (**97**)[57] (Scheme **2.20**). To determine the effect of the presence of these alkyl substituents with variable carbon units, the acetyl-group was first reduced with sodium borohydride, which on reacting with HBr gas and an appropriate alcohol produced the corresponding alkyl ether derivatives of bacteriochlorin (**98**) in high yield. These compounds are stable both in vitro and in vivo, exhibit long-wavelength absorption near 790 nm, and show high tumor uptake. In preliminary in vitro and in vivo studies, some of these compounds have been found to be quite effective at low injected doses.[58a] Earlier, it was shown that fluorinated analogs of purpurin showed enhanced photodynamic efficacy compared to the nonfluorinated analogs.[40f] The same group in order to investigate the effect of fluorine in bacteriopurpurinimide reacted bacteriopurpurinimide methyl ester with 3,5-bis(trifluoromethyl)benzyl amine (Scheme **2.21**).[58b] The compound (**101**) was found to be quite effective in vivo, and a drug dose of 1 μm/kg and light dose of 135/75 produced a 60% long-term tumor cure in C3H mice bearing RIF tumor.[58b]

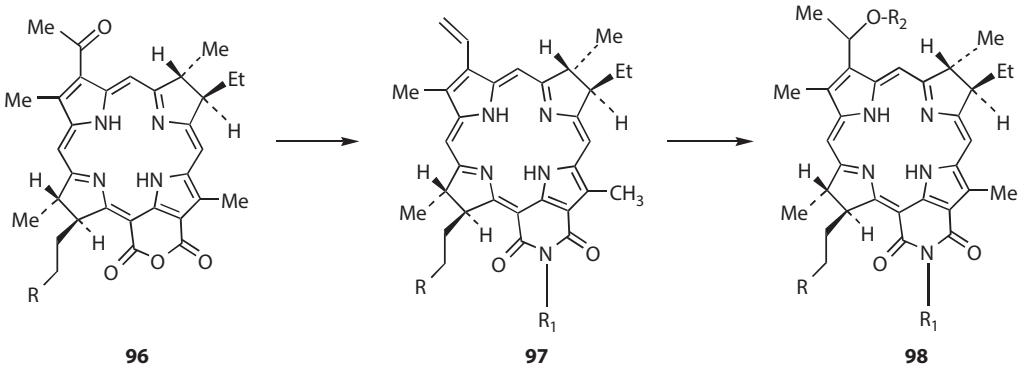

SCHEME 2.20 Synthesis of alkyl ether derivatives of *N*-substituted bacteriopurpurinimides.

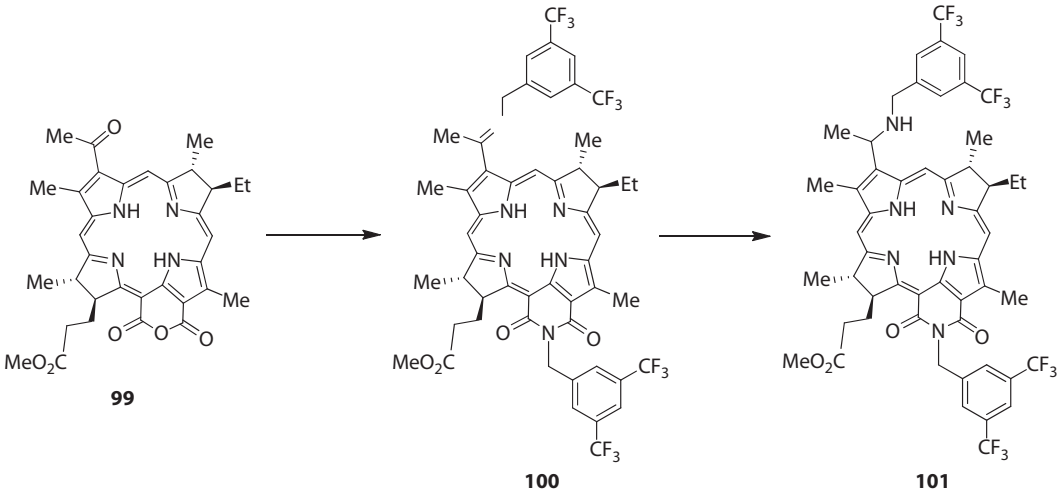

SCHEME 2.21 Synthesis of fluorinated bacteriopurpurimides.

2.3 Expanded Porphyrins

2.3.1 Texaphyrin

The texaphyrins are aromatic tripyrrolic, pentaaza, Schiff-base macrocycles that bear a strong, but *expanded*, resemblance to the porphyrins and other naturally occurring tetrapyrrolic prosthetic groups.[59] Similar to porphyrins, the texaphyrins are fully aromatic and colored compounds (Scheme **2.22**). However, they are 22π-electron electron systems rather than 18π-electron ones. This class of compounds exhibit long-wavelength absorption >700 nm depending on the nature of substituents present at the peripheral position. Also in contrast to porphyrins, the texaphyrins are monoanionic ligands that contain five, rather than four, coordinating nitrogen atoms within the central core that is roughly 20% larger than that of the porphyrins. High-yield production of long-lived triplet states and their remarkable singlet oxygen-producing efficiency are of important features of this class of photosensitizers. Currently, two different water-solubilized lanthanide(III)texaphyrin complexes, namely, the gadolinium(III) (**104**)[60] and lutetium(III) (**105**)[61a] derivatives (Gd-Tex and Lu-Tex, respectively), are being tested clinically. The first of these, XCYTRIN™, is in a pivotal phase III clinical trial as a potential enhancer of radiation therapy for patients with metastatic cancers of the brain receiving whole-brain radiation therapy. The second, in various formulations, is being

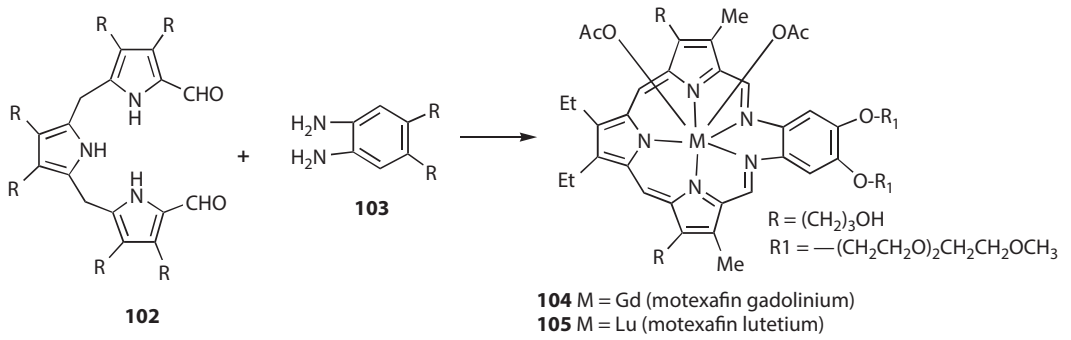

SCHEME 2.22 Synthesis of metallated saphyrins.

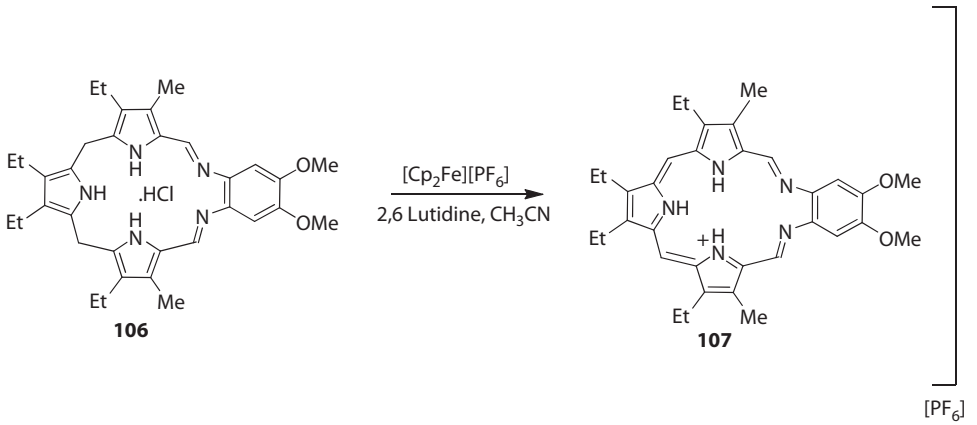

SCHEME 2.23 Synthesis of substituted nonmetallated saphyrins.

tested as a photosensitizer for use in the treatment of recurrent breast cancer (LUTRIN) and is in phase II clinical trials, photoangioplastic reduction of atherosclerosis involving peripheral arteries (ANTRIN), and light-based treatment of AMD (OPRTIN), currently phase I clinical trials.[59]

Earlier, texaphyrins could only be obtained in the form of metal complexes. In 2001, Sesseler et al. reported the synthesis of a metal-free form of texaphyrin (Scheme **2.23**).[61b] The metal-free oxidized texaphyrin 107 as its HPF6 salt was isolated by using ferrocenium cation as oxidizing agent and using a reduced porphyrinogen-like nonaromatic form of texaphyrin.[61b]

Recently, Lu et al. synthesized a benzotexaphyrin with an extensively delocalized π-electron system.[61c] Benzotexaphyrin absorbs at 810 nm and has high efficiency in generating singlet oxygen in methanol (0.65).

2.3.2 Sapphyrins

Another class of expanded porphyrins are the sapphyrins (**5**), which were discovered accidentally during the synthesis of vitamin B_{12}.[61d] These have a 22π-electron pathway, and as a result, they have more electron affinity than the corresponding porphyrin system.[61e]

They absorb in the near-infrared region and produce high singlet oxygen yields, which makes them potential PDT agent.[61f] Sesseler and coworkers synthesized and characterized a series of novel water-soluble sapphyrins that were found to localize selectively in pancreatic carcinoma tissue in a xenographic murine model (Scheme **2.24**).[61g] Among these, the sapphyrins bearing neutral solubilizing groups (compounds **111–113**) were found to have selectivities for tumor tissue over surrounding tissues. The incorporation of

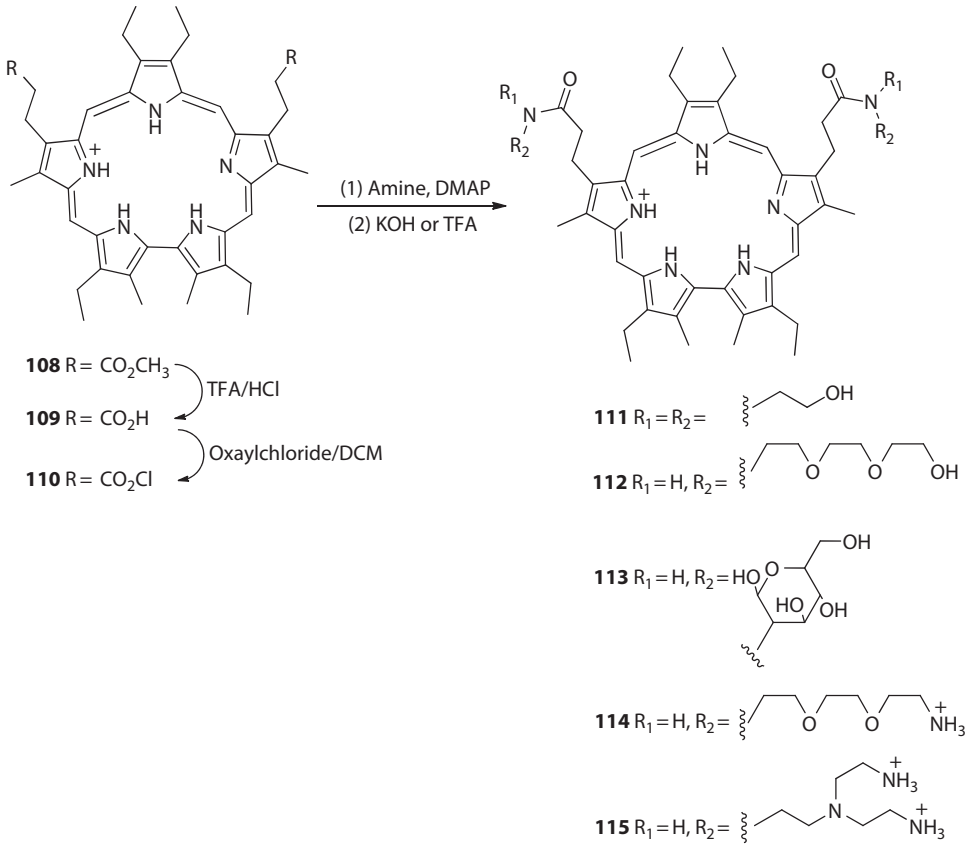

SCHEME 2.24 Synthesis of substituted saphyrins.

charged moieties into the sapphyrin (compounds **114** and **115**) significantly reduced the tumor localization. The tetrahydroxy sapphyrin (**111**) exhibited the best tumor-to-muscle ratio, whereas the incorporation of glucosamine into the sapphyrin (**119**) cores afforded the best tumor-to-liver ratio.

Recently Hooker et al. showed the activity of sapphyrins and heterosapphyrins in the presence of light against *Leishmania* parasites.[61h]

2.4 Phthalocyanines and Naphthalocyanines

Phthalocyanines (**6**, Pc) and naphthalocyanines (**7**, Nc) can be regarded as azaporphyrins containing four isoindoles linked by nitrogen atoms[62] (Scheme **2.25**). Compared to porphyrins, Pc and Nc offer high molar-extinction coefficients and red shift maximums at 680 nm for Pc and 780 nm for Nc resulting from the benzene or naphthalene rings condensed at the periphery of the porphyrin-like macrocycle. They possess high singlet oxygen producing efficiency, and interestingly, chelation of the metal ions such as zinc or aluminum increases the singlet oxygen yield to nearly 100%. Therefore, metal complexes of the Pc and Nc have attracted attention for their use as photosensitizers in PDT. In recent years, a large number of metalated or nonmetalated phthalocyanine-based photosensitizers have been synthesized by introducing a variety of substituents at the peripheral position(s). If the valency of the central metal is higher than 2, it binds various axial ligands. All of these chemical changes of Pc and Nc skeleton alter their PDT efficacy. Aggregated Pc and Nc are inactive photochemically because of a greatly enhanced rate of excited singlet state deactivation by internal conversion of the ground state. In the phthalocyanine series, Olenick and coworkers in collaboration with Kenney[63] synthesized and evaluated four silicon analogs with variable

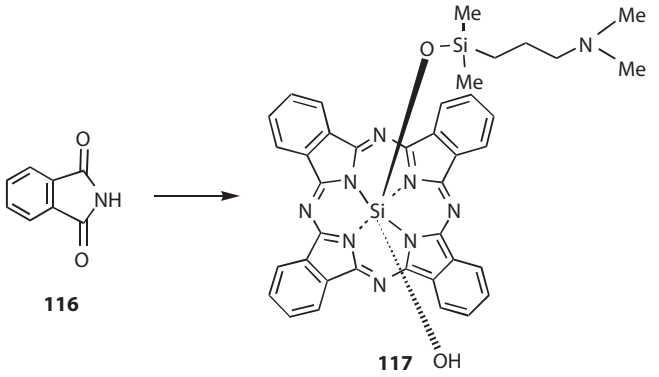

SCHEME 2.25 Substituted silicon phthalocyanines.

lipophilicity to learn more about the structural features that silicon phthalocyanine must have in order to be a good PDT photosensitizer. All these analogs produced similar photophysical properties; however, the photosensitizer denoted as Pc4, bearing a long-chain amino axial ligand (**117**), has shown promising results both in vitro and in vivo and is presently entering clinical trials.[64] Further, it was concluded that the presence of structural features leading to improvement in the association between the photosensitizers and important cellular targets is more useful than those leading to improvements in their already acceptable photophysical and photochemical characteristics. A series of benzyl-substituted phthalonitriles were converted into the corresponding Zn(II) hydroxyphthalocyanines (phthalocyanine phenol analogs). Their efficacy as sensitizers for PDT was evaluated on the EMT-B mammary tumor cell line. In vitro, the 2-hydroxy Zn Pc was the most active, followed by 2,3- and 2,9-dihydroxy ZnPc, with the 2,9,16-trihydroxy ZnPc exhibiting the least activity. In vivo, the monohydroxy derivative and the 2,3-dihydroxy analog were both efficient in inducing tumor necrosis, but complete tumor regression was poor even at high doses. In contrast, the 2,9-dihydroxy isomer at 2 μM/kg induced tumor necrosis in all animals treated, with 75% complete regression. These results underline the importance of the position of the substituents on the Pc macrocycle to optimize tumor response and confirm the PDT potential of the unsymmetrical Pcs bearing functional groups on adjacent benzene rings.[65a]

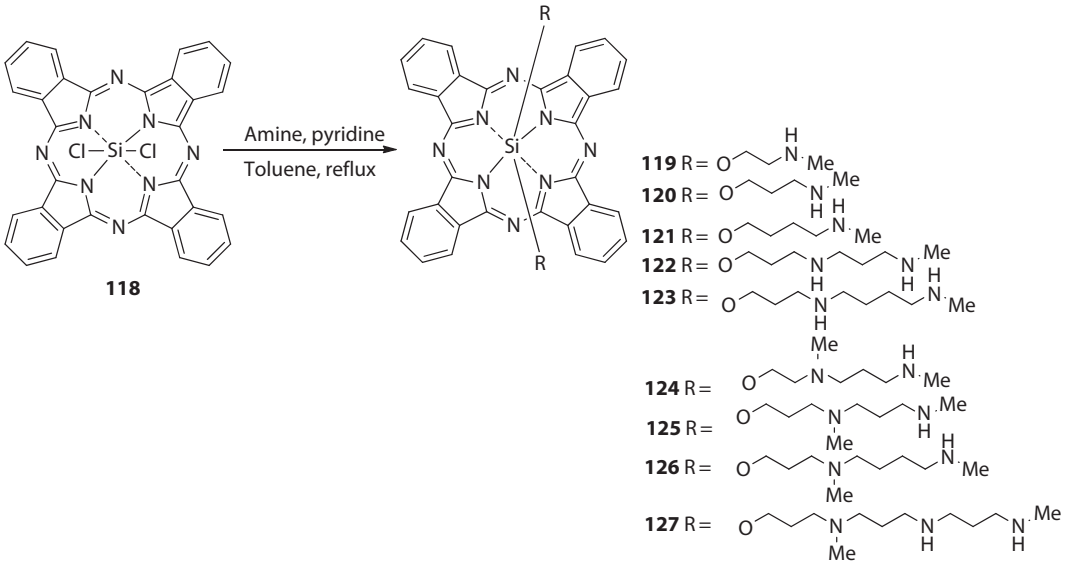

SCHEME 2.26 Substituted silicon phthalocyanines.

Jiang and coworkers synthesized a series of silicon (IV) phthalocyanines with polyamine moieties at axial positions (Scheme **2.26**).[65b] These compounds (**119–127**) were found to be potent PSs toward the HT29 cells with IC_{50} values as low as 1 nm, and also compounds **120** and **123** suppressed the growth of tumors in nude mice bearing HT29 tumor.[65b]

Recently, Dumoulin et al. synthesized a chalcone phthalocyanine conjugate (**130**) to combine the vascular disrupting effect of chalcones with the photodynamic effect of phthalocyanines.[65c] For this, they converted the aminochalcone to the activated isocyanate chalcone (**129**), and then the isocyanate chalcone was coupled to tetrahydroxylated Zn (II) phthalocyanine (**128**) under basic conditions (Scheme **2.27**). The photophysical and biological studies of chalcone phthalocyanine conjugate (**130**) are under progress.[65c]

Recently, certain water-soluble dual-function photosensitizers containing phthalocyanine-ALA (5-aminolevulinic) conjugate (**135, 140**) were synthesized by Oliveira et al. These compounds produce good singlet oxygen yields and could be efficient agents for the use in PDT (Scheme **2.28**).[65d]

The pegylated zinc phthalocyanines were found to be highly cytotoxic toward HT29 human colorectal carcinoma and HepG2 human hepatocarcinoma on illumination with light with IC_{50} as low as 0.02 μM.[65e]

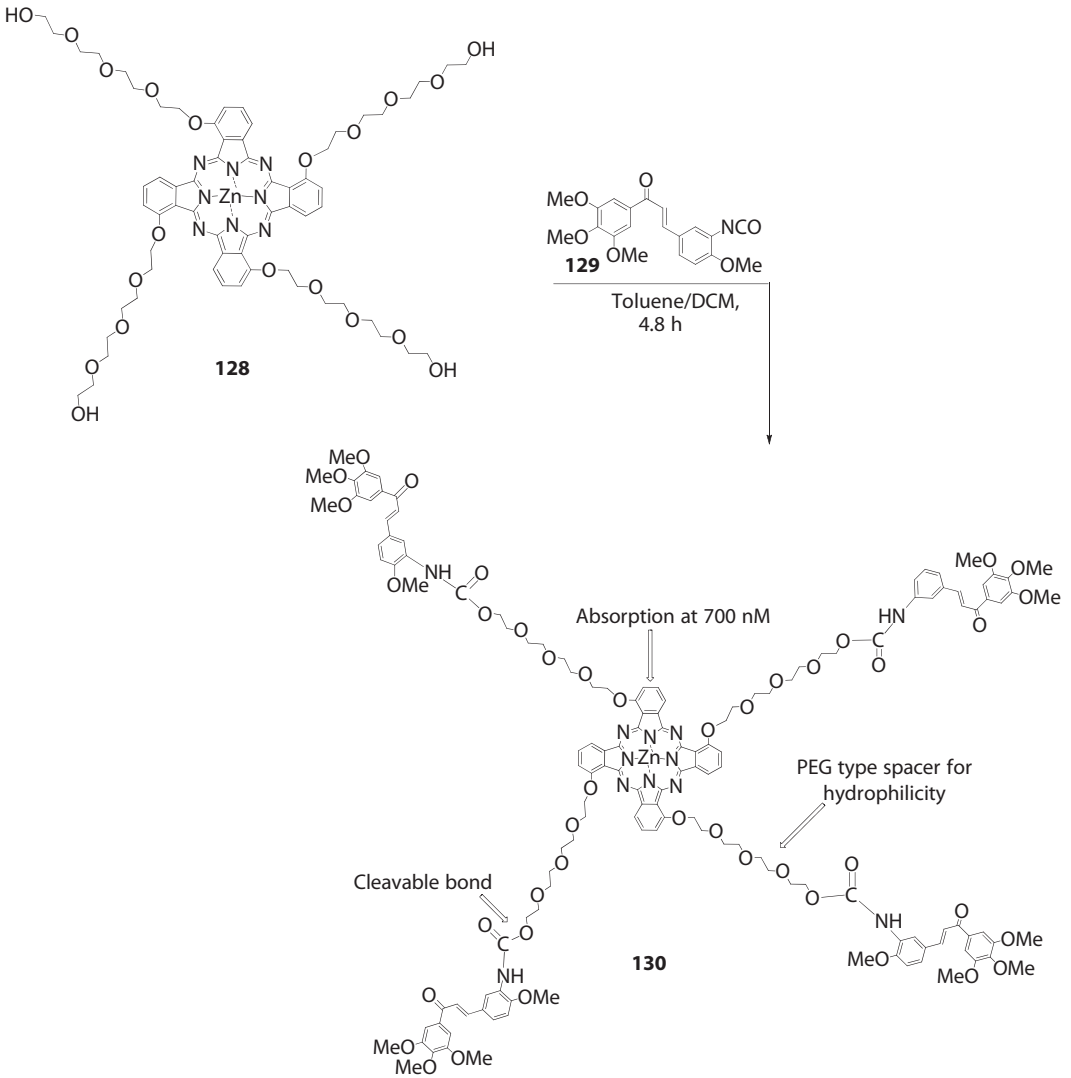

SCHEME 2.27 PEG-substituted tetraphenylporphyrins.

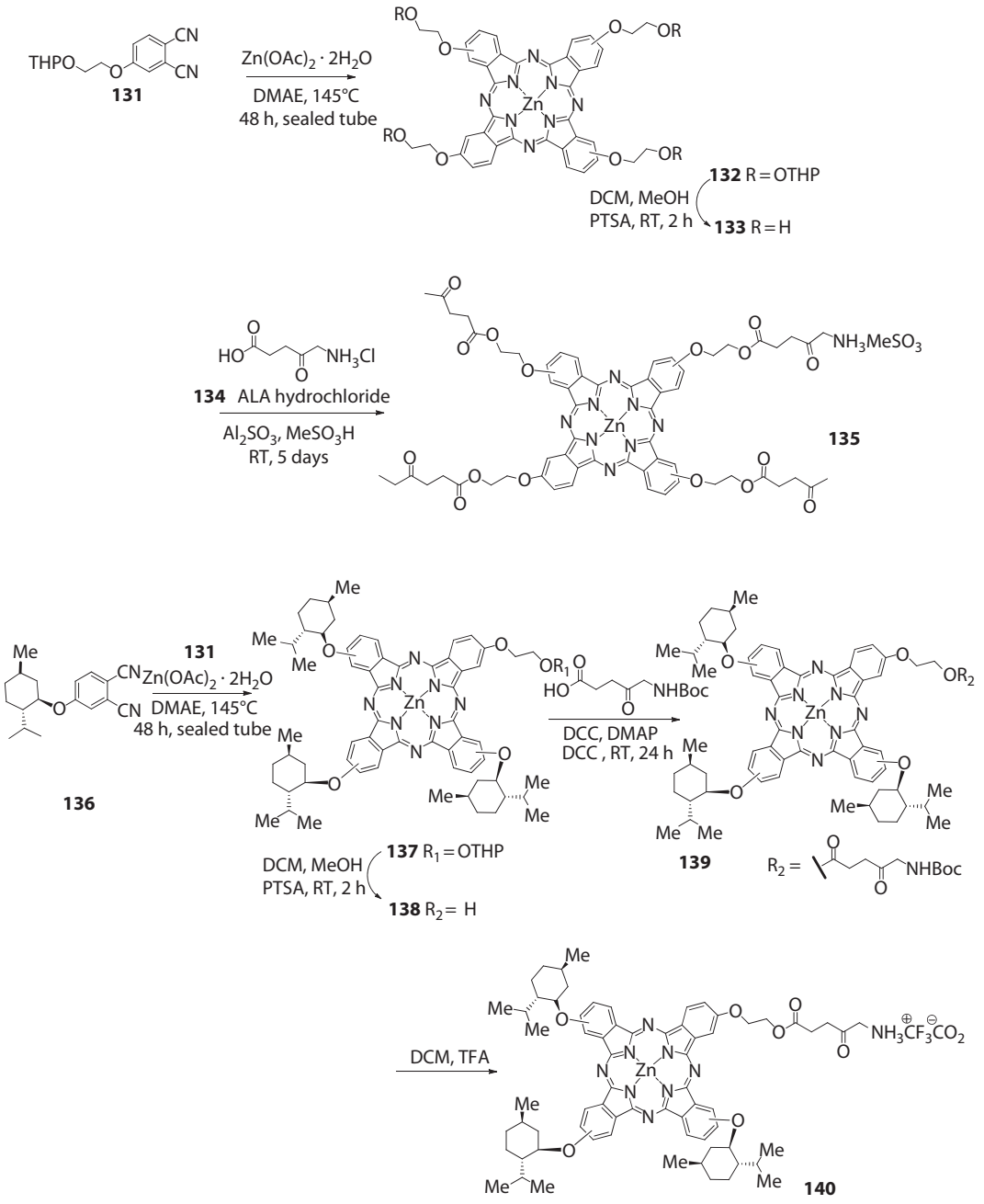

SCHEME 2.28 Phthalocyanines substituted at peripheral positions.

Water-soluble, 3-hydroxypyridin tetrasubstituted indium (III) phthalocyanines (**143**, **147**) and their quarternized derivatives (**144**, **148**) were synthesized by Durmus and coworkers and showed to have high singlet oxygen yield (>0.55) (Scheme **2.29**).[65f]

Rodgers et al. in collaboration with Kenney and collaborators[66] developed a new route to silicon-substituted phthalocyanines and phthalocyanines-like compounds that is robust and flexible. One